

**VISUAL SYSTEM DEVELOPMENT IN PEOPLE WITH ONE EYE:
BEHAVIOUR AND STRUCTURAL NEURAL CORRELATES**

KRISTA KELLY

A DISSERTATION SUBMITTED TO
THE FACULTY OF GRADUATE STUDIES
IN PARTIAL FULFILLMENT OF THE REQUIREMENTS
FOR THE DEGREE OF
DOCTOR OF PHILOSOPHY

GRADUATE PROGRAM IN PSYCHOLOGY
YORK UNIVERSITY
TORONTO, ONTARIO

MAY 2014

©Krista Kelly, 2014

GENERAL ABSTRACT

Postnatal monocular deprivation from the surgical removal (enucleation) of one eye in humans results in intact spatial form vision, although its consequences on motion perception development are less clear. Changes in brain structure following early monocular enucleation have either been assessed in species whose visual system is quite different from humans, or in enucleated monkeys and humans following short-term survival. In this dissertation, I sought to determine the long-term effects of enucleation on visual system development by examining behavioural visual abilities and visual system morphology in adults who have had one eye enucleated early in life due to retinoblastoma. In Chapter II, I conducted a series of speed and luminance contrast discrimination tasks not yet implemented in this group. Early monocular enucleation results in impaired speed discrimination but intact contrast perception compared to binocular and monocular viewing controls. These findings suggest differential effects of enucleation on the development of spatial form vision and motion perception. In Chapters III and IV, I obtained high-resolution structural magnetic resonance images to assess the morphological development of subcortical (Chapter III) and cortical (Chapter IV) structures in the visual pathway. Early monocular enucleation resulted in decreased optic chiasm width and volume, optic tract diameters, and lateral geniculate nuclei (LGN) volumes compared with binocularly intact controls. Surprisingly, however, optic tract diameter and LGN volume decreases were less severe contralateral to the remaining eye. Early monocular enucleation also resulted in increased grey matter surface area of visual and non-visual cortices compared with binocularly intact controls.

Consistent with the LGN asymmetry, increased surface area of the primary visual cortex was restricted to the hemisphere contralateral to the remaining eye. Surprisingly, however, these increases were found for those with right- but not left-eye enucleation, suggesting different developmental time periods for each hemisphere. Possible mechanisms of altered development following early monocular enucleation include: 1) recruitment of deafferented cells by the remaining eye, 2) retention of deafferented cells due to feedback from visual cortex, and 3) a disruption in synaptic pruning. These data highlight the importance of receiving normal levels of binocular visual input during infancy for typical visual development.

ACKNOWLEDGEMENTS

First, I would like to sincerely thank my advisor, Dr. Jennifer Steeves, for allowing me to be part of such an amazing, thriving lab for the past 8 years. Through your support and guidance, I have obtained invaluable skills that have aided in my development as a researcher. You pushed me to think critically and independently, and taught me the importance of collaborations and publishing. You went above and beyond the duties of a supervisor, and your passion for research and teaching are inspirational. I hope some day to be as great of a mentor as you!

A huge thank you to my Perceptual Neuroscience labmates, both past and present, especially Caitlin Mullin, Stefania Moro, and Adria Hoover who have been at my side since the beginning. It was so much easier experiencing all of the ups and downs of grad school with you gals! Lily Solomon-Harris and Sara Rafique, thank you for your friendship and support over the past year. I am grateful to have made such amazing friends in the workplace!

Thank you to my committee members, Drs. Laurie Wilcox, Frances Wilkinson, and Keith Schneider. Your invaluable input has greatly improved my dissertation. I would also like to thank Drs. Jason Barton and Anne Moore for reading my dissertation and for their insightful questions and comments during my oral exam. A very special thank you to Dr. Martin Steinbach for the various roles you have played throughout my graduate career and for your continuing guidance. It was a privilege working with you for so many years! I would also like to thank Dr. Brenda Gallie from The Hospital for Sick Children who provided the rare patient population for me to test.

I would also like to thank many others at York University. Dr. Suzanne MacDonald, my minor area paper advisor. Thank you for the opportunity to conduct animal behaviour research with polar bears. It was an experience that I thoroughly enjoyed! Thank you to my colleagues in the Sherman Health Sciences centre, Kevin DeSimone, Joy Williams, Joseph Viviano, and Aman Ish Goyal for your MRI scanning and analyses expertise. Thank you to those in the Graduate Psychology department, Freda Soltau, Lori Santos, Sandra Locke, Susanna Talanca, and Ann Pestano. You were always so pleasant and had answers to all of my questions. A special thank you to Teresa Manini for all of your help and for allowing me to be part of the CVR Summer School. I have really enjoyed working with you and getting to know you!

Thank you to all of those who have participated in my experiments over the years. I would never have been able to do this without you. I would also like to thank all of the volunteers and research assistants that have helped me with my research over the years, especially Sarah Zohar. It was a privilege working with you.

I would like to thank the granting agencies that have supported me during my dissertation — the Ontario Graduate Scholarship and the Ontario Graduate Scholarship in Science and Technology. Research funds were also provided from CUPE, The Faculty of Graduate Studies, and the Graduate Student Association.

Thank you to all of my friends who have supported me in many ways. Larissa McKetton, I consider you to be an honorary Steeves' Lab member and a great friend! Joel Dmitruk, David Carey, Marwan Daar, and the rest of my Toronto friends, thank you

for taking me in and showing me how amazing Toronto can be! To my far away friends, Susan Bouzane and Sarah Lloyd, thank you for always being there.

Lastly, I would like to express a heartfelt thank you to my family - Mom, Dad, Mike, Jen and Jase, Terri, Nathan and Ethan (and soon-to-be Paige). You have all supported me in every way possible and for that I am eternally grateful!

TABLE OF CONTENTS

| | |
|------------------------------------------------------------------------------------------------|-----|
| General Abstract | ii |
| Acknowledgements..... | iv |
| Table of Contents | vii |
| List of Tables | ix |
| List of Figures | xi |
| Chapter I:..... | 1 |
| General Introduction..... | 1 |
| Typical Visual Development: Behaviour | 5 |
| Typical Visual Development: Morphology | 11 |
| Atypical Visual Development: Early Monocular Pattern Deprivation | 19 |
| Atypical Visual Development: Early Monocular Enucleation | 21 |
| Limitations of Previous Studies | 34 |
| Purposes and Hypotheses | 36 |
| Chapter II:..... | 40 |
| Impaired speed perception but intact luminance contrast perception in people with one eye..... | 40 |
| Methods..... | 46 |
| Results..... | 50 |
| Discussion | 59 |
| Conclusions | 63 |
| Chapter III:..... | 65 |
| Altered anterior visual system development following early monocular enucleation..... | 65 |
| Methods..... | 71 |
| Results..... | 79 |
| Discussion | 92 |
| Conclusions | 99 |

| | |
|--------------------------------------------------------------------------|-----|
| Chapter IV: | 100 |
| Altered cortical development following early monocular enucleation | 100 |
| Methods | 107 |
| Results..... | 116 |
| Discussion..... | 129 |
| Conclusions | 139 |
| Chapter V: | 140 |
| General Discussion | 140 |
| Summary and Conclusions | 141 |
| Limitations | 148 |
| Future Directions | 152 |
| Concluding Remarks | 156 |
| References | 158 |
| Appendices..... | 213 |
| Appendix A: Glossary of terms..... | 213 |
| Appendix B: Copyright permissions..... | 218 |

LIST OF TABLES

| | |
|--------------------------------------------------------------------------------------------------------------------------------------------------------------------------------------------------------------------------------------------------------------------------------------------------------------------------------------------------------------------------------------------------------------------------------------------------------------------------------------|----|
| Table 2.1. Patient histories for ME participants including age, sex, Snellen acuity, enucleated eye, and age at enucleation (AAE)..... | 47 |
| Table 3.1. ME patient histories. All participants took part in the chiasm phase of the experiment. Participants that took part in the LGN phase are indicated under LGN volume. Age, sex, Snellen acuity, enucleated eye, and age at enucleation (AAE) are also reported..... | 73 |
| Table 3.2 Mean (SD) left and right optic nerve and optic tract diameter, and LGN volume in the control group..... | 81 |
| Table 3.3. Percent (%) decrease of chiasm structures and LGN volume for the early ME group and the late ME participant relative to controls. Percent decrease relative to the average of two age- and sex-matched controls and one age- and sex-matched early ME participant for the chiasm are also shown for the late ME participant for the chiasm structure, and relative to one age- and sex-matched control for LGN volume. [% decrease = (Controls – ME)/Controls × 100]..... | 90 |

Table 3.4. Descriptive statistics for the control and early ME groups showing the mean ($\pm 95\%$ CIs) optic nerve diameter, optic chiasm width in the X and Y planes, optic chiasm volume, optic tract diameter, LGN volume, and whole brain volume. Values for each measurement are also shown for one late ME participant91

Table 4.1. Patient histories for ME participants including age, sex, Snellen acuity, enucleated eye, and age at enucleation (AAE)109

Table 4.2. Descriptive statistics for the control and early ME groups showing the mean (\pm SEM) global estimates for surface area and cortical thickness of the cortical grey matter in the right and left hemisphere117

Table 4.3. Information for clusters flagged as significantly different between groups, including region, cluster size (mm^2), maximum $-\log(10)p$ value, and MNI coordinates120

Table 4.4. Descriptive statistics for the control, early ME_L and early ME_R groups showing group averages (\pm SEM) for surface area (cm^2) and cortical thickness (mm) estimates for V1 and V2 in the right and left hemispheres. Surface area and cortical thickness estimates are also shown for the late ME_L participant, a group of controls and one early ME_L participant age- and sex-matched to the late ME_L participant128

LIST OF FIGURES

Figure 1.1. Schematic of the binocularly intact visual pathway. Visual information from each eye travels through the optic nerve via the temporal (T: green fibres) and nasal (N: purple fibres) retinal ganglion axons and converges at the optic chiasm. Uncrossed temporal fibres project to laminae of the (i) ipsilateral LGN and crossed nasal fibres project to laminae of the (c) contralateral LGN. As a result, the LGN receives information from each eye in separate layers. The magnocellular (m) and parvocellular (p) laminae receive axons from magnocellular and parvocellular ganglion cells of the retina, respectively. Geniculate axons travel via the optic radiations to carry visual information to primary visual cortex (V1), which sends feedback to the LGN for further processing. Figure from Kelly et al. (2014) (adapted from the freely available image from ©John Wiley and Sons, Inc)15

Figure 1.2. Schematic of the monocularly enucleated visual pathway where half of the inputs to subcortical and cortical substrates are removed. Visual information from the remaining eye travels through the optic nerve via the temporal (T: green fibres) and nasal (N: purple fibres) retinal ganglion axons and converges at the optic chiasm. Uncrossed temporal fibres project to laminae of the (i) ipsilateral LGN and crossed nasal fibres project to laminae of the (c) contralateral LGN, which receive information from each eye in separate layers. Geniculate axons travel via the optic radiations to carry visual information to primary visual cortex (V1), which sends feedback to the LGN.

Figure from Kelly et al. (2014) (adapted from the freely available image from ©John Wiley and Sons, Inc)30

Figure 2.1. Speed discrimination Weber fractions ($\Delta X/X$) for BV (filled grey square) and ME (open circle) groups for (A) leftward and (B) rightward motion. In general, the ME group exhibited elevated speed discrimination thresholds compared with the BV group. Error bars represent $\pm 95\%$ confidence intervals (CIs)52

Figure 2.2. Speed discrimination Weber fractions thresholds ($\Delta X/X$) for MV (filled grey triangle) and ME (open circle) groups for (A) nasalward and (B) temporalward motion. The ME group exhibited elevated speed discrimination thresholds compared with ME group for nasalward speeds only. Error bars represent $\pm 95\%$ CIs.....54

Figure 2.3. Contrast detection thresholds (%) for BV (filled grey square), MV (filled grey triangle), and ME (open circle) groups for (A) 0.5 cpd and (B) 4 cpd gratings. The MV and ME groups exhibited elevated luminance contrast detection thresholds compared with the BV group for both 0.5 and 4 cpd gratings. The MV group showed a tendency for elevated luminance contrast detection thresholds at 4 cpd compared with the ME group. Error bars represent $\pm 95\%$ CIs.....55

Figure 2.4. Contrast discrimination Weber fractions thresholds ($\Delta X/X$) for BV (filled grey square), MV (filled grey triangle), and ME (open circle) groups for (A) 0.5 cpd and (B) 4

cpd gratings. No significant differences were found between groups for 0.5 cpd, but the MV group exhibited tendencies for elevated luminance contrast discrimination thresholds compared with the ME group at 4 cpd. Error bars represent $\pm 95\%$ CIs.....57

Figure 3.1. Schematic of the (A) binocularly intact and (B) monocularly enucleated visual pathways. (A) In the intact visual pathway, visual information from each eye travels through the optic nerve via the temporal (T: green) and nasal (N: purple) retinal fibres and converges at the optic chiasm. Uncrossed temporal fibres project to the ipsilateral LGN and crossed nasal fibres project to the contralateral LGN, which receive information from each eye in separate layers. From here, the optic radiations carry information to primary visual cortex (cortical area V1). (B) In the monocularly enucleated visual pathway, the right eye is removed in this diagram and half of the inputs received by the LGN and visual cortex are deafferented. Figure adapted from ©John Wiley and Sons, Inc68

Figure 3.2. An axial image of a reformatted T_1 weighted scan from a control participant displaying optic nerves (a) ipsilateral and (b) contralateral to the dominant eye, optic tracts (c) ipsilateral and (d) contralateral to the dominant eye, and optic chiasm widths in the (x) X and (y) Y planes76

Figure 3.3. Coronal slice of an averaged PD weighted image depicting the LGN (white arrows) of a control participant when the PD images were (A) not interpolated and when

they were (B) interpolated. Left and right ROI tracings of the LGN (white) in the averaged, interpolated PD weighted image are also shown (C)78

Figure 3.4. Bar graphs depicting mean optic chiasm volume (mm^3), and mean optic chiasm width (mm) in the X and Y planes, for the control (blue bars) and early ME (grey bars) groups. The early ME group exhibited significant decreases in all chiasm measures compared with the control group. Error bars represent $\pm 95\%$ confidence intervals (CIs). $**p < 0.01$; $***p < 0.001$ 80

Figure 3.5. The optic nerves, chiasms, and tracts of a (A) typical control and (B) early ME participant are shown in reformatted T_1 weighted images. Bar graphs are also shown depicting the mean diameter (mm) for (C) optic nerves and (D) optic tracts ipsilateral (Ipsi: green bars) and contralateral (Contra: purple bars) to the dominant eye in the control group and remaining eye in the early ME group. The early ME group exhibited significantly decreased diameter for the contralateral optic nerve and both optic tracts compared with the control group. The early ME group also exhibited an asymmetry that was not present in the control group: the contralateral optic tract (purple arrow) was significantly increased compared with the ipsilateral optic tract (green arrow) relative to the remaining eye. Error bars represent $\pm 95\%$ CIs. $***p < 0.001$ 83

Figure 3.6. PD weighted images depicting the LGN ipsilateral (green arrow) and contralateral (purple arrow) to the dominant eye for a (A) typical control and remaining

eye in a (B) typical early ME participant. A bar graph is shown (C) depicting mean LGN volumes (mm³) ipsilateral (Ipsi: green bars) and contralateral (Contra: purple bars) to the dominant eye in the control group and remaining eye in the early ME group.

Compared with the control group, the early ME group exhibited volume decreases in both LGN. The early ME group also exhibited an asymmetry that was not present in the control group: contralateral LGN volume was significantly increased relative to ipsilateral LGN relative to the remaining eye. Error bars represent $\pm 95\%$ CIs. $*p < 0.05$;

$***p < 0.001$ 86

Figure 3.7. A T₁ weighted image showing the (A) optic nerves, chiasm, and tracts, and (B) an averaged PD image showing both LGN from the late ME (right eye enucleated) participant. The chiasm and LGN were decreased in size compared with controls. While the late ME participant showed an increase in contralateral (purple arrow) relative to ipsilateral (green arrow) optic tract diameter, there was no asymmetry between ipsilateral and contralateral LGN volumes89

Figure 4.1. Coronal, transverse, and sagittal views of an extracted brain depicting automatic segmentation of the pial matter (red) and white matter (yellow) borders....112

Figure 4.2. Three-dimensional examples of thresholded V1 (yellow) and V2 (blue) ROIs on the pial and inflated surface of a typical binocularly intact control115

Figure 4.3. Average inflated brain showing regional group differences in the left hemisphere for (A) total surface area between the control and early ME_L groups, and for (B) mean cortical thickness between the early ME_L and early ME_R groups. (A) The early ME_L group exhibited significantly larger total surface area compared with the control group in three clusters located in the inferior supramarginal, superior temporal, and superior parietal regions ($p < 0.05$, FDR corrected). (B) The early ME_L group also exhibited significantly larger mean cortical thickness compared with the early ME_R group in one cluster located in the middle occipital region ($p < 0.05$, FDR corrected).....119

Figure 4.4. Bar graphs depicting group averages for (A) total surface area (cm²) and (B) mean cortical thickness (mm) for right and left V1 and V2 in the control (blue), early ME_L (light grey), and early ME_R (dark grey) groups. In general, the early ME_L group exhibited increases in total surface area and mean cortical thickness compared with controls and the early ME_R group, while the early ME_R group exhibited decreases in mean cortical thickness compared to the control group. Error bars represent \pm SEM. * $p < 0.10$; ** $p < 0.05$; *** $p < 0.01$124

Figure 4.5. Bar graphs depicting (A) total surface area (cm²) and (B) mean cortical thickness (mm) for right and left V1 and V2 for the late ME_L participant (black), an age- and sex-matched control group (green), the early ME_L group (light grey), and one age- and sex-matched early ME_L participant (pink). The late ME_L participant exhibited decreases in total surface area in V2 compared with the early ME_L group, and overall

decreases in mean cortical thickness compared to all groups. Error bars represent \pm

SEM. * $p < 0.10$; ** $p < 0.05$; *** $p < 0.01$127

CHAPTER ONE

GENERAL INTRODUCTION

As humans, we rely on vision more than any other sense to interact with our world. We must gather visual cues from the environment such as the shape, colour, and texture of objects, whether or not they are moving, and in which direction. Information-gathering occurs very quickly and easily, allowing us to make instantaneous decisions regarding our movements and intentions. Visual abilities develop very early in life, but are not fully mature and can be disrupted by visual disorders that occur postnatally (reviewed in Atkinson, 2000 & Daw, 2006). The brain, however, is quite adept at compensating for atypical circumstances, particularly when these circumstances occur early in life during a time when the brain is still developing. A complete loss of vision often results in a sharpening of the remaining senses, such as enhancements in the perception of tactile (e.g., Van Boven, Hamilton, Kauffman, Keenan, & Pascual-Leon, 2000) and auditory (e.g., Gougoux et al., 2004) stimuli. Further, occipital brain regions normally responsible for processing vision in the sighted population have been recruited during auditory (Gougoux, Zatorre, Lassonde, Voss, & Lepore, 2005) and tactile (Ptito Moesgaard, Gjedde, & Kupers, 2005) perception tasks in blind individuals. Enhancements in non-vision modalities and altered brain activity provide evidence of the brain's reorganization abilities in order to compensate for the complete loss of one sensory system. But what happens when only HALF of a sensory system is disrupted, such as in the case of losing one eye?

Throughout history, there have been instances of individuals who have lost one eye, including *Columbo* actor Peter Falk, legendary musician Sammy Davis Jr., and author Frank Brady. In his book, *A Singular View* (2004), Brady discusses his

experience with monocular vision loss and the functional consequences that occur when half of the inputs to the binocular visual system are removed. In brief, these consequences include: 1) A lack of binocular summation, which is an enhancement in detecting or discriminating visual stimuli when viewing with two eyes compared with one (Banton & Levi, 1991; Cagnello, Arditi, & Halpern, 1993; Legge, 1984). Binocular summation may be due to: a) low-level factors such as greater pupil constriction and fixation stability during binocular compared with monocular viewing (e.g., González, Wong, Niechwiej-Szwedo, Tarita-Nistor, & Steinbach, 2012; Thomson, 1947), b) probability summation, which refers to a statistical increase in ability to detect light by a factor of $\sqrt{2}$ when two signal detectors (i.e., two eyes) are present compared to when only one detector is present (Pirenne, 1954), and c) neural summation, which refers to the notion that signals from both eyes are summed when they are received by binocular cells in visual cortex (reviewed in Howard, 2002). When one eye is missing, the binocular advantage for detecting visual information is removed. 2) A narrowing of the horizontal visual field by 20 – 40%. This narrowing occurs because vision is restricted to only one eye, and that eye's visual field is blocked on one side by the nose. This reduction can lead to an increased frequency of bumping into things on the side of the lost eye. 3) A lack of stereoscopic (3D) depth perception. Stereopsis is the process of depth perception induced by using a binocular cue to depth — binocular disparity. Binocular disparity refers to the fact that each eye has a slightly different view of the world; when the brain perceives these two slightly different images, depth is perceived. This phenomenon occurs more strongly in animals with frontally placed eyes, such as monkeys and humans (reviewed in Howard, 2002). A lack of stereopsis due to eye loss

can lead to mobility issues involved in driving, walking, and playing sports. My dissertation investigates the effects of these consequences on the behavioural and morphological development of the visual system.

While functional impairments do occur as a result of losing one eye, they are relatively minor. People with one eye lead quite normal and active lives, and can navigate their world with ease, likely due to compensatory behaviours. For example, to compensate for the loss of stereopsis, people with one eye make more head movements than those with two eyes. These head movements create a monocular depth cue called motion parallax (Marotta, Perrot, Nicolle, Servos, & Goodale, 1995). To compensate for the visual field reduction, people with one eye turn their head to align the remaining eye to the centre of their body (Goltz, Steinbach, & Gallie, 1997). These individuals also exhibit a decrease in visual dominance during an audiovisual task, suggesting that they rely more on their sense of hearing (Moro & Steeves, 2012).

For my dissertation, I explored the developmental consequences of complete monocular deprivation in adults who had one eye enucleated (surgically removed) early in life due to retinoblastoma (cancer of the retina). Studying the consequences of early monocular enucleation not only provides information about how the visual system is affected during development, but also informs on the binocular mechanisms required for typical visual maturation. While there are many developmental consequences to assess with this form of deprivation, I focus my research on two areas: behavioural changes in visual abilities, and structural within the visual pathway of the brain.

The following introductory sections provide a comprehensive review of the literature pertinent to understanding my research. I begin by describing the typical

development of behavioural visual abilities, including spatial form vision and motion perception. I then explain the morphological configuration of the adult visual pathway and how it typically develops. Following this, I present data showing the consequences of early monocular deprivation of pattern information on behavioural and morphological visual development. Subsequently, I describe the advantages of studying early monocular enucleation over early monocular pattern deprivation. From here, I discuss the epidemiology and proper treatment of retinoblastoma. Next, I describe research showing the behavioural development of spatial form vision and motion perception following early monocular enucleation. I then explain previous research investigating the morphological development of the visual pathway in enucleated non-primates, non-human primates, and humans. Lastly, I point out the limitations of previous research and briefly outline the specific purposes and hypotheses for each of the experimental chapters that follow.

Typical Visual Development: Behaviour

Before discussing the effects of early eye enucleation on the development of behavioural visual abilities, it is important to first discuss how and when these abilities first emerge in the typical developing infant. Although infants are able to “see” at birth, visual function is quite immature and requires experience in order to refine its many aspects. In general, some functions mature faster than others and there exist multiple

critical periods¹ during which these functions emerge and can be altered. One example is the emergence of stereopsis, which occurs between 4 – 6 months of age (Birch, Shimofo, & Held, 1985; Fox, Asin, Shea, & Dumais, 1980; Takai, Sato, Tan, & Hirai, 2005), yet has different developmental time courses for more specific forms of stereopsis. For example, coarse stereopsis matures around 4 years of age, while fine stereopsis does not mature until adolescence (Giaschi, Narasimhan, Solski, Harrison, & Wilcox, 2013). Coarse stereopsis refers to depth perception that is achieved with very large disparities that are not able to be fused into one image, whereas fine stereopsis refers to the perception of depth that is achieved with smaller disparities that are able to be fused into one image (Giaschi et al., 2013). Similarly, face perception emerges very early in life and continues to develop until early adolescence. For example, newborns can recognize their mother's face (Bushnell, 2001) and discriminate novel faces (Turati, Macchi Cassia, Simion, & Leo, 2006) but cannot recognize faces based on feature-spacing, an ability that is not mature until adolescence (e.g., Baudoin, Gallay, Durand, & Robichon, 2010). For the purpose of this dissertation, the development of two broad aspects of vision – spatial form vision and motion perception – will be discussed in relation to typical and atypical development.

¹ A critical period is the postnatal period during which rapid development of a function occurs and during which that function is most vulnerable to abnormal experience. There are three types of critical periods relative to a function: 1) *critical period of development* where environmental experience can have a great impact on a function during a time when that function is rapidly developing, 2) *critical period for disruption* where atypical postnatal experience can have adverse effects on development of a function, and 3) *critical period for recovery* where a function can be recovered after it has been disrupted. Critical periods for different functions can emerge at different times and have varying time courses (reviewed in Daw, 2006).

Spatial form vision. Spatial form vision refers to the ability to resolve the spatial features of objects and of our environment. Basic, low-level spatial visual abilities include, but are not limited to, acuity (the ability to resolve fine detail) and contrast sensitivity (the level of contrast required to resolve fine detail at various spatial frequencies²). Brain regions implicated in low-level spatial form vision include visual areas V1 and V2 (Anzai, Peng, & Van Essen, 2007; Hubel & Livingstone, 1990; Tootell, Hamilton, & Switkes, 1988). In contrast, mid- to high-level spatial form vision tasks include detecting and recognizing forms, such as letters, faces, and objects. These stimuli bring together many aspects of low-level spatial form vision, such as contrast and spatial frequency, and are processed in cortices beyond V1 (e.g., fusiform gyrus, lateral occipital complex, V4) (e.g., Grill-Spector, Kourtzi, & Kanwisher, 2001; Kanwisher, McDermott, & Chun, 1997; Wilkinson et al., 2000). (The development of spatial form vision has extensively been reviewed in: Atkinson, 2000; Daw, 2006; Teller, 1997).

Binocular summation, the advantage of viewing with two eyes compared with one, does not occur in infants until the onset of stereopsis between 4 – 6 months of age. Once stereopsis emerges, binocular acuity is already superior to monocular acuity (Birch, 1985; Birch & Swanson, 1992). Grating acuity, the highest resolvable spatial frequency, is quite immature at birth as newborns are most sensitive to spatial frequencies between 1 – 3 cycles per degree (cpd) (~ 20/200). Acuity improves rapidly during the first six months of life where sensitivity increases to approximately 10 cpd (~20/60), then it develops slowly until adult sensitivity levels are reached at 40 cpd between 4 – 6 years of age (Ellemberg, Lewis, Liu, & Maurer, 1999; Mayer & Dobson,

² The number of light/dark cycles per degree (cpd) of visual angle.

1982). In contrast, Snellen acuity, which is measured using letters in a line, is not adult-like until 10 years of age (Hohmann & Haase, 1982). Vernier acuity is the smallest misalignment between two lines that can be detected. This form of acuity is poorer at birth compared with grating acuity and reaches adult levels later at approximately 5 – 8 years of age (Drover, Morale, Wang, Stager, & Birch, 2010; Skoczenski & Norcia, 1999; Zanker, Mohn, Weber, Zeitler-Driess, & Fahle, 1992). However, vernier acuity is superior to grating acuity when adult levels are reached (Zanker et al., 1992). This is because vernier acuity is a form of hyperacuity, which means that we are able to resolve visual information to a level that is finer than the spacing of cones in the retina allows (Westheimer, 1975). Hyperacuity is thought to reflect processing beyond the retina at the level of the cortex, and is limited by the development of cortical visual regions (Skoczenski & Norcia, 1999).

Contrast sensitivity is also poor at birth and improves rapidly during the first 12 weeks of age (Atkinson, Braddick & Moar, 1977; Norcia, Tyler, & Hamer, 1990). Contrast sensitivity continues to develop at different rates for different spatial frequencies. By 2 – 3 months of age, the inverted U-shape of the contrast sensitivity function is similar to that of adults; however, infants are more sensitive to lower contrasts at lower spatial frequencies compared with higher contrasts and higher spatial frequencies (Adams & Courage, 1993 & 2002; Atkinson, Braddick, & Braddick, 1974; Banks & Salapatek, 1978; Norcia et al., 1990). Although at birth sensitivity is best for lower spatial frequencies, sensitivity to higher spatial frequencies matures more rapidly, with high spatial frequencies reaching adult levels before those for low spatial frequencies (Adams & Courage, 1993 & 2002). By 7 – 9 years of age, contrast

sensitivity at all spatial frequencies has reached adult levels (Adams & Courage, 2002; Bradley & Freeman, 1982; Ellemberg, et al., 1999).

Motion perception. While spatial form vision incorporates static aspects of objects, motion perception incorporates temporal aspects, such as discerning the direction and speed of moving objects in our environment, or the movement of information across the retina as we make eye movements or move in the environment. This is an important visual ability that has real-world applications such as driving, crossing the road, and participating in sports. The perception of visual motion is processed by extrastriate cortices, including V3/V3a, V5/middle temporal (MT), and medial superior temporal (MST). The MT/MST complex is often referred to as MT+ (McKeefry, Burton, Vakrou, Barrett, & Morland, 2008; Tootell et al., 1995).

Similar to spatial form vision, motion perception is present but relatively crude at birth. Optokinetic nystagmus, a reflexive, involuntary eye movement in response to motion, is elicited at birth by full-field, high-contrast, low spatial frequency gratings (Kremenitzer, Vaughan, Kurtzberg, & Dowling, 1979). Further, 1 – month olds prefer to view moving rather than static stimuli (Volkman & Dobson, 1976) and can detect flicker rates at about 75% of adult levels at 40 Hz (Regal, 1981). However, some aspects of motion perception, such as direction and speed discrimination, are quite poor early in life compared with adults. For example, sensitivity to fast speeds [6 – 9 degrees per second (deg/s)] matures earlier than that to slow speeds (e.g., 1.5 deg/s) (Ahmed, Lewis, Ellemberg, & Maurer, 2005; Aslin & Shea, 1990; Ellemberg et al., 2003, 2004; Manning, Aagten-Murphy, & Pellicano, 2012). Similarly, first-order (luminance-defined) motion is

initially more mature than second-order (texture- or contrast-defined) motion, but second-order motion reaches adult levels first (Bertone, Hanck, Cornish, & Faubert, 2006; Ellemborg, et al., 2003, 2004). Directional sensitivity for global motion (e.g., coherent motion) does not emerge until 6 – 8 weeks of age (Banton, Dobkins, Berenthal, 2001; Banton, Berenthal, & Seaks, 1999; Wattam-Bell, 1994, 1996).

However, the literature is inconsistent regarding the age of maturation for this ability, with studies showing adult levels being achieved between 3 years of age and adolescence (Ellemborg, Lewis, Maurer, Brar, & Brent, 2002; Hadad, Maurer, & Lewis, 2011; Parrish, Giaschi, Boden, & Dougherty, 2005).

In addition to immature motion perception, a directional asymmetry in the form of a temporalward to nasalward preference is found in infants, but not adults, during monocular viewing. An asymmetrical optokinetic nystagmus response emerges around 2 months of age and substantially reduces to almost symmetrical levels between 6 months to 2 years of age, depending on the study (Lewis, Maurer, Chung, Holmes-Shannon, & Van Schaik, 2000; Naegele & Held, 1982; Roy, Lachapelle, & Lepore, 1989; Valmaggia et al., 2004; Wattam-Bell, 2003). An asymmetry has also been found for electrophysiological measures of motion perception, specifically motion visual evoked potentials (mVEPs), indicating the presence of a nasalward bias at 3 months of age that becomes symmetrical between 6 – 8 months of age (Birch, Fawcett, & Stager, 2000; Bosworth & Birch, 2007; Norcia et al., 1991). Further, asymmetries have been observed for behavioural measures such as preferential looking and habituation tasks. These studies show that a nasalward bias emerges between 6 – 12 weeks and disappears at around 8 months of age (Bosworth & Birch, 2005, 2007; Wattam-Bell, 2003). Separate

neural pathways have been posited to account for directional asymmetries found for optokinetic nystagmus, and for mVEPs and other motion perception tasks.

Optokinetic nystagmus is mediated by subcortical mechanisms [i.e., nucleus of the optic tract (NOT), dorsal terminal nucleus (DTN)], that mature earlier than cortical mechanisms (e.g., V3/MT+) associated with mVEPs and motion perception tasks, such as direction discrimination for coherent motion (Distler & Hoffmann, 2011; Mason, Braddick, & Wattam-Bell, 2003; Wattam-Bell, 2003).

The nasalward bias in optokinetic nystagmus likely reflects cortical immaturity of the eye movement system. Cells within the direct subcortical pathway from the retina to contralateral NOT-DNT, even when mature, are responsive to ipsiversive motion (left NOT-DNT prefers leftward motion, right NOT-DNT prefers rightward motion) (Distler & Hoffmann, 2011; Hoffmann, 1986). The emergence of symmetrical optokinetic nystagmus may reflect maturation of binocular inputs to NOT-DNT from cortical visual regions such as primary visual cortex and MT+ (Braddick, Atkinson, & Wattam-Bell, 2003; Hoffmann, Bremmer, Thiele, & Distler, 2002). The nasotemporal asymmetry present in the subcortical pathway is then masked by the cortical pathway. The cortical asymmetry found for mVEPs and other motion perception tasks has been suggested to reflect immaturities in directional tuning in early visual cortex and MT+ (Braddick, 1996).

Typical Visual Development: Morphology

Adult visual pathway. Visual information in the adult primate visual system travels along the retinogeniculocortical pathway (see Figure 1.1). After reaching the

retina, visual input exits each eye via retinal ganglion cell (RGC) axons that form the optic nerve and converges at the optic chiasm. Approximately half of these axons project ipsilaterally (uncrossed temporal retinal fibres) while the other half project contralaterally (crossed nasal retinal fibres) via the optic tracts (Fukuda, Sawai, Watanabe, Wakakuwa, & Morigiwa, 1989; Kupfer, Chumbley, & Downer, 1967). Consequently, each optic tract consists of RGC axons from the nasal hemiretina of the contralateral eye and the temporal hemiretina of the ipsilateral eye. While a small percentage (~10%) of optic tract axons project to subcortical structures including the superior colliculus (involved in the control of eye movements and multisensory integration), pretectum (involved in regulating pupillary light reflexes), and hypothalamus (involved in regulating circadian rhythms), the majority of these fibres (~90%) terminate in the lateral geniculate nucleus (LGN) which is located in the thalamus (Perry & Cowey, 1984; Perry, Oehler, & Cowey, 1984; Wallace, Wilkinson, & Stein, 1996).

The thalamus is a subcortical sensory relay station with nuclei that process all sensory modalities except olfaction (Gottfried & Zald, 2005). These nuclei send sensory information to subcortical and cortical regions for further processing. For example, the medial geniculate nucleus relays auditory information to primary auditory cortex (Pandya, Rosene, & Doolittle, 1994), and the ventral posterior nucleus relays touch and proprioception information to primary somatosensory cortex (Vázquez, Salinas, & Romo, 2013). Each of these relays also receives feedback from the cortical regions to which they project. In Chapter III of my dissertation, I focused on the development of the LGN, which is the visual relay station. The LGN receives information from each eye in six separate, eye-specific laminae. Ipsilateral eye connections project to layers 2, 3, and 5

while contralateral connections project to layers 1, 4, and 6 (reviewed in Howard, 2002). Midget³ RGCs respond preferentially to colour and project to parvocellular (P) cells within the four dorsal geniculate laminae (layers 3 – 6). Geniculate P cells have small receptive fields and thus have high spatial (peak sensitivity = 40 cpd gratings) but poor temporal (peak sensitivity = 10 Hz) resolution. In contrast, parasol⁴ RGCs respond preferentially to motion and achromatic stimuli and project to magnocellular (M) cells within the two ventral geniculate layers. Geniculate M cells have large receptive fields and thus have high temporal (peak sensitivity = 20 Hz) but poor spatial (peak sensitivity = 10 cpd gratings) resolution (Derrington & Lennie, 1984; Kaplan & Shapley, 1982; Schiller, Logothetis, & Charles, 1990).

LGN afferents project via the optic radiations to layer IVc of ipsilateral primary visual cortex (V1, striate cortex), which is located in the calcarine sulcus of the occipital lobe. V1 contains six functionally distinct layers and each hemisphere processes input from the contralateral hemifield (reviewed in Howard, 2002). While cells within V1 are innervated by both eyes, the majority of these cells respond predominantly to input from one eye or the other eye. This preference is called ocular dominance, and cells with the same preference are grouped into ocular dominance columns (Hubel & Wiesel, 1969; Horton, Dagi, McCrane, & de Monasterio, 1990; LeVay, Hubel, & Wiesel, 1975). The M and P segregation in the LGN also persists in layer IVc, with sublayers IVc α and IVc β innervated by their respective M and P geniculate afferents (Hubel & Wiesel, 1977).

³ Not to be confused with magnocellular (M) cells of the LGN, which are innervated by *parasol* retinal ganglion cells.

⁴ Not to be confused with parvocellular (P) cells of the LGN, which are innervated by *midget* retinal ganglion cells.

Response properties of these cells reflect those found within the LGN (Blasdel & Fitzpatrick, 1984). Once processed, information from V1 is sent to areas beyond V1, such as V2 and MT+ (Ho & Giaschi, 2009; Hubel & Livingstone, 1987; McKeefry et al., 2008; Tootell et al., 1995). Feedback connections are also sent from V1 to the LGN, and from extrastriate areas back to V1 (Beatty, Sadun, Smith, Vonsattel, & Richardson, 1982; Wunderlich, Schneider, & Kastner, 2005; reviewed in Hubel & Wiesel, 1977 and Howard, 2002).

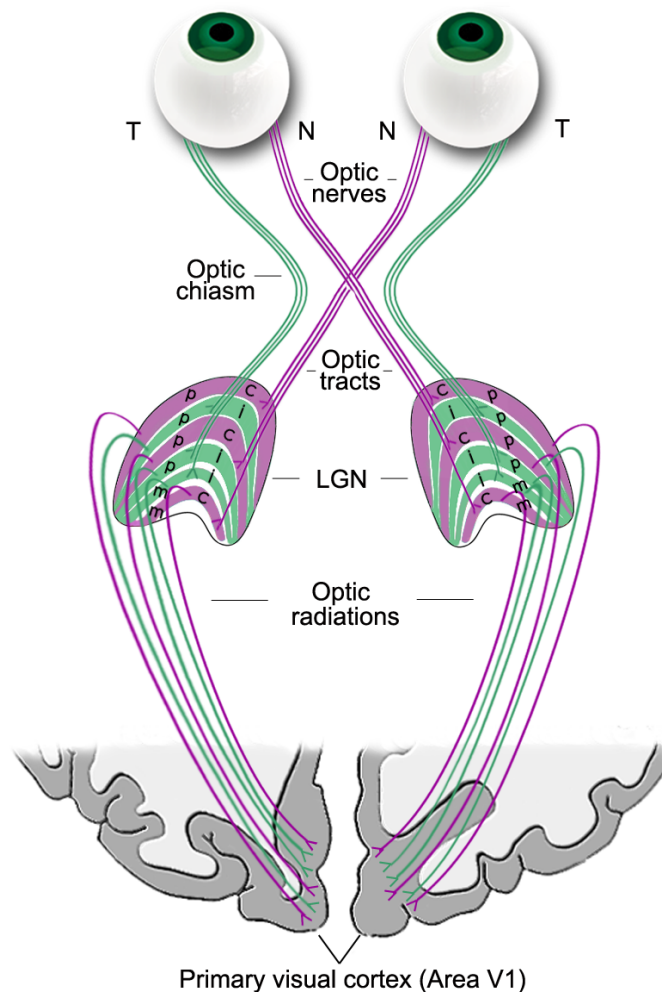


Figure 1.1. Schematic of the binocularly intact visual pathway. Visual information from each eye travels through the optic nerve via the temporal (T: green fibres) and nasal (N: purple fibres) retinal ganglion axons and converges at the optic chiasm. Uncrossed temporal fibres project to laminae of the (i) ipsilateral LGN and crossed nasal fibres project to laminae of the (c) contralateral LGN. As a result, the LGN receives information from each eye in separate layers. The magnocellular (m) and parvocellular (p) laminae receive axons from magnocellular and parvocellular ganglion cells of the retina, respectively. Geniculate axons travel via the optic radiations to carry visual information

to primary visual cortex (V1), which sends feedback to the LGN for further processing.

Figure from Kelly et al. (2014) (adapted from the freely available image from

©John Wiley and Sons, Inc).

Developing visual pathway. Behavioural improvements in spatial form vision and motion perception during typical visual development likely reflect morphological and physiological changes occurring not only in the retina but also in visual regions of the brain (Banks & Bennett, 1988; reviewed in Daw, 2006). Maturation of all aspects of the visual system depend on some level on other developing aspects of the system. Further, subcortical regions of the visual system tend to develop at earlier stages compared with cortical regions. For example, retinogeniculate afferents are formed prior to those reaching visual cortex (Khan, Wadhwa, & Bulani, 1994). Renowned Canadian neuroscientist, Donald Hebb (Hebb, 1949), first described the functional process by which synapses form in the brain. He explained that neurons form new connections and are strengthened by the degree of correlated sensory information, such as visual input, received by the cells. Those connections and cells that do not receive strong visual input will eventually atrophy.

Maturation of the visual system occurs in two stages: 1) prenatal period prior to visual experience during which genetic factors control development, and 2) postnatal period during which visual experience is necessary for development and refinement of the visual system. Experience-dependent plasticity, the brain's ability to change based on environmental circumstances, occurs in the second stage. Postnatal development of the visual system relies heavily on environmental stimulation and binocular interactions,

including competition and cooperation (Horton & Hocking, 1998a; Rakic, 1976; Sloper, 1993), a point that will become evident during discussion of the typical and atypical development of this system.

RGC axons segregate into the adult pattern of contralateral and ipsilateral projections gradually *in utero*. Further, the laminar organization of the primate LGN and generation of geniculate cells are both complete before birth (Rakic, 1976, 1977). Because vision is not yet possible at this point, these processes depend heavily on spontaneous electrical activity in the retina (Shatz & Stryker, 1988). Although, the LGN is quite developed at birth, immaturities are present. For example, LGN synaptic connections are visible *in utero*, but cell and synapse sizes are small, and dendritic spine numbers are larger than adults in both monkeys and humans (Brauer, Leuba, Garey, & Winkelman, 1985; Garey & de Courten, 1983; Hickey, 1977; Khan et al., 1994). The number of spines reaches its maximum at birth in monkeys and by 4 months of age in humans. Once the maximum is reached, a pruning period begins where dendritic numbers decrease to reach adult levels by 3 and 9 months of age in monkeys and humans, respectively (Garey & de Courten, 1983; Huttenlocher, de Courten, Garey, & Van der Loos, 1982). The size of cells in the LGN rapidly increases between 6 and 12 months of age in humans, with P cells developing earlier (~12 months) than M cells (~24 months) (Brauer et al., 1985; Hickey, 1977). A similar pattern is also found in monkeys (Boothe, Greenough, Lund, & Wrege, 1979; Headon, Sloper, Hiorns, & Powell, 1981). In general, the human LGN is morphologically mature by 9 months of age; however, it continues to develop physiologically (de Courten & Garey, 1982; Blakemore & Vital-Durand, 1986; Garey & de Courten, 1983). The maintenance of geniculate cells during

development relies heavily on Hebbian activity-driven competition and cooperation between the two eyes (Sloper, Headon, & Powell, 1987a; Sloper, 1993).

In visual cortex, the volume of V1 increases four-fold between birth and 4 months of age to reach adult size (Garey & de Courten, 1983; Huttenlocher & De Courten, 1987). Yet, V1 is still quite immature early in life and continues to develop into adolescence. For instance, synaptic density increases slowly during the first 1 – 2 months of age, and then rapidly reaches its maximum between 6 – 9 months of age (Garey & de Courten, 1983). Following this period of synaptogenesis, a period of pruning occurs characterized by a progressive loss of synapses so that by age 11, adult levels are reached. The adult level of synaptic density in the brain is only about half of the maximum synaptic density present during infancy (Huttenlocher, 1990; Huttenlocher et al., 1982, Garey & De Courten, 1983). Pruning may serve to fine-tune the visual system and create more efficient connections for processing visual information.

Unlike layers of the LGN, ocular dominance columns in V1 are only partially segregated at birth in primates, and neurons initially respond equally to both eyes (Rakic, 1976, 1977; LeVay et al., 1980; Sloper, 1993). Columnar segregation occurs rapidly following birth and completes postnatally around 6 weeks for monkeys (LeVay et al., 1980), and 6 months for humans (Hickey & Peduzzi, 1987). Similar to geniculate development, this process relies heavily on binocular competition between the eyes for space within visual cortex (Horton & Hocking, 1998b; reviewed in Howard, 2002; Katz & Crowley, 2002). In humans, columnar segregation occurs when stereopsis first emerges (Hickey & Peduzzi, 1987), suggesting that binocular competition occurs between 4 – 6

months of age, and that this process is necessary for developing ocular dominance columns.

Atypical Visual Development: Early Monocular Pattern Deprivation

Given the immaturity of the postnatal visual system, it stands to reason that abnormal visual experience can disrupt its development. Early monocular deprivation of pattern information from disorders such as strabismus (misaligned visual axes), congenital cataract (cloudy lens), or anisometropia (unequal refractive error in the two eyes) leads to an imbalance of visual inputs to the brain. These visual disorders frequently lead to amblyopia, which is a permanent reduction of visual function in the deprived eye due to the disruption of visual development early in life (reviewed in Barret, Bradley, & McGraw, 2004). Because of an imbalance of visual input found in amblyopia, the non-deprived eye suppresses the deprived eye (Baker & Meese, 2007). An imbalance of visual input during the critical periods for development and disruption of visual abilities can lead to behavioural deficits in both spatial form vision and motion perception that persist throughout life in the deprived and non-deprived eye, even after treatment (Ellemberg et al., 2002, 2005; Ellemberg, Lewis, Maurer, & Brent, 2000; Hess & Howell, 1977; Hess, Wang, Demanins, Wilkinson, & Wilson, 1999; Ho et al., 2005; Lewis, Maurer, Tytla, Bowering, & Brent, 1992; Reed, Steeves, Steinbach, Kraft, & Gallie, 1996; Simmers, Ledgeway, Hess, & McGraw, 2003; Woo & Irving, 1991). These deficits will be described briefly below.

Spatial form vision. Forms of monocular deprivation such as strabismus, cataracts, and anisometropia result in small contrast sensitivity losses for high spatial frequencies, grating acuity, and vernier acuity (Ellemberg et al., 2000; Lewis et al., 1992; McKee, Levi, & Movshon, 2003). Further impairments are observed in the perception of global form in Glass (1969) patterns, contrast letter recognition, and global shape discrimination (Lewis et al., 2002; Hess et al., 1999; Reed et al., 1996).

Motion perception. Deficits are observed for global direction of motion (Ellemberg et al., 2002, Ho et al, 2005; Simmers et al., 2003) and motion-defined form (Ho et al., 2005). These deficits also translate into reduced activation in areas known to process vision such as primary visual cortex (Barnes et al. 2001; Goodyear, Nicolle, Humphrey, & Menon 2000) and MT+ (Ho & Giaschi, 2009).

Visual pathway morphology. Monocular deprivation of patterned information not only produces behavioural deficits, but morphological and physiological changes also occur in the visual pathway of both animals and humans. Seminal research by David Hubel and Torsten Wiesel provided the first evidence for permanent changes in the architecture of the brain following restricted visual input during postnatal development. They showed that eyelid suture in kittens produced atrophy of geniculate cells, and a shift in ocular dominance columns in favour of the non-deprived eye (Wiesel & Hubel, 1963a,b; Wiesel & Hubel, 1965). However, monocular deprivation in adult cats did not alter ocular dominance columns, which suggests a critical period of development of the visual system (Wiesel & Hubel, 1965). The implications of these findings have since led

to an abundance of research examining the effects of various forms of visual deprivation on many different species. For example, eyelid suture in infant monkeys also produces reductions in geniculate laminae size corresponding to the deprived eye, as well as a shift in ocular dominance in favour of the non-deprived eye (Blakemore, Garey, & Vital-Durand, 1978; Hubel, Wiesel, & LeVay, 1977; LeVay et al., 1980).

In humans, strabismic amblyopia is associated with decreased grey matter concentration in the LGN and atrophy of LGN layers (Barnes et al., 2010). A case study of an adult who experienced eye trauma at an early age resulting in a corneal opacity showed shrunken ocular dominance columns associated with the damaged eye (Adams, Sincich, & Horton, 2007). Further, children and adults with strabismic and anisometropic amblyopia exhibit grey matter volume reductions in visual cortices (Mendola et al., 2005; Xiao et al., 2007). These findings suggest altered morphological visual system development following early monocular deprivation that leads to an uneven stream of visual inputs, and consequently uneven binocular interactions in the brain. But how does the visual system develop in response to a complete lack of binocular, rather than uneven, interactions?

Atypical Visual Development: Early Monocular Enucleation

Why study monocular enucleation? Early monocular pattern deprivation results in uneven visual input, and thus uneven binocular interactions. Weak input from the deprived eye to binocular cells in visual cortex may indirectly affect the non-deprived eye, a notion supported by low-level spatial form vision deficits found in the non-deprived eye in individuals with amblyopia (e.g., Woo & Irving, 1991). These deficits may

indicate a general vulnerability of a compromised visual system, and may be compounded by treatments, such as patching, which acts as monocular deprivation for the non-deprived eye. Further, motion stimuli inherently possess spatial attributes such as luminance contrast and spatial frequency. Those with early monocular pattern deprivation are impaired on tasks that assess these spatial attributes. Thus, it is unclear which aspect of vision actually underlies the motion perception impairments found with these disorders. Examining a monocularly deprived population with motion perception impairments but intact spatial form vision is ideal to help tease apart the effects of early monocular deprivation on the development of these two systems. One such population does exist – those who have had one eye enucleated early in life due to retinoblastoma.

Monocular enucleation is inherently different from other forms of monocular pattern deprivation because the eye is completely removed, resulting in only one stream of information to the visual system and a lack of competitive binocular interactions. In contrast to other forms of monocular deprivation, enucleation is associated with equivalent or enhanced spatial form vision compared to controls (reviewed in Kelly, Moro, & Steeves, 2013a; Steeves, González, & Steinbach, 2008). To assess the effects of monocular deprivation on maturation of the visual system, it is advantageous to examine those who have experienced early monocular enucleation since no anomalous visual input is being projected to the visual system from the removed or remaining eye.

Retinoblastoma. Most research examining early monocular enucleation in humans has tested a rare group of individuals whose eye was removed early in life due to retinoblastoma. Retinoblastoma is a rare malignant tumor of the retina that generally occurs before 5 years of age and accounts for approximately 6% of all childhood cancers (Broaddus, Topham, & Singh, 2009a). Roughly 60% of these cases present as unilateral retinoblastoma with no family history of the disease. The mean age of diagnosis for unilateral retinoblastoma is 24 months and the most frequent and effective treatment is enucleation of the cancerous eye (Lohmann & Gallie, 2013). With a high survival rate (Broaddus, Topham, & Singh, 2009b) and the lack of binocular visual input associated with retinoblastoma, it is imperative to investigate the consequences of the most effective treatment, enucleation, on the developing visual system. My dissertation describes in detail behavioural and morphological effects on the developing visual system following early monocular enucleation due to unilateral retinoblastoma.

Spatial form vision. The development of various spatial visual abilities has previously been investigated in adults who had one eye enucleated early in life due to retinoblastoma (see Kelly et al., 2013a and Steeves et al., 2008 for reviews). In general, monocular enucleation leaves low-level visual spatial perception intact and in some cases, enhances this ability relative to binocular controls. Early monocular enucleation results in superior performance compared with controls viewing monocularly with a patch over their non-dominant eye on a hyperacuity task, alignment acuity, which measures the accuracy of aligning a dot to a horizontally- or obliquely-oriented bar (Reed, Steinbach, Ono, Kraft, & Gallie, 1995). Contrast sensitivity is also enhanced at 2,

4, and 8 cpd relative to monocular viewing controls (Nicholas, Heywood, & Cowey, 1996). In addition, a developmental relationship exists wherein earlier eye enucleation (< 4 years of age) results in superior contrast sensitivity at 2 and 4 cpd compared with later enucleation (> 4 years of age), and superior contrast sensitivity at 4 cpd compared with binocular viewing controls (Nicholas et al., 1996). These data indicate different critical developmental periods for neural mechanisms sensitive to different spatial frequencies. Unlike contrast sensitivity, no developmental relationship exists for alignment acuity, suggesting differential effects of enucleation on various spatial visual abilities that have different developmental critical periods and perhaps different underlying cortical mechanisms.

Mid-level aspects of spatial form vision have also been assessed following early monocular enucleation. For example, this form of deprivation leads to intact texture-defined letter detection and recognition (Steeves, González, Gallie, & Steinbach, 2002), as well as intact foveal acuity for illiterate 'E' optotypes compared to binocular viewing controls. Early monocular enucleation is also associated with superior foveal acuity at 96%, 13.5% and 4.7% contrasts and superior peripheral acuity at 13.5% and 4.7% contrasts relative to monocular viewing controls (González, Steeves, Kraft, Gallie, & Steinbach, 2002). A similar pattern has also been demonstrated for low-contrast letter acuity (Reed et al., 1996; Reed, Steeves, & Steinbach, 1997). In addition, acuity in the fellow eye of individuals with strabismus is much worse than that of the remaining eye of enucleated participants (Reed et al., 1996), suggesting that completely deafferenting the affected eye is less detrimental to visual development of spatial form vision in the

remaining eye than receiving unbalanced binocular visual input from misaligned visual axes where one stream of information is anomalous.

More complex, higher-level aspects of spatial form vision have also been measured following early monocular enucleation that include object and face perception. Similar to lower-level aspects of vision, this form of deprivation results in enhanced low-contrast global shape discrimination compared with monocular viewing controls (Steeves, Wilkinson, González, Wilson, & Steinbach, 2004). However, not all aspects of spatial form vision remain intact; mild impairments have been found for face perception compared with binocular and monocular viewing controls (Kelly, Gallie, & Steeves, 2012). More specifically, enucleation results in equal accuracy but significantly slower response latencies compared with controls for face discrimination. Nonetheless, these deficits do not translate to the perception of another class of objects – houses that were manipulated in a similar manner to that of the face stimuli. These findings suggest that mild impairments are unique to face perception. Similar deficits are present with monocular deprivation from congenital cataract (Le Grand, Mondloch, Maurer, & Brent, 2003, 2004) and indicate that atypical visual input of any manner during maturation negatively affects the development of the highly specialized ability of face perception. At present, face perception in terms of accurate but slower processing is the only spatial form vision deficit found in early monocular enucleation participants. Thus, it appears that spatial form vision remains relatively intact in this group.

Motion perception. Despite the relatively large body of research conducted on spatial visual abilities following early monocular enucleation, research on motion

perception in this group is sparse. Early enucleation results in mild motion perception deficits compared with controls for the recognition of letters defined by the relative motion of dots inside and outside the letter boundary (i.e., motion-defined letters) (Steeves et al., 2002). Further, this group is impaired in perceiving motion-in-depth; enucleation participants overestimate whereas binocular controls tend to underestimate the time-to-collision of an approaching object (Steeves, Gray, Steinbach, & Regan, 2000). However, not all aspects of motion are disrupted following early enucleation. For example, this form of deprivation results in comparable thresholds to controls for relative velocity detection using texture-defined shearing stimuli (Bowns, Kirshner, & Steinbach, 1994). Further, while enucleation leads to impaired motion-defined letter *recognition*, motion-defined letter *detection* and discrimination of the direction of coherent horizontal motion are intact relative to controls (Steeves et al., 2002).

Although some aspects of motion perception remain intact, response asymmetries have been reported in individuals with early monocular enucleation. For example, this group favours lower over upper hemifield motion for relative velocity discrimination of shearing stimuli (Bowns et al., 1994), and nasalward over temporalward motion for coherent motion discrimination (Steeves et al., 2002). A nasalward bias is also observed for optokinetic nystagmus while viewing full-field motion (Day, 1995; Reed et al., 1991). The optokinetic nystagmus asymmetry may reflect a disruption in earlier maturing regions that mediate eye movement responses, such as NOT, whereas motion processing asymmetries may reflect a disruption in the development of higher cortical regions associated with motion perception, such as MT+ (Distler & Hoffmann, 2011; Mason et al., 2003; Wattam-Bell, 2003). This notion is

consistent with nasalward biases reported in the immature visual system (Lewis et al., 2000), and an earlier critical period for nasalward motion perception (Braddick, et al., 2003; Wattam-Bell, 2003).

Dissociation in visual ability. It is clear that a dissociation in visual ability occurs following early monocular enucleation such that spatial form vision remains intact but motion perception is mildly impaired. A dissociation suggests differential effects of enucleation during the critical periods of development of these two systems, and that an intact binocular visual system is required for typical maturation of motion perception. In addition, this dissociation indicates a greater postnatal vulnerability of cortical areas that process motion, likely V3 and MT+. To further support this notion, motion perception impairments have been reported for other developmental disorders such as Williams syndrome and autism (Atkinson et al., 1997; Koldewyn, Whitney, & Rivera, 2010). Most cells in MT+ are binocular and cannot be driven by one eye. Further, these binocular cells are tuned to disparity (Maunsell & Van Essen, 1983; Roy, Komatsu, & Wurtz, 1992). Therefore, a common physiological mechanism that links binocularity and motion perception may account for motion perception deficits in the enucleated population.

Visual pathway morphology. A moderate body of research exists on the behavioural visual abilities following long-term survival from monocular enucleation in humans, yet few studies have investigated the morphological consequences of this form

of deprivation on visual pathway development. Below, I will discuss morphological changes in the visual system of various species following monocular enucleation.

Non-primate species. Morphological changes are well established in non-primate mammalian models of early monocular enucleation. Briefly, an increase in crossed fibres of the remaining eye at the expense of uncrossed fibres is found in enucleated mice, ferrets, and rabbits (Godement, Salaun, & Metin, 1987; Grigonis, Pearson, & Murphy, 1986; Guillery, 1989). The region of LGN that receives projections from the ipsilateral, remaining eye is decreased in volume by about 50% while the region that receives contralateral projections remains intact in early-enucleated rabbits (Grigonis et al., 1986). Further, contralateral retinal projections from the remaining eye terminate in deafferented regions of the LGN, indicating reorganization as a result of the enucleation (Grigonis et al., 1986). Early monocular enucleation in mice affects neuron density and metabolic activity less in visual cortex contralateral compared with ipsilateral to the remaining eye (Chow et al., 2011; Heumann & Rabinowicz, 1982). Enucleation in mice also expands and accelerates the refinement of retinotopic area V1 of the remaining eye during development (Faguet, Maranhao, Smith, & Trachtenberg, 2009; Smith & Trachtenberg, 2007).

Non-human primates. In monocularly enucleated primates, including humans, half of the inputs to the visual system are removed (see Figure 1.2 for a depiction of the removal of the inputs associated with enucleation to subcortical and cortical visual areas). In the adult monkey, enucleation results in degeneration of the optic nerve, but

this degeneration does not immediately occur and is more pronounced 4 years compared with 6 months after enucleation (Horton, 1997). Interestingly, a phenomenon referred to as Wilbrand's knee is present wherein the nasal crossed fibres of the remaining eye loop into the optic nerve of the removed eye prior to traveling to the chiasm. It has been suggested that this phenomenon occurs only after long-term survival, and that it occurs due to optic chiasm shrinkage (Horton, 1997).

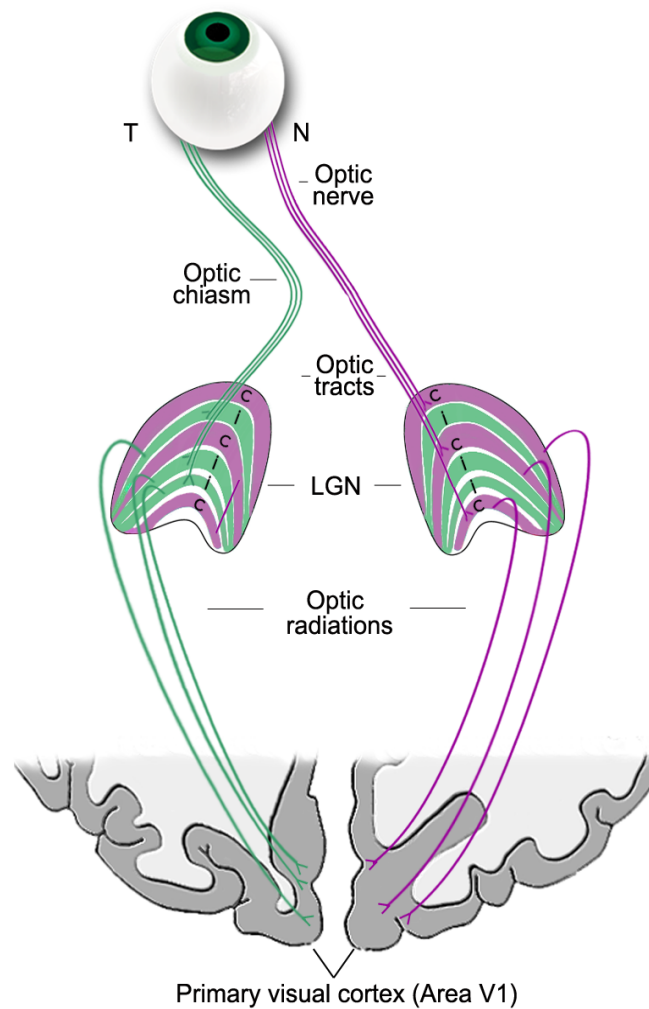


Figure 1.2. Schematic of the monocularly enucleated visual pathway where half of the inputs to subcortical and cortical substrates are removed. Visual information from the remaining eye travels through the optic nerve via the temporal (T: green fibres) and nasal (N: purple fibres) retinal ganglion axons and converges at the optic chiasm. Uncrossed temporal fibres project to laminae of the (i) ipsilateral LGN and crossed nasal

fibres project to laminae of the (c) contralateral LGN, which receive information from each eye in separate layers. Geniculate axons travel via the optic radiations to carry visual information to primary visual cortex (V1), which sends feedback to the LGN. Figure from Kelly et al. (2014) (adapted from the freely available image from ©John Wiley and Sons, Inc).

In the monkey LGN, laminae fail to segregate (Rakic, 1981), deafferented and non-deafferented cells shrink (Hendrickson & Tigges, 1985; Hubel et al., 1977; Sloper et al., 1987a), and deafferented cells die following early monocular enucleation (Sloper et al., 1987a & b). Further, enucleation in the adult macaque monkey produces shrinkage and death of geniculate cells in deafferented laminae (Matthews, 1964). Geniculate P cells compared with M cells are more adversely affected following enucleation (Hendrickson & Tigges, 1985; Sloper et al., 1987a), suggesting differential effects of enucleation on these two systems. A developmental effect on non-deafferented geniculate P cells indicates that enucleation at birth causes these cells to undergo hypertrophy and then return to normal size, whereas enucleation at 7 months of age causes these cells to shrink in size. Further, these cells were unaffected if the enucleation occurred in adulthood (Sloper et al., 1987a). Interestingly, aberrant connections are formed between the remaining eye and deafferented geniculate cells in prenatally enucleated monkeys (Rakic, 1981; Wefers, Dehay, Berland, Kennedy, & Chalupa, 2000), suggesting compensatory reorganization in response to the loss of one eye. However, this finding is inconsistent with another study showing no innervation of deafferented laminae by the remaining eye in postnatally enucleated monkeys (Hubel et

al., 1977) and indicates a critical period of development for the formation of retinogeniculate synaptic connections.

In visual cortex, monocular enucleation one week after birth in monkeys is associated with decreased ocular dominance columns in layer IVc β (i.e., parvocellular) but not layer IVc α (i.e., magnocellular). In contrast, enucleation before birth completely eliminates ocular dominance columns in monkey cortex (Horton & Hocking, 1998a). Although the parvocellular layer is more adversely affected, the magnocellular and parvocellular division found in the binocularly intact visual cortex is still achieved in V1 following early enucleation (Rakic, 1981). Further, area V2 appears unaffected by enucleation, and supports the notion that the visual information from both eyes is integrated by this point (Horton & Hocking, 1998a). Ocular dominance columns are significantly diminished in squirrel monkeys but are normal in macaques enucleated in adulthood (Hendrickson & Tigges, 1985; Horton & Hocking, 1998b), indicating differential consequences for different species of monkeys.

Human primates. Late enucleation. Monocular enucleation in adulthood is associated with atrophy of the anterior visual pathway that comprises the optic nerves, optic chiasm, optic tracts, LGN, and optic radiations years following enucleation (Beatty et al., 1982; Goldby, 1957; Hardmann, Halpin, Hourihan, Mars, & Lane, 1997; Horton, 1997). Similar to monkeys, Wilbrand's knee is also present following long-term survival from enucleation (Horton, 1997). In the LGN, neuronal loss occurs in deafferented laminae (Beatty et al., 1982; Goldby, 1957). For example, surface area of deafferented

laminae is reduced by approximately 50% compared with non-deafferented laminae. Further, deafferented cells (40 – 52%) are reduced in size more than non-deafferented cells (30 – 35%) (Goldby, 1957). Similar to enucleated monkeys (Hendrickson & Tigges, 1985; Sloper et al., 1987a), deafferented parvocellular laminae of the LGN are more affected by enucleation compared with deafferented magnocellular laminae (Goldby, 1957). At the cortical level, one postmortem study found that although ocular dominance columns were present and uniform 1 year following late enucleation, a region of striate cortex that represents the monocular crescent exhibited attenuated and fragmented columns ipsilateral to the remaining eye (Adams et al., 2007). This is inconsistent with another study showing normal cytoarchitecture of the calcarine in a postmortem brain 38 years following late enucleation (Beatty et al., 1982). This discrepancy may reflect the different survival period lengths after the enucleation and/or the different staining methods used.

Early enucleation. One study examining the postmortem brain of an adult who lost one eye at the age of 6 years due to trauma shows degeneration in geniculate laminae associated with the enucleated eye, indicative of transneuronal degeneration; however only one LGN could be dissected (Hickey & Guillery, 1979). Thus, it is unclear how early monocular enucleation affects bilateral LGN development. Similar to monkeys (Horton & Hocking, 1998a), a post-mortem examination of visual cortex found a lack of ocular dominance columns in layer IVc in two children (aged 28 months and 51 months) enucleated in infancy due to retinoblastoma (Horton & Hocking, 1998a). However, one child was born with tumors in the remaining eye that were treated with laser photocoagulation, resulting in decreased acuity in that eye. Further, both children died

from brain tumors that may have had an effect on neural development independent of the effects of the removal of one stream of visual input to the brain. One recent functional imaging study examined cortical activation in alive, albeit sedated, children enucleated in infancy due to retinoblastoma (Barb et al, 2011). The researchers found cortical dominance in V1 corresponding to the projection from the nasal hemiretina in the remaining eye (i.e., contralateral hemisphere to the remaining eye). This asymmetry is also present in binocularly intact individuals during monocular viewing (Toosy et al., 2001), suggesting that no physiological changes have occurred in primary visual cortex as a result of the enucleation. Thus, it is important to study the structural integrity of visual cortex to determine the effects of enucleation on morphological development.

Limitations of Previous Studies

Several limitations of the existing research on early monocular enucleation have motivated the experiments in my dissertation. Behavioural data are inconsistent with monocularly enucleated participants exhibiting intact performance for motion-defined letter detection and direction discrimination (Steeves et al., 2002), but impaired motion-defined letter recognition and motion-in-depth perception (Steeves et al., 2000 & 2002). Therefore, motion perception must be probed further to determine the behavioural consequences of the loss of one eye during development. Further, no studies have directly compared performance for spatial form vision and motion perception in the same individuals to determine whether enucleation has differential effects on these two systems. In Chapter II of my dissertation, I addressed these limitations by studying the effects of early monocular enucleation on the development of speed discrimination. I

also contrasted speed discrimination performance with contrast discrimination performance to address the question of whether the spatial form vision and motion perception systems are affected in a different manner by enucleation.

It is difficult to make assumptions based on previous research regarding the morphological effects of early monocular enucleation following long-term survival. First, the majority of enucleation studies have been conducted on non-primate species whose visual pathway is set-up in a different manner compared with primates. Specifically, rabbits, mice, and ferrets exhibit predominantly crossed retinal fibres due to laterally placed eyes resulting in less binocular overlap⁵ of the visual fields for each eye. In contrast, non-human and human primates exhibit hemisdecussation of retinal fibres due to frontally placed eyes and a great deal of binocular overlap (e.g., Chalupa & Lia, 1991; Jeffery, Cowey, & Kuypers, 1981; Neveu et al, 2006; Provis & Watson, 1981; reviewed in Horton, 2006 and Howard, 2002). The varying degrees of binocularity would thus translate into differing degrees of binocular interactions, namely binocular competition and binocular cooperation. While these studies provide valuable information regarding the effects of complete deafferentation of one eye on the visual system, it is unclear whether these results can be generalized to humans given the fundamental differences in each species' visual system. Second, it is difficult to extrapolate data from non-human primate research to long-term development following early enucleation in humans since the majority of monkey studies focus on enucleation that occurred during adulthood

⁵ Newton-Müller-Gudden law. The proportion of crossed/uncrossed retinal fibres is related to the size of the binocular visual field. Primates have frontally placed eyes and approximately 50% of retinal fibres crossing over. Rodents and rabbits have more laterally placed eyes and approximately 80% and 98 – 99% of retinal fibres crossing over, respectively (Giolli & Guthrie, 1969; reviewed in Howard, 2002).

(Hendrickson and Tigges, 1985; Horton & Hocking, 1998b; Matthews, 1964) or following relatively short-term survival periods (Hendrickson and Tigges, 1985; Hubel et al., 1977; Matthews, 1964; Rakic, 1981; Sloper et al, 1987a). Third, the majority of human studies report brain changes following enucleation that occurs in adulthood when critical periods for development have long been surpassed (Beatty et al, 1982; Goldby, 1957; Hardmann et al., 1997; Horton, 1997). The last two experiments in my dissertation examined whether early monocular enucleation disrupts the morphological development of subcortical (Chapter III) and cortical (Chapter IV) structures in the human visual pathway following long-term survival.

Purposes and Hypotheses

The general goal of this dissertation is to determine how the human visual system develops following monocular enucleation that occurs postnatally during a time of rapid brain development. To accomplish this, I have tested a group of adults who have experienced early monocular enucleation due to unilateral retinoblastoma. I have tested this group using a variety of techniques that inform on the behavioural and morphological development of the enucleated visual system and compared these results to binocularly intact controls. Behaviourally, I have assessed spatial form vision and motion perception development following enucleation by conducting a series of speed and luminance contrast discrimination tasks. Subsequent to these behavioural experiments, I have examined morphological development at different levels of the visual pathway (i.e., optic chiasm – LGN – visual cortex) using state-of-the art structural neuroimaging techniques. Findings from these experiments will add to the literature on

the consequences of early monocular enucleation in humans following long-term survival. Further, these data will help elucidate the role that binocularity plays in developing the visual system. The purposes and hypotheses of each experiment are described in detail below.

In Chapter II, I report on the speed and luminance contrast discrimination abilities of a group of adults with early monocular enucleation relative to binocular and monocular viewing controls. Previous literature has shown that spatial form vision abilities are relatively intact in this group; however, the findings are inconsistent regarding motion perception. The main goals of this experiment were twofold. *Goal 1.* To further measure motion perception development by testing an aspect of motion not yet assessed in this population, speed perception. *Hypotheses 1.* Consistent with previous research showing impaired performance for the recognition of motion-defined form (Steeves et al., 2002) and the perception of motion-in-depth (Steeves et al., 2000), I predicted further deficits for speed discrimination in the enucleation group compared with controls. Alternatively, since enucleation results in equivalent relative motion detection thresholds (Bowns et al., 1994), motion-defined form detection, and direction discrimination for coherent motion (Steeves et al., 2002) compared to controls, speed discrimination abilities may remain intact. *Goal 2.* To further examine the reported naso-temporal asymmetry found with early monocular enucleation. *Hypothesis 2.* Consistent with previous nasal biases found for optokinetic nystagmus (Day, 1995; Reed et al., 1991) and direction discrimination (Steeves et al., 2002), I predicted that the enucleation group would display better speed discrimination thresholds for nasalward compared with temporalward motion. Alternatively, enucleation is associated with no motion

asymmetries for motion-defined form detection and recognition (Steeves et al., 2002). Therefore, the enucleation group may not exhibit nasotemporal asymmetries for speed discrimination. *Goal 3.* To determine whether spatial form vision and motion perception development are affected differently by early monocular enucleation as the previous dissociation in visual ability suggests. *Hypothesis 3.* If these two systems are differentially affected by enucleation (i.e., impaired speed discrimination, intact contrast discrimination), I predicted that speed discrimination performance would not be correlated with that for contrast discrimination.

In Chapter III, I examined the structure of the anterior visual pathway including the optic chiasm and LGN in a group of adults enucleated early in life and compared the results to binocularly intact controls. A vast literature exists examining changes in this pathway in enucleated animal models, such as rodents and primates. Yet, few studies have examined the anterior visual pathway in humans, and those that have report on late rather than early enucleation using postmortem and histological methods. Thus, the precise effects of early monocular enucleation in humans are unclear and the goal of this experiment was to address this issue. I accomplished this by using noninvasive, state-of-the art structural neuroimaging methods to obtain morphological measurements of the optic chiasm and LGN. Consistent with animal models and with late enucleation in humans, I predicted morphological decreases in both optic chiasm measures and LGN volume following enucleation relative to controls. Alternatively, if early monocular enucleation during the postnatal critical period affects development of the anterior visual pathway in a different manner compared with late enucleation, a different pattern of results may emerge.

In Chapter IV, I continued examining the morphological development of the human visual pathway following enucleation by moving beyond subcortical structures to examine the cortex. For this experiment, I used structural neuroimaging methods to conduct whole brain and region-of-interest (ROI) analyses to examine cortical thickness and surface area estimates of grey matter in visual cortex. For the ROI analyses, I focused specifically on regions associated primarily with spatial form vision, namely V1 and V2. Consistent with decreased cortical thickness of grey matter in the occipital lobe in amblyopia (Du et al., 2009) and morphological changes in visual cortex of enucleated monkeys and humans such as a lack of ocular dominance columns (e.g., Horton, 1997; Rakic, 1981), I predicted that enucleation would result in decreases of cortical thickness and surface area in regions associated with vision. Alternatively, if early enucleation produces compensatory reorganization during development, I predict little to no decreases relative to controls.

CHAPTER II

IMPAIRED SPEED PERCEPTION BUT INTACT LUMINANCE CONTRAST PERCEPTION IN PEOPLE WITH ONE EYE⁶

⁶ Kelly, K.R., Zohar, S., Gallie, B.L. & Steeves, J.K.E. (2013). *Investigative Ophthalmology and Visual Science*, 54(4), 3058-64. Copyright ARVO

The visual system is not fully developed at birth (Daw, 2006) and relies on normal levels of balanced visual input during postnatal maturation (Wiesel & Hubel, 1963, 1965). For example, imbalanced visual input from monocular deprivation during infancy due to congenital cataract, anisometropia, and strabismus results in deficits in spatial form vision (e.g., contrast sensitivity, acuity) and motion perception (e.g., direction discrimination) that persist throughout life in both the deprived and non-deprived eye (Ellemberg, Lewis, Maurer, & Brent, 2000; Ellemberg, Lewis, Maurer, Barr, & Brent, 2002; Ellemberg et al., 2005; Ho et al., 2005; Kandel, Grattan, & Bedell, 1980; Lewis, Maurer, Tytla, Bowering, & Brent, 1992; Reed, Steeves, Steinbach, Kraft, & Gallie, 1996; Simmers, Ledgeway, Hess, & McGraw, 2003; Woo & Irving, 1991). Considering that motion stimuli intrinsically possess spatial attributes, it is difficult to determine which aspect of vision underlies motion processing deficits in these disorders. In fact, one study has shown that motion deficits in amblyopia are related to contrast sensitivity impairments rather than poor local motion perception (Qiu, Xu, Zhou, & Lu, 2007). To determine how spatial form vision and motion perception develop following visual deprivation, it may be helpful to examine populations that are impaired on only one of these aspects of vision, specifically a monocularly deprived population with intact contrast sensitivity.

One such population does exist, those who have experienced early monocular enucleation (ME; surgical removal of one eye) due to cancer of the retina (retinoblastoma), a disease with onset generally before 2 years of age. Enucleation provides a valuable model for examining the effects of early monocular deprivation on visual system development since it results in a more complete form of monocular

deprivation compared with other forms, such as strabismus or amblyopia, where disrupted patterned visual input is received by the deprived eye. Enucleated individuals demonstrate intact spatial form vision compared to binocular viewing (BV) controls for contrast sensitivity (Nicholas, Heywood, & Cowey, 1996), luminance contrast letter acuity (González, Steeves, Kraft, Gallie, & Steinbach, 2002; Reed et al., 1996; Reed, Steeves, & Steinbach, 1997), and global shape discrimination (Steeves, Wilkinson, González, Wilson, & Steinbach, 2004). Further, enucleated individuals actually have enhanced ability for the majority of these tasks compared with controls viewing monocularly with a patch over one eye (González et al., 2002; Reed et al., 1996; Reed et al., 1997; Steeves et al., 2004). Moreover, participants who underwent enucleation before 4 years of age have enhanced contrast sensitivity at 4 cpd compared with BV controls (Nicholas et al., 1996). These data suggest cortical reorganization, which may compensate for the early loss of one eye (reviewed in Kelly, Moro, & Steeves, 2013a and Steeves, González, & Steinbach, 2008). It is important to note, however, that enucleated individuals exhibit mild deficits in face perception, suggesting that higher-level spatial form vision is somewhat disrupted in this group (Kelly, Gallie, & Steeves, 2012).

Despite the generally intact or enhanced spatial form vision ability following ME, small motion perception deficits are found for motion-defined form (Steeves, González, Gallie, & Steinbach, 2002) and the perception of motion in depth (Steeves, Gray, Steinbach, & Regan, 2000). This dissociation in visual ability suggests a greater vulnerability during atypical postnatal visual development of cortical regions associated with motion processing, likely the middle temporal/medial superior temporal (MT/MST)

complex (MT+) (Tootell et al., 1995). However, not all aspects of motion are disrupted, enucleated participants demonstrate intact relative velocity detection (Bowns, Kirschner, & Steinbach, 1994) and direction discrimination for coherent motion (Steeves et al., 2002) compared to controls. Binocular congenital cataracts corrected during the first year of life disrupt global motion perception more than monocular cataracts, suggesting that normal visual input from one eye spares some vision (Ellemberg et al., 2002). Thus, normal visual input from the remaining eye in the enucleated population may result in a relative sparing of motion perception for some tasks, but not others. Nonetheless, response asymmetries have been shown in enucleated individuals favoring lower over upper hemifield motion for relative velocity discrimination (Bowns et al., 1994), as well as nasalward over temporalward motion for coherent motion discrimination (Steeves et al., 2002) and for eye movement responses to full field motion, specifically optokinetic nystagmus (Reed et al., 1991; Day, 1995). The optokinetic nystagmus asymmetry indicates a disruption in the earlier developing subcortical regions that mediate optokinetic nystagmus (e.g., nucleus of the optic tract [NOT]), whereas motion asymmetries point to a higher-level cortical disruption and are consistent with evidence for an earlier maturation period for the processing of nasalward motion (Braddick, Atkinson, & Wattam-Bell, 2003; Wattam-Bell, 2003).

Given the inconsistent nature of previous findings, it is worthwhile to further examine the effects of ME on motion perception development. One aspect of motion processing not yet studied in this population, the perception of speed, has real-world applications such as playing sports, crossing the road, and driving. While research implicates visual areas such as cortical area MT in the coding of speed perception

(Chawla, Phillips, Buechel, & Edwards, 1998; Huk & Heeger, 2000), other studies suggest extrastriate visual areas V3 and V3a are also involved (Kau et al., 2013; McKeefry, Burton, Vakrou, Barrett, & Morland, 2008). Further, speed processing occurs in cortical regions distinct from those for processing coherent motion (Kau et al., 2013). The development of speed perception appears to have a number of sensitive periods with fast speeds (e.g., 6°/s and 9°/s) maturing earlier than slow speeds (e.g., 1.5°/s) (Ahmed, Lewis, Ellemberg, & Maurer, 2005; Aslin & Shea, 1990; Ellemberg et al., 2003, 2004; Manning, Aagten-Murphy, & Pellicano, 2012). Consistent with developmental data, individuals who experienced binocular and monocular congenital cataracts exhibit stronger deficits in direction discrimination for slow compared with fast speeds (Ellemberg et al., 2005), indicating an earlier critical period for the development of neural regions sensitive to speeds that have not yet reached their optimal sensitivity.

We compare speed discrimination and luminance contrast detection and discrimination performance of a group of early ME participants to that of controls viewing binocularly and monocularly. We predict speed discrimination deficits as well as the presence of nasotemporal asymmetries in the enucleated group compared with controls, similar to disruptions observed in other tasks of motion processing with this population (Steeves et al., 2002). We also predict that these impairments will be more pronounced for slow than high speeds, consistent with developmental (Ahmed et al., 2005; Aslin & Shea, 1990; Ellemberg et al., 2003, 2004; Manning et al., 2012) and cataract (Ellemberg et al., 2005) studies. However, since some aspects of motion processing are not impaired in enucleated participants (Steeves et al., 2002; Bowns et al., 1994), we may find no speed perception deficits. For luminance contrast perception, we predict that the

early monocular enucleation group will perform in a similar manner as controls, consistent with previous findings (Nicholas et al., 1996; Reed et al., 1997; González et al., 2002; Steeves et al., 2004). Finally, we correlate speed and luminance contrast perception performance within individuals to determine whether spatial form vision and motion perception development are affected independently by enucleation as the previously described dissociation in visual ability would suggest. Data from these experiments will contribute to our understanding of the role that binocular vision plays in visual system development.

Methods

Participants

Monocular Enucleation (ME) group. Twelve adults (8 males) from The Hospital for Sick Children in Toronto who had one eye enucleated (7 right eye enucleated) due to retinoblastoma were tested. Mean age (\pm SD) was 23.9 ± 2.4 years (range = 17 – 43 years) and mean age at enucleation (AAE) (\pm SD) was 24.3 ± 5.0 months (range = 4 – 60 months). Participants had normal or corrected to normal Snellen acuity (Precision Vision, La Salle, IL). Enucleated participants are regularly seen by their ophthalmologist and no known ocular abnormalities were reported in the remaining eye. Table 2.1 lists individual patient histories.

Binocular (BV) and Monocular (MV) Viewing controls. Seventeen adults (6 males) were recruited who were approximately age-matched to the ME group. Participants were tested binocularly (BV) and monocularly (MV) on two separate occasions with semitransparent medical tape over their non-dominant eye (12 left eye patched) to reduce the effects of binocular rivalry. Mean age (\pm SD) was 25.2 ± 1.6 years (range = 19 – 40 years). Participants had normal or corrected to normal Snellen acuity and normal stereoacuity (Stereo Optical Co., Inc., Chicago, IL). Acuity and the Porta test (described in Durand & Gould, 1910) were used to assess eye dominance for the MV condition.

Table 2.1. Patient histories for ME participants including age, sex, Snellen acuity, enucleated eye, and age at enucleation (AAE).

| Patient | Age (years) | Sex | Acuity | Enucleated Eye | AAE (months) |
|---------|----------------|--------|---------|-------------------|-----------------|
| ME01 | 27 | Male | 20/16 | Right | 4 |
| ME02 | 43 | Female | 20/12.5 | Right | 18 |
| ME03 | 20 | Male | 20/20 | Right | 39 |
| ME04 | 34 | Female | 20/12.5 | Left | 18 |
| ME05 | 21 | Male | 20/20 | Right | 23 |
| ME06 | 18 | Female | 20/16 | Left | 48 |
| ME07 | 18 | Male | 20/16 | Right | 13 |
| ME08 | 17 | Male | 20/20 | Right | 9 |
| ME09 | 18 | Male | 20/20 | Left | 60 |
| ME10 | 29 | Female | 20/20 | Left | 11 |
| ME11 | 24 | Female | 20/16 | Right | 35 |
| ME12 | 30 | Male | 20/20 | Left | 13 |

Stimuli

Stimuli were created based on previously described methods (Chen, Bedell, & Frishman, 1996; Chen, Nakayama, Levy, Mathysse, & Holzman, 1999; Chen et al., 2008) using VPixx v.2.71 software (VPixx Technologies Inc., Saint-Bruno, QC, Canada). Stimuli consisted of 0.5 cpd vertical sine wave gratings with a 1° Gaussian blur applied to minimize edge effects.

Speed Discrimination. Leftward and rightward moving stimuli retained a constant luminance contrast of 20%. Base speed values, the speed levels to which an increment was added, were 3.8°/s, 6.2°/s, 10°/s, 16.2°/s, and 24°/s.

Luminance Contrast Detection and Discrimination. Luminance contrast stimuli were static versions of the gratings described for speed discrimination. Contrast was defined using Michaelson contrast⁷. Base luminance contrast values were 0% for detection and 5%, 11%, 22%, 44%, and 78% for discrimination. Since individuals who were enucleated prior to 4 years of age have shown higher contrast sensitivity at 4 cpd compared with BV controls (Nicholas et al., 1996), we also administered a set of luminance contrast detection and discrimination tasks at 4 cpd using 0%, 5%, and 11% base luminance contrasts. All other parameters were similar to those above.

Procedure

This research was conducted according to the doctrine of the Declaration of Helsinki and was approved by the research ethics boards of both The Hospital for Sick Children and York University. Informed consent was obtained from all participants prior to testing. Participants completed the tasks in a darkened room and sat 50 cm from the computer display with their chin resting on a chinrest. Stimuli were presented on a 17.5 inch Viewsonic G90fb CRT monitor (Viewsonic Corporation, Walnut, CA) with a refresh

⁷ Michaelson contrast is often used for stimuli such as sine-wave gratings and is defined as the difference in luminance between the highest (I_{\max}) and lowest (I_{\min}) luminance in the pattern divided by the sum of the two luminances. The formula is $(I_{\max} - I_{\min}) / (I_{\max} + I_{\min})$.

rate of 80 Hz. The monitor was driven by an Apple Macintosh Pro computer (Apple, Cupertino, CA). Participants' responses were recorded with a keyboard.

The sets of speed and luminance contrast perception tasks were blocked and counterbalanced. Leftward and rightward trials were interleaved in the speed discrimination tasks. A three-down one-up staircase procedure with a two-interval forced choice task was used to determine thresholds for each of the base speeds (one staircase each for leftward and rightward motion) and luminance contrasts. The value of the target stimuli decreased with three consecutive correct answers and increased with one incorrect answer by an increment of 30% of the difference between the base and target on the previous trial. The staircase ended after 12 reversals so that all participants performed at 79.4% accuracy. Thresholds were calculated by analyzing the last nine reversals. Four practice trials were provided prior to completing each set of tasks to ensure participants understood the procedure. Since the just-noticeable-difference between two perceived stimuli is proportional to the magnitude of the stimuli (i.e., Weber's Law: Weber, 1894), we expressed speed and luminance contrast discrimination thresholds as Weber Fractions ($\Delta X/X$). Luminance contrast detection thresholds could not be expressed as Weber Fractions, thus we expressed these thresholds as a percent (%) contrast.

Participants viewed two sequentially presented gratings, one base and one target, and were asked to indicate which of the two intervals contained: (1) a grating moving at a faster speed (speed discrimination), (2) a grating (luminance contrast detection), or (3) a grating of higher contrast (luminance contrast discrimination). The presentation sequence of the base and target was randomized and trials began with a

“ping” sound. Each grating was presented for 250 ms with an interstimulus interval of 200 ms. The second grating was jittered to the right of the first by 0.7° in order to prevent point by point comparisons between the two stimuli. A fixation window $15^\circ \times 15^\circ$ in size was presented for 200 ms before the first and second intervals in order to focus participants’ attention to the center of the display, but not cause afterimages on the region where the gratings appeared.

One ME and one MV participant did not complete the speed discrimination tasks due to time constraints. All control participants completed the set of 4 cpd tasks at all contrasts in both BV and MV conditions. Nine participants from the original ME group also completed the 4 cpd discrimination tasks at 5% and 11% contrasts, and eight completed the 4 cpd detection task at 0% contrast.

Results

Leftward/Rightward Speed Discrimination

An omnibus three-way ANOVA with group (BV, ME) as the between-groups variable, and direction (left, right) and base speed (3.8°/s, 6.2°/s, 10°/s, 16.2°/s, 24°/s) as the within-groups variables revealed no significant interactions ($ps \geq 0.146$). Significant main effects of group, $F(1,26) = 13.68$, $p = 0.001$, speed, $F(2.1,54.1) = 38.32$, $p < 0.001$, and direction, $F(1,26) = 12.54$, $p = 0.002$, were found. Both groups showed the typical pattern of lower thresholds for fast compared with slow speeds (Ahmed et al., 2005; Manning et al., 2012).

Collapsed across direction, post-hoc pairwise comparisons (Bonferroni-adjusted alphas = 0.01) revealed that the ME group exhibited significantly elevated thresholds (i.e., lower sensitivity) compared with the BV group for 10°/s ($p = 0.004$) and 24°/s ($p = 0.003$). The ME group also displayed tendencies for elevated thresholds compared with the BV group that approached significance for 3.8°/s ($p = 0.032$), 6.2°/s ($p = 0.015$), and 16.2°/s ($p = 0.037$). Collapsed across speed, post-hoc pairwise comparisons (Bonferroni-adjusted alphas = 0.025) revealed that the ME group exhibited significantly elevated thresholds compared with the BV group for both leftward ($p = 0.003$) and rightward ($p = 0.001$) motion. Further, the ME group exhibited significantly elevated thresholds for rightward compared with leftward motion ($p = 0.005$), and the BV group exhibited only a tendency for the same pattern that approached significance ($p = 0.074$). No simple effects analyses were conducted due to the lack of significant interactions. Figure 2.1 depicts (A) leftward and (B) rightward speed discrimination mean thresholds per group.

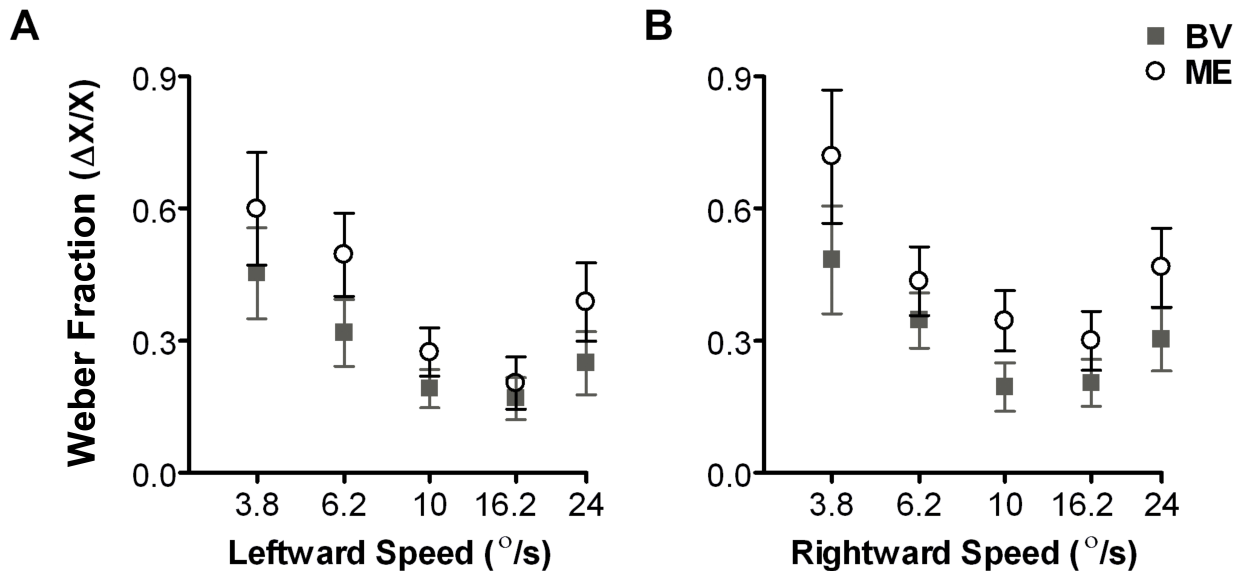


Figure 2.1. Speed discrimination Weber fractions ($\Delta X/X$) for BV (filled grey square) and ME (open circle) groups for (A) leftward and (B) rightward motion. In general, the ME group exhibited elevated speed discrimination thresholds compared with the BV group. Error bars represent $\pm 95\%$ confidence intervals (CIs).

Nasalward/Temporalward Speed Discrimination

An omnibus three-way ANOVA with group (MV, ME) as the between-groups variable, and direction (nasalward, temporalward) and base speed (3.8°/s, 6.2°/s, 10°/s, 16.2°/s, 24°/s) as the within-groups variables revealed a significant two-way speed by direction interaction, $F(2.4, 60.7) = 3.10$, $p = 0.043$. No other interactions were significant ($ps \geq 0.418$). Significant main effects of group, $F(1, 25) = 5.56$, $p = 0.027$, and speed, $F(4, 100) = 45.42$, $p < 0.001$, but not direction, $F(1, 25) = 0.83$, $p = 0.370$ were found. Both groups showed the typical pattern of elevated thresholds for slow compared with fast speeds (Ahmed et al., 2005; Manning et al., 2012).

Collapsed across direction, post-hoc pairwise comparisons (Bonferroni-adjusted alphas = 0.01) revealed tendencies for the ME group to have elevated speed discrimination thresholds compared with the MV group that approached significance for 6.2°/s ($p = 0.044$) and 10°/s ($p = 0.018$). The significant speed by direction interaction allowed a simple effects analysis (Bonferroni-adjusted alphas = 0.01), which revealed that the ME group had significantly elevated nasalward thresholds for 10°/s ($p = 0.001$) and tendencies for elevated nasalward thresholds that approached significance for 3.8°/s ($p = 0.081$) and 6.2°/s ($p = 0.018$) compared with the MV group. The ME group showed no nasotemporal asymmetries at any speed ($ps \geq 0.221$), but the MV group showed tendencies for elevated temporalward compared with nasalward thresholds that approached significance for 3.8°/s ($p = 0.065$) and 10°/s ($p = 0.057$), but tendencies for lower temporalward compared with nasalward thresholds that approached significance for 24°/s ($p = 0.033$). Figure 2.2 depicts (A) nasalward and (B) temporalward speed discrimination mean thresholds per group.

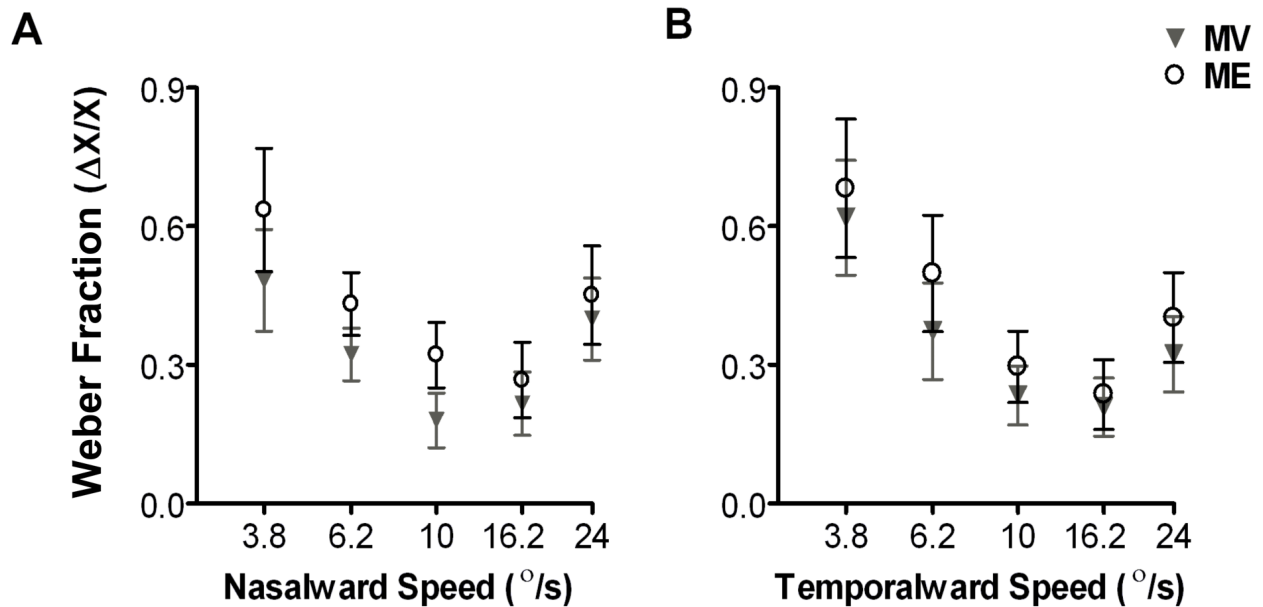


Figure 2.2. Speed discrimination Weber fractions ($\Delta X/X$) for MV (filled grey triangle) and ME (open circle) groups for (A) nasalward and (B) temporalward motion. The ME group exhibited elevated speed discrimination thresholds compared with ME group for nasalward speeds only. Error bars represent $\pm 95\%$ CIs.

Luminance Contrast Detection

Luminance contrast detection thresholds could not be converted into Weber fractions and were, thus, analyzed independently from those for contrast discrimination using separate one-way ANOVAs for 0.5 cpd and 4 cpd spatial frequency with group (BV, MV, ME) as the between-groups variable. Significant main effects of group were found for 0.5 cpd, $F(2,43) = 22.73$, $p < 0.001$, and for 4 cpd, $F(2,39) = 11.16$, $p < 0.001$. All groups showed the typical pattern of significantly elevated thresholds for 0.5 cpd compared with 4 cpd ($ps < 0.001$).

Post-hoc pairwise comparisons (Bonferroni-adjusted alphas = 0.017) revealed that the ME and MV groups exhibited significantly elevated detection thresholds compared with the BV group for 0.5 cpd and 4 cpd ($p \leq 0.006$). However, the MV group exhibited a tendency for an elevated detection threshold compared with ME group that approached significance for 4 cpd ($p = 0.070$). Figure 2.3 depicts (A) 0.5 cpd and (B) 4 cpd mean luminance contrast detection thresholds.

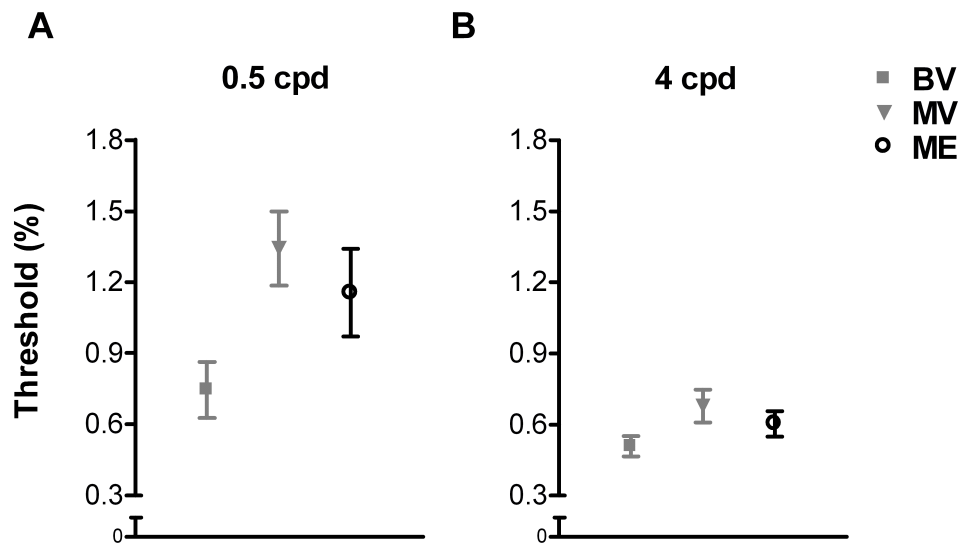


Figure 2.3. Contrast detection thresholds (%) for BV (filled grey square), MV (filled grey triangle), and ME (open circle) groups for (A) 0.5 cpd and (B) 4 cpd gratings. The MV and ME groups exhibited elevated luminance contrast detection thresholds compared with the BV group for both 0.5 and 4 cpd gratings. The MV group showed a tendency for elevated luminance contrast detection thresholds at 4 cpd compared with the ME group. Error bars represent $\pm 95\%$ CIs.

Luminance Contrast Discrimination

A two-way ANOVA with group (BV, MV, ME) as the between-groups variable and base contrast (5%, 11%, 22%, 44%, 78%) as the within-groups variable for luminance contrast discrimination at 0.5 cpd spatial frequency revealed no significant group by contrast interaction, $F(2.1, 92.9) = 0.48$, $p = 0.767$, and no significant main effect of group, $F(2, 43) = 0.64$, $p = 0.530$. However, a significant main effect of luminance contrast was found, $F(2.1, 92.9) = 59.71$, $p < 0.001$. All groups showed the typical pattern of decreasing thresholds for increasing luminance contrast.

Another two-way ANOVA with group (BV, MV, ME) as the between-groups variable and base contrast (5%, 11%) as the within-groups variable for luminance contrast discrimination at 4 cpd spatial frequency revealed no significant group by contrast interaction, $F(2, 40) = 0.53$, $p = 0.593$. A significant main effect of luminance contrast, $F(1, 40) = 19.82$, $p < 0.001$, and a marginally significant main effect of group, $F(2, 40) = 3.21$, $p = 0.051$ were observed. All groups showed the typical pattern of elevated thresholds for 5% compared with 11% contrast ($ps \leq 0.06$).

Post-hoc pairwise comparisons (Bonferroni-adjusted alphas = 0.025) revealed that the MV group exhibited tendencies for elevated thresholds compared with the ME group that approached significance for 5% ($p = 0.056$) and 11% ($p = 0.090$) at 4 cpd spatial frequency. Figure 2.4 depicts (A) 0.5 cpd and (B) 4 cpd luminance contrast discrimination mean thresholds per group.

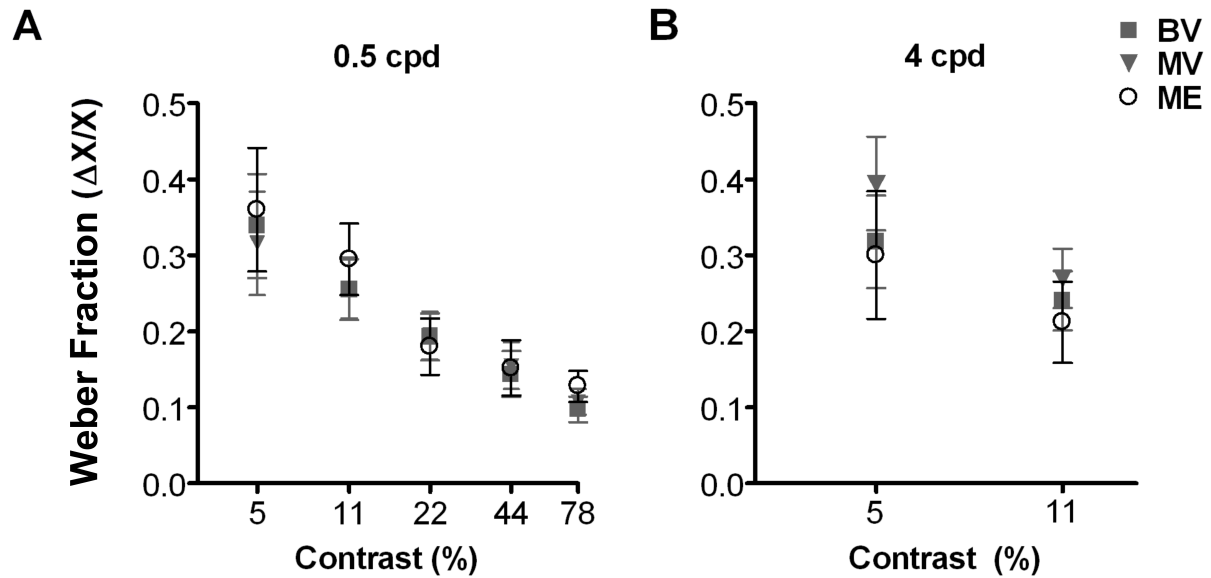


Figure 2.4. Contrast discrimination Weber fractions ($(\Delta X/X)$ for BV (filled grey square), MV (filled grey triangle), and ME (open circle) groups for (A) 0.5 cpd and (B) 4 cpd gratings. No significant differences were found between groups for 0.5 cpd, but the MV group exhibited tendencies for elevated luminance contrast discrimination thresholds compared with the ME group at 4 cpd. Error bars represent $\pm 95\%$ CIs.

Timing of Deprivation

Partial correlations controlling for age revealed no significant correlations between AAE in the ME group and their luminance contrast detection and discrimination, or speed discrimination thresholds (p s ≥ 0.123).

Relationship Between Luminance Contrast Detection/Discrimination and Speed

Discrimination

Since the ME group did not exhibit nasotemporal asymmetries, nasalward and temporalward thresholds were averaged. Each speed discrimination threshold was then correlated with each luminance contrast detection and discrimination threshold using partial correlations controlling for age to determine if development of speed and luminance contrast processing are affected in the same way by ME. Only correlations that reached $p < 0.05$ (uncorrected alpha) subsequent to outlier removal are reported. Only two positive correlations were found: (1) 10°/s speed and 44% luminance contrast perception, $r(7) = 0.74$, $p = 0.024$, and (2) 24°/s and 78% luminance contrast perception, $r(8) = 0.75$, $p = 0.013$. To compare against the ME group, the same correlations were conducted for the BV group with leftward and rightward thresholds averaged and for the MV group with nasalward and temporalward thresholds averaged. No significant correlations were found for the BV group; however, two positive correlations were found for the MV group: (1) 24°/s and 0% luminance contrast at 0.5 cpd, $r(11) = 0.58$, $p = 0.047$, and (2) 24°/s and 0% luminance contrast at 4 cpd, $r(12) = 0.69$, $p = 0.013$. These few correlations may be due to the problem of multiple comparisons when conducting many correlations and, thus, must be interpreted with caution.

Discussion

We demonstrate speed discrimination impairments in early ME individuals compared with BV controls for all speeds regardless of direction. This is consistent with previously reported motion processing deficits in this group (Steeves et al., 2000, 2002). Moreover, we also report the first instance of motion perception deficits for the early ME group compared with MV controls. While the ME group showed elevated speed thresholds at all speeds relative to BV controls, they only showed deficits at slower speeds when compared with MV controls. This finding supports research indicating later maturation for the perception of slow speeds (Ahmed et al., 2005; Aslin & Shea, 1990; Ellemberg et al., 2003, 2004, 2005; Manning et al., 2012) and suggests an interruption to this critical period with ME. Further, the enucleation group's speed processing deficits were less pronounced when compared with monocular rather than BV controls indicating that the control condition of MV with an eye patch over one eye appears to interfere with the visual processing of motion. This is likely due to inhibitory binocular interactions from the eye patch such as binocular inhibition or rivalry. Binocular inhibitory effects may also contribute to the mild nasotemporal asymmetries observed in our MV controls. Nonetheless, MV controls are better than ME participants at speed discrimination. This finding suggests that binocular inhibitory effects from eye patching disrupt speed perception minimally in controls, which is supported by the lack of asymmetry for global motion perception with eye patching (Steeves et al., 2002). Remarkably, enucleated observers displayed deficits for nasalward motion only compared with MV controls, suggesting that at least for the perception of speed, the earlier developing perception of nasalward motion may be more vulnerable to early visual deprivation when assessing

local rather than global motion. Thresholds for temporalward motion appear to be slightly elevated (Fig. 2.2B), and perhaps there may exist a disruption in the development of processing temporalward motion as well; however, these elevations did not reach significance.

Motion perception deficits have been documented in developmental disorders affecting visual ability such as Williams Syndrome and autism (Atkinson et al., 1997; Koldewyn, Whitney, & Rivera, 2010), suggesting that a vulnerability of the dorsal motion processing system may exist with atypical development (Braddick et al., 2003). Deficits in speed perception for our enucleated group may also be attributed to a disruption in dorsal regions associated with processing speed that are beyond V1, such as V3/V3a and MT+ (Kau et al., 2013; McKeefry et al., 2008; Tootell et al., 1995). Cells in MT+ and V3a are also tuned to binocular disparity and there is considerable functional overlap between stereopsis and motion processing (Backus, Fleet, Parker, & Heeger, 2001; Maunsell & Van Essen, 1983; Roy, Komatsu, & Wurtz, 1992). Indeed, strabismic individuals with weak stereopsis exhibit deficits in speed judgments similar to our ME group (Tychsen & Lisberger, 1986). Thus, a common physiologic link between motion perception and binocular integration may account for the motion deficits in our enucleated group, for whom no binocular interaction in the visual cortex is possible. Consequently, intact binocularity may be required for the normal maturation of motion systems.

Unlike previous research (Day, 1995; Reed et al., 1991; Steeves et al., 2002), no nasotemporal asymmetries were observed in our ME group. Attending to speed rather than direction has been shown to activate different neural regions for motion (Kau et al.,

2013) and could account for the lack of asymmetry in our study. It is also possible that a nasotemporal asymmetry does not manifest during tasks where motion is easily determined by local cues such as speed. Individuals who have experienced early-onset strabismus show larger nasalward biases for the perceived speed of sine wave gratings (Brosnahan, Norcia, Schor, & Taylor, 1998; Tychsen & Lisberger, 1986), though this is a very different form of deprivation than enucleation. A lack of nasotemporal asymmetries may also reflect a brief period of binocular vision with normal input through the removed eye prior to enucleation since the majority of our participants underwent enucleation later than 6 months of age. However, central vision is usually obstructed approximately 6 months prior to when retinoblastoma is diagnosed and the eye is enucleated; therefore, this brief period of normal vision is likely even shorter. It is possible that complete deafferentation of one eye with enucleation is fundamentally different from other forms of monocular deprivation and results in speed discrimination deficits but no nasotemporal asymmetries.

The ME group exhibited substantially elevated luminance contrast detection thresholds regardless of spatial frequency compared with the BV group, which is consistent with a previously reported elevated threshold for luminance contrast letter acuity at 4% contrast compared with BV controls (Reed et al., 1997). More importantly, these deficits disappear when performance in the ME group is compared with MV controls in our study. This indicates a binocular advantage when viewing with two eyes (i.e., binocular summation) compared to one. Binocular summation effects have been implicated in the superior resolution of vernier acuity as well as luminance contrast detection and discrimination, and its effect is strongest at lower luminance contrasts

(Banton & Levi, 1991; Cagnello, Arditi, & Halpern, 1993; Legge, 1984;). Therefore, the reduction in luminance contrast detection in our study for both the MV and ME groups can be largely attributed to the lack of binocular summation and not to a deficit in the development of luminance contrast perception.

Despite the lack of binocular summation, the ME group nonetheless had a tendency for superior luminance contrast detection and discrimination of 5% and 11% luminance contrast 4 cpd gratings compared with the MV group. This finding is consistent with previous luminance contrast tasks in this population (González et al., 2002; Nicholas et al., 1996; Reed et al., 1996, 1997; Steeves et al., 2004). Several suggestions have been put forth to account for the superior performance of ME patients compared with MV controls at low contrast visual tasks (Steeves et al., 2008) including: (1) binocular interference of binocular rivalry when wearing an eye patch for the MV controls, which of course is absent in the ME group, (2) years of monocular practice for the ME group, and (3) compensatory reorganization within visual cortex of ME patients in favor of the remaining eye. For instance, the complete removal of one eye eliminates binocular inhibitory interactions and binocular competition for cortical space during postnatal visual development. Consequently, neurons in the visual pathway that would otherwise have been allocated to the enucleated eye may be recruited by the remaining eye at various levels of the visual system such as the lateral geniculate nucleus and V1 (Horton & Hocking, 1998; Rakic, 1981). Recruitment within V1 may prevent spatial form vision deficits following ME, and in some cases may actually enhance this ability.

No timing of deprivation effects were found for luminance contrast detection and discrimination. This finding is consistent with previous studies of spatial form vision in

enucleation, which have not found an effect of age at enucleation (Reed et al., 1996, 1997; González et al., 2002; Steeves et al., 2004; Kelly et al., 2012). Apart from two individuals, all of our participants had their eye surgically removed before 44 months of age, which may be outside developmental critical periods or may not span a large enough period in early development to be sensitive to developmental critical period effects. Further, when we removed participants who underwent eye enucleation after 24 months of age from our analyses, we found the same pattern of results. The relative lack of relationship between luminance contrast detection and discrimination and speed discrimination for either group, coupled with the dissociation in visual ability, suggests that early ME affects the development of the motion perception and spatial form vision pathways differently.

Conclusions

In conclusion, our study shows that enucleated observers have deficits in speed but not luminance contrast processing, which is consistent with the previously reported dissociation in visual ability. This is the first study to measure both luminance contrast and speed processing in the same individuals. These findings, coupled with a relative lack of correlation between the sets of speed and luminance contrast tasks, point to independent effects of enucleation on these two systems. It is possible that the visual system undergoes compensatory reorganization in response to the loss of one eye during infancy for spatial form vision to remain intact. Yet, such reorganization may not be sufficient for the development of motion perception. This study highlights the

importance of normal and balanced levels of binocular postnatal visual input for the normal development of the motion processing systems.

CHAPTER III

ALTERED ANTERIOR VISUAL SYSTEM DEVELOPMENT FOLLOWING EARLY MONOCULAR ENUCLEATION⁸

⁸ Kelly, K.R., McKetton, L., Schneider, K.A., Gallie, B.L. & Steeves, J.K.E. (2014). *NeuroImage: Clinical*, 4, 72-81. Copyright Elsevier

Retinoblastoma is a rare eye cancer that accounts for approximately 6% of all childhood cancers and generally occurs before 5 years of age (Broaddus, Topham, & Singh, 2009a). The most frequent and effective treatment for unilateral retinoblastoma is monocular enucleation (surgical removal) of the cancerous eye, which, in turn, deprives the brain of one half of visual inputs. Due to the high survival rate (97%) (Broaddus, Topham, & Singh, 2009b) and lack of balanced binocular input associated with retinoblastoma, it is crucial to study the consequences of the most effective treatment, monocular enucleation, on visual system development following long-term survival. In both animals and humans, postnatal monocular deprivation from lid suture, congenital cataracts, and strabismus negatively affects visual development (e.g., Barnes et al., 2010; Ellemberg, Lewis, Maurer, & Brent, 2000; Wiesel & Hubel, 1963a) given that, at birth, the visual system is not fully mature (reviewed in Daw, 2006). This finding highlights the importance of receiving binocular balanced input during the critical postnatal developmental period of the visual pathway.

Here, we focus on the morphological development of the anterior visual pathway in adults who have had one eye enucleated early in life due to retinoblastoma. In the primate visual pathway, RGC axons from each eye converge at the optic chiasm. Approximately half of these axons project ipsilaterally (uncrossed temporal fibres) while the other half project contralaterally (crossed nasal fibres) via the optic tracts to each lateral geniculate nucleus (LGN) (Figure 3.1). The LGN is a subcortical thalamic visual relay station that receives information from each eye in segregated, eye-specific laminae. At birth, this structure is relatively adult-like in volume and laminar organization

and is morphologically mature by 9 months of age; however, it continues to develop physiologically (Blakemore & Vital-Durand, 1986; de Courten & Garey, 1982; Garey & de Courten, 1983). Frontally placed eyes and thus an overlap of the visual fields in primates results in binocular vision, specifically stereopsis and binocular depth perception, that occurs at a cortical level in striate and extrastriate visual areas. Hemidecussation of retinal fibres allows binocular cells within these regions to receive information from both eyes about corresponding points in the binocular visual field (reviewed in Howard, 2002). Since monocular enucleation results in only one stream of visual information to the brain and thus a lack of binocularity within the cortex, development of the enucleated visual system is likely to be disrupted.

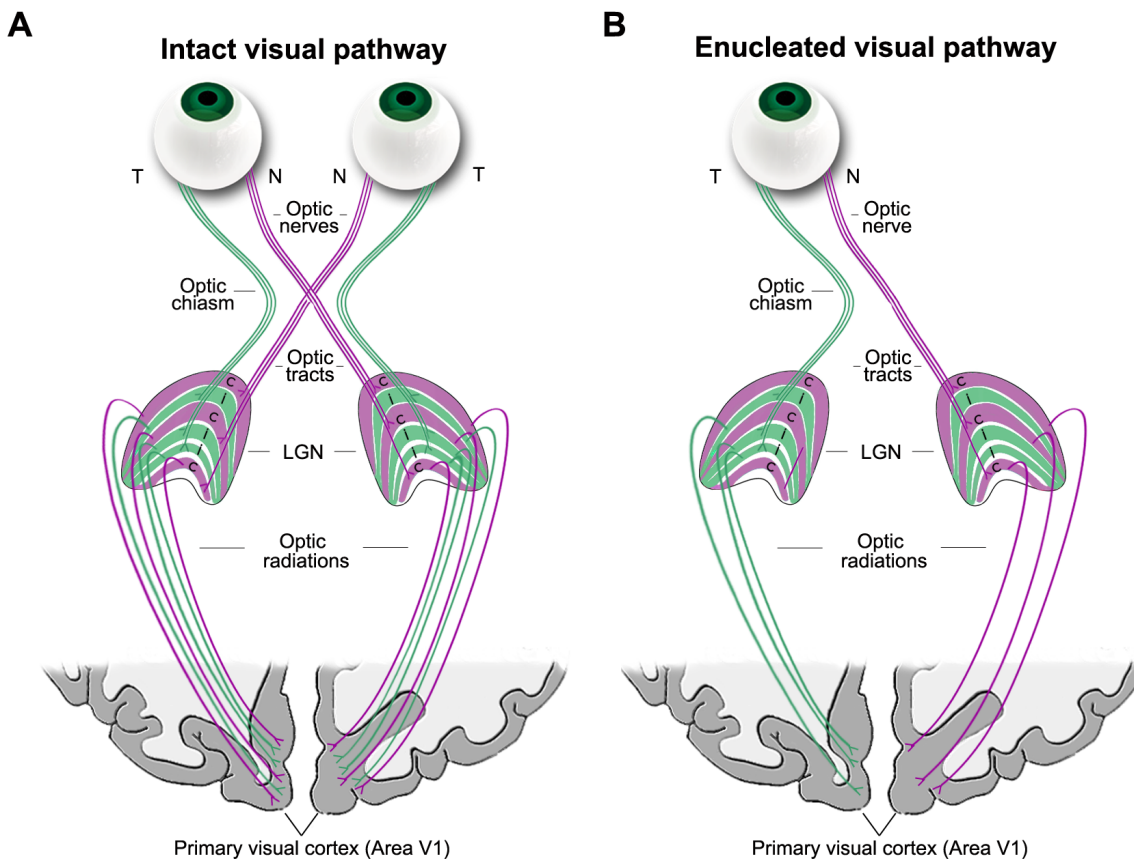


Figure 3.1. Schematic of the (A) binocularly intact and (B) monocularly enucleated visual pathways. (A) In the intact visual pathway, visual information from each eye travels through the optic nerve via the temporal (T: green) and nasal (N: purple) retinal fibres and converges at the optic chiasm. Uncrossed temporal fibres project to the ipsilateral LGN and crossed nasal fibres project to the contralateral LGN, which receive information from each eye in separate layers. From here, the optic radiations carry information to primary visual cortex (cortical area V1). (B) In the monocularly enucleated visual pathway, the right eye is removed in this diagram and half of the inputs received by the LGN and visual cortex are deafferented. Figure adapted from ©John Wiley and Sons, Inc.

Behavioural consequences of early monocular enucleation in adult humans are well documented. In general, this population exhibits intact or enhanced spatial form vision, such as contrast sensitivity (Kelly, Zohar, Gallie, & Steeves, 2013b, Nicholas, Heywood, & Cowey, 1996; Steeves, Wilkinson, González, Wilson, & Steinbach, 2004), but mildly impaired motion perception, such as speed discrimination (Kelly et al., 2013b; reviewed in Kelly, Moro, & Steeves, 2013a and Steeves, González, & Steinbach, 2008). Few researchers have had the opportunity to investigate morphological changes in the enucleated human visual pathway. Morphological changes have been relatively well established in animal models of enucleation, although most of these models are from species with more laterally placed eyes and therefore predominantly crossed retinal fibres. These studies show an increase in crossed fibres of the remaining eye at the expense of uncrossed fibres in enucleated mice, ferrets, and rabbits (Godement, Salaun, & Metin, 1987; Grigonis, Pearson, & Murphy, 1986; Guillery, 1989). In enucleated rabbits, LGN size contralateral to the enucleated eye is reduced (Khan, 2005). While these studies demonstrate changes as a result of early eye enucleation, it is difficult to extrapolate these results to the primate visual system given the fundamental differences in the species' visual systems: rodents exhibit a crossing over of the majority of retinal fibres and a lack of binocular disparity and stereopsis while primates exhibit hemidecussation of retinal fibres and no lack of binocular disparity and stereopsis (Chalupa & Lia, 1991; Jeffery, Cowey, & Kuypers, 1981; Neveu et al., 2006; Provis & Watson, 1981). In non-human primates, geniculate laminae fail to segregate (Rakic, 1981), and deafferented and non-deafferented cells shrink following enucleation (Hendrickson & Tigges, 1985; Hubel, Wiesel, & LeVay, 1977; Matthews, 1964; Sloper,

Headon, & Powell, 1987a). Yet, it is also difficult to generalize non-human primate studies to early enucleated humans since some non-human primate studies focus on enucleation in adulthood (e.g., Hendrickson & Tigges, 1985) and all studies only report consequences following a relatively short survival period in late or early enucleation (Hendrickson & Tigges, 1985; Hubel et al., 1977; Matthews, 1964; Rakic, 1981; Sloper et al., 1987a).

Only a handful of studies have focused on morphological changes following early monocular enucleation in humans. For example, reduced optic chiasm width (Horton, 1997), degenerated optic tracts, and transneuronal degeneration of deafferented geniculate cells (Beatty, Sadun, Smith, Vonsattel, & Richardson, 1982; Goldby, 1957; Hickey & Guillery, 1979) are reported years following enucleation. However, most studies have only reported brain changes in those who have lost one eye during adulthood when the developmental critical periods have long been surpassed. Moreover, these examinations were all completed postmortem. One study did examine the LGN of an adult who lost one eye at 6 years of age due to trauma and found transneuronal degeneration of layers associated with the enucleated eye (Hickey & Guillery, 1979), but this examination was only conducted on the left LGN and it is unknown how the right LGN was affected.

Our goal in the present study was to assess how early eye enucleation affects the maturation of the anterior visual system given that this system is not receiving information from the enucleated eye that is required during postnatal development. More specifically, we sought to examine these effects following long-term survival. To do so, we used noninvasive structural magnetic resonance imaging (MRI) to assess the optic

nerves, optic chiasm, optic tracts, and LGN in adults who had one eye enucleated during infancy due to retinoblastoma and compared them to binocularly intact controls.

Although previous research has reported on late-enucleated participants and the structure of the anterior visual system, we had the opportunity to test one late-enucleated participant and compare his results to the control and early enucleation groups. Consistent with early-enucleated monkeys (Matthews, 1964; Rakic, 1981; Sloper et al., 1987a) and late-enucleated humans (Beatty et al., 1982; Goldby, 1957; Horton, 1997), we predict reductions in optic chiasm and LGN measures in the early enucleation group. This finding would suggest degeneration of cells in a system that relies on Hebbian synaptic learning for refinement during maturation. Alternatively, if early enucleation alters the complex development of the visual system rather than triggering cell loss, we predict a different pattern of results that would be present with early, but not late, enucleation. These data will help elucidate the role of balanced binocular vision during postnatal maturation in the developing anterior visual system.

Methods

Participants

Early Monocular Enucleation (ME) group. The first phase of this study consisted of analyzing the morphology of the chiasm of twelve adults (6 males) who were former patients at The Hospital for Sick Children in Toronto and who had one eye enucleated (9 right eye enucleated) due to retinoblastoma (cancer of the retina). Mean age (\pm SD) was 27.4 ± 11.9 years (range = 17 – 54 years) and mean age at enucleation (AAE) (\pm SD) was 18.7 ± 11.3 months (range = 4 – 48 months). Based on the size and

position of the tumour under retinal examination prior to enucleation, it is estimated that typically the tumour would have lead to disrupted vision approximately 6 months prior to enucleation. Eight of these participants (3 males; 6 right eye enucleated) also took part in the second phase of this study, which consisted of analyzing LGN volume. Mean age (\pm SD) was 27.8 ± 9.7 years (range = 17 – 45 years) and mean AAE (\pm SD) was 15.0 ± 6.4 months (range = 4 – 26 months). All participants had normal or corrected-to-normal acuity as assessed by an EDTRS eye chart (Precision VisionTM, La Salle, IL). Enucleated participants are regularly seen by their ophthalmologist. No known ocular abnormalities in the remaining eye, or neurological abnormalities in the brain, were reported. Table 3.1 lists individual patient histories.

Late ME participant. We also tested one late ME participant (male, age = 65 years) who experienced trauma to the eye at 50 years of age that eventually resulted in a detached retina and subsequent eye enucleation approximately 6 years prior to testing (AAE = 708 months). All data from the late ME participant was analysed separately from the early ME group to compare late versus early enucleation (see Table 3.1 for late ME patient history).

Table 3.1. ME patient histories. All participants took part in the chiasm phase of the experiment. Participants that took part in the LGN phase are indicated under LGN volume. Age, sex, Snellen acuity, enucleated eye, and age at enucleation (AAE) are also reported.

| Patient | Age (years) ^a | Sex | Acuity | Enucleated Eye | AAE (months) | LGN Volume ^b |
|-----------|-----------------------------|--------|------------|-------------------|-----------------|----------------------------|
| ME01 | 54 | Male | 20/16 -1 | Right | 24 | No |
| ME02 | 43/45 | Female | 20/12.5 +2 | Right | 18 | Yes |
| ME03 | 21 | Male | 20/20 | Right | 23 | No |
| ME04 | 18 | Female | 20/20 | Right | 48 | No |
| ME05 | 18/19 | Male | 20/20 +4 | Right | 13 | Yes |
| ME06 | 17 | Male | 20/20 +2 | Right | 9 | No |
| ME07 | 29 | Female | 20/20 | Left | 11 | Yes |
| ME08 | 28 | Male | 20/16 | Right | 4 | Yes |
| ME09 | 30 | Male | 20/20 +3 | Left | 13 | Yes |
| ME10 | 18 | Female | 20/16 +3 | Right | 17 | Yes |
| ME11 | 17 | Female | 20/12.5 +1 | Right | 26 | Yes |
| ME12 | 36 | Female | 20/16 +4 | Left | 18 | Yes |
| ME13 | 65 | Male | 20/20 | Right | 708 | Yes |
| (Late ME) | | | | | | |

^a The first number indicates age for the chiasm phase, the second number indicates age for the LGN phase.

^b Indicates whether participant took part in the LGN phase of the study.

Control group. Twenty-eight binocularly intact controls (15 males) took part in the chiasm phase of the study and were approximately age- and sex-matched to the early ME group. Mean age (\pm SD) was 29.9 ± 11.6 years (range = 18 – 60 years). Fifteen of these participants (8 males) also took part in the LGN phase and mean age (\pm SD) was 29.9 ± 11.2 years (range = 18 – 60 years). Participants had normal or corrected-to-normal acuity (Precision Vision TM, La Salle, IL) and normal Titmus stereoacuity (Stereo Optical Co., Inc. Chicago, IL). Acuity and the Porta test (described in Durand & Gould, 1910) were used to assess eye dominance (Chiasm: 18 right eye dominant; LGN: 11 right eye dominant).

Data Acquisition, Processing, and Measurements

This research followed the Declaration of Helsinki doctrine and was approved by the Research Ethics Boards of both The Hospital for Sick Children and York University. Informed consent was obtained from all participants prior to testing and after explanation of the nature and possible consequences of the study.

All scans were acquired on a Siemens MAGNETOM Trio 3T MRI scanner with a 32-channel head coil at the Sherman Health Sciences Research Centre, York University. A T_1 weighted three-dimensional MPRAGE scan of the entire head was acquired sagittally with the following parameters: rapid gradient echo, 1 mm^3 isotropic voxels, TR = 1900 ms, TE = 2.52 ms, 256×256 matrix, and flip angle = 9° . All T_1 images were re-oriented on the MRI console (Syngo; Siemens, Munich, Germany) to ensure the optic nerves, optic chiasm, and optic tracts were observed in the same plane and a reformatted image with a 1mm slice thickness was obtained parallel to the

optic chiasm. Processing of these reformatted images was conducted using tools from the freely available FMRIB's Software Library (FSL; version 4.1.8) (<http://www.fmrib.ox.ac.uk/fsl>). Chiasm region-of-interest (ROI) masks were manually traced by three independent raters blind to group membership in FSLview. Chiasm masks from each rater were merged using `fslmerge` and a median mask was created using `fslmaths` that was comprised of voxels chosen in at least 2 of the 3 original masks. From the median mask, chiasm volumes were calculated using the `fslstats` tool. Several chiasm measurements (Figure 3.2) were also taken by four independent raters blind to group membership using the Osirix® length measurement tool, which computes selected distances using bicubic interpolation⁹ (Rosset, Spadola, & Ratlib, 2004): optic nerve diameter (a) ipsilateral and (b) contralateral to the dominant eye for controls and the remaining eye for ME participants, optic tract diameter (c) ipsilateral and (d) contralateral to the dominant/remaining eye, and optic chiasm width in the (x) X and (y) Y planes. Each rater took three measurements and the average of these measurements across raters was calculated per structure. To ensure whole brain volume was not a factor affecting our results, we also calculated whole brain volumes excluding the cerebellum and brain stem using volumetric segmentation performed with the FreeSurfer image analysis suite (<http://surfer.nmr.mgh.harvard.edu/>).

⁹ Bicubic interpolation is the interpolation of data points on a 2D grid, which results in a smoother image (Keys, 1981; Pan, Yang, & Tang, 2012).

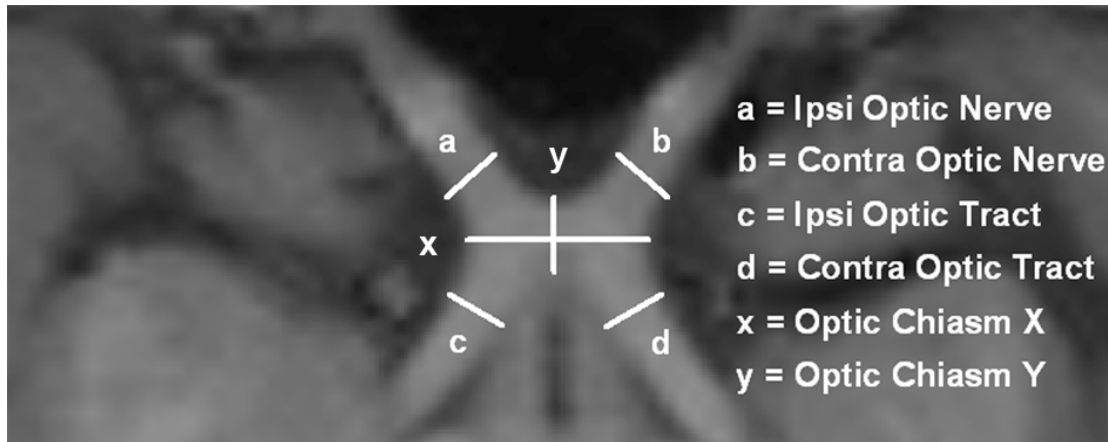


Figure 3.2. An axial image of a reformatted T_1 weighted scan from a control participant displaying optic nerves (a) ipsilateral and (b) contralateral to the dominant eye, optic tracts (c) ipsilateral and (d) contralateral to the dominant eye, and optic chiasm widths in the (x) X and (y) Y planes.

While T_1 weighted images have good contrast between grey and white matter in the cortex, the contrast between the LGN and surrounding tissue is low making it difficult to differentiate the LGN. Proton density (PD) weighted images have been shown to successively distinguish thalamic nuclei (Devlin et al., 2006). PD weighted images use a long repetition time and a short echo time to minimize T_1 and T_2 weightings, thus the tissue contrast is primarily dependent on the number of protons per unit tissue (i.e., proton density) (Jackson, Ginsberg, Schomer, & Leeds, 1997). A higher density of protons gives rise to brighter signals on the PD image, and vice versa. Following T_1 acquisition, participants underwent between 30 to 40 PD weighted scans each lasting approximately 1.5 mins. Slices were acquired coronally with the following parameters:

turbo spin echo, $800\mu\text{m} \times 800\mu\text{m}$ in-plane resolution, slice thickness = 2 mm or 1 mm, TR = 3000 ms, TE = 22 or 26 ms, 256×256 matrix, flip angle = 120° .

Processing of PD weighted images was also conducted using FSL's toolbox. All PD weighted images for each participant were first interpolated to twice the resolution and half the voxel size to create a higher resolution image with FLIRT (Jenkinson & Smith, 2001; Jenkinson, Bannister, Brady, & Smith, 2002). To increase the signal-to-noise ratio (SNR), these interpolated images were then concatenated using `fslmerge`, motion corrected using MCFLIRT (Jenkinson et al., 2002), and a mean high-resolution image was created using `fslmaths` (Figure 3.3). Three independent raters manually traced left and right LGN ROI masks three times each per participant using the mean PD weighted image. For each rater, ROIs were merged using `fslmerge` and a median mask was created using `fslmaths`. Finally, median masks from each of the three raters were merged together and a final median mask across raters was created. LGN volumes (left and right) were calculated per participant from this final median mask using `fslstats`.

The methods used in this study are the gold standard and most appropriate methods for evaluating the chiasm and LGN in clinical settings (e.g., Bridge, Cowey, Ragge, & Watkins 2009; Schmitz et al., 2003). While contrasts on the T_1 and PD weighted images may be sensitive to other factors such as extracellular space, gliosis, and axon diameter (e.g., Sloper et al., 1987a) that may affect the quantitative interpretation of our findings, the measurements in our study are consistent with those found using histological or post mortem measurements (e.g., Andrews, Halpern, Scott, & Purves 1997; Horton, 1997).

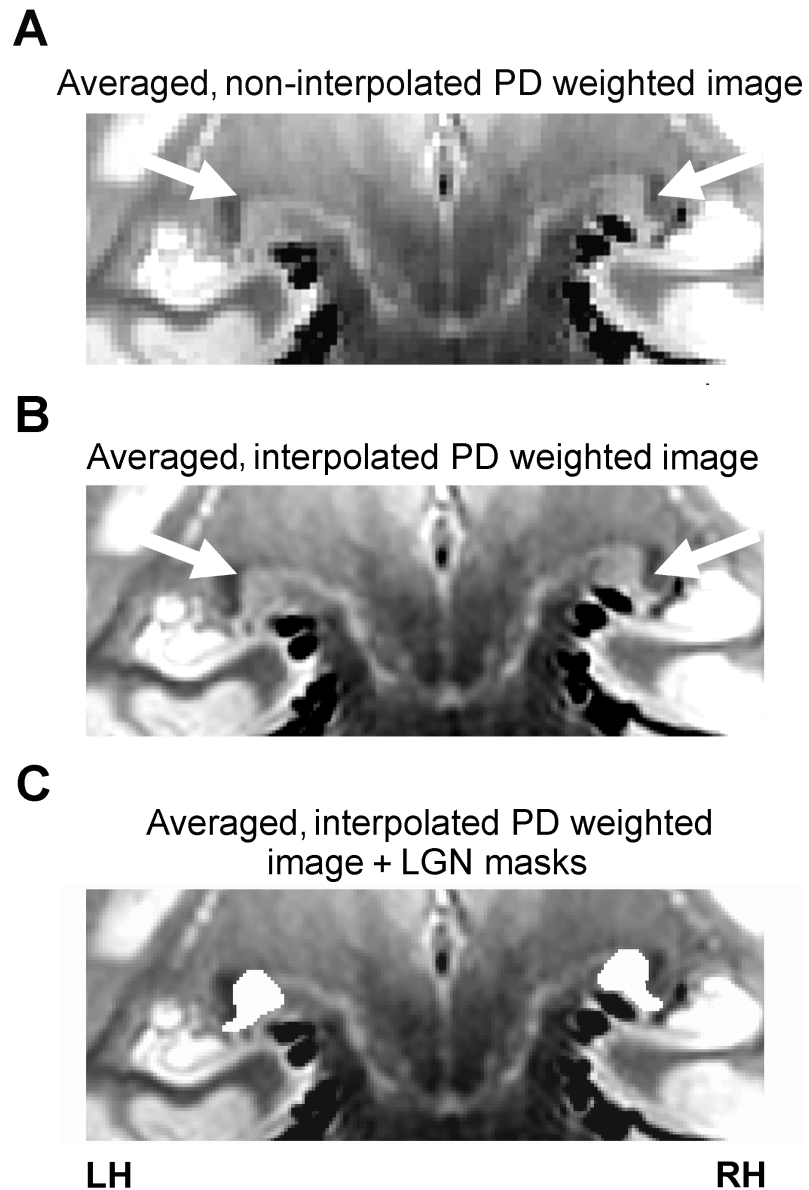


Figure 3.3. Coronal slice of an averaged PD weighted image depicting the LGN (white arrows) of a control participant when the PD images were (A) not interpolated and when they were (B) interpolated. Left and right ROI tracings of the LGN (white) in the averaged, interpolated PD weighted image are also shown (C).

Results

Whole Brain Volume

No significant difference in whole brain volume was found for the early ME compared to control group, $t(38) = -0.90$, $p = 0.373$, and the whole brain volume of both groups were within the range previously reported for healthy controls (Allen, Damasio, & Grabowski, 2002; Ge et al., 2002). Therefore, whole brain volume was not factored into our analyses. (See Table 3.4 at the end of the results section for whole brain volumes per group).

Intra- and Inter-Rater Reliability

Intraclass correlation coefficient (ICC) reliability analyses were conducted to ensure consistent measurements within (intra) and between (inter) raters. For chiasm measurements, all intra-rater ICCs were above 0.71 and all inter-rater ICCs were above 0.79. For LGN volume, all intra-rater ICCs were above 0.98 and all inter-rater ICCs were above 0.87. ICCs above 0.7 are considered to reflect a strong agreement between measures (Cohen, 2001), thus our ICCs indicate that measurements were consistent both within and between raters.

Optic Chiasm Measurements

Optic chiasm measurements were within the range previously reported for healthy controls (Parravano, Toledo, & Kucharczyk 1993; Schmitz et al., 2003. Wagner, Murtagh, Hazlett, & Arrington, 1997). Consistent with other research (Wagner et al.,

1997), no significant sex differences in optic chiasm width (X and Y planes) or volume were found for the control group ($ps \geq 0.264$).

A 2×3 analysis of variance (ANOVA) with age as a covariate, group (control, early ME) as the between-groups variable, and chiasm measurement (volume, X plane width, Y plane width) as the within-groups variable revealed a significant group \times chiasm measurement interaction, $F(1,37) = 68.92$, $p < 0.001$. A significant main effect of group was also found, $F(1,37) = 68.99$, $p < 0.001$.

Post-hoc pairwise comparisons (Bonferroni-adjusted alphas = 0.017) revealed that the early ME group had significantly decreased chiasm volume, and chiasm widths in the X and Y planes compared with the control group ($ps \leq 0.002$). Figure 3.4 shows mean optic chiasm X and Y plane width and chiasm volume per group. (See also Table 3.4 at the end of the results section for optic chiasm measurements per group).

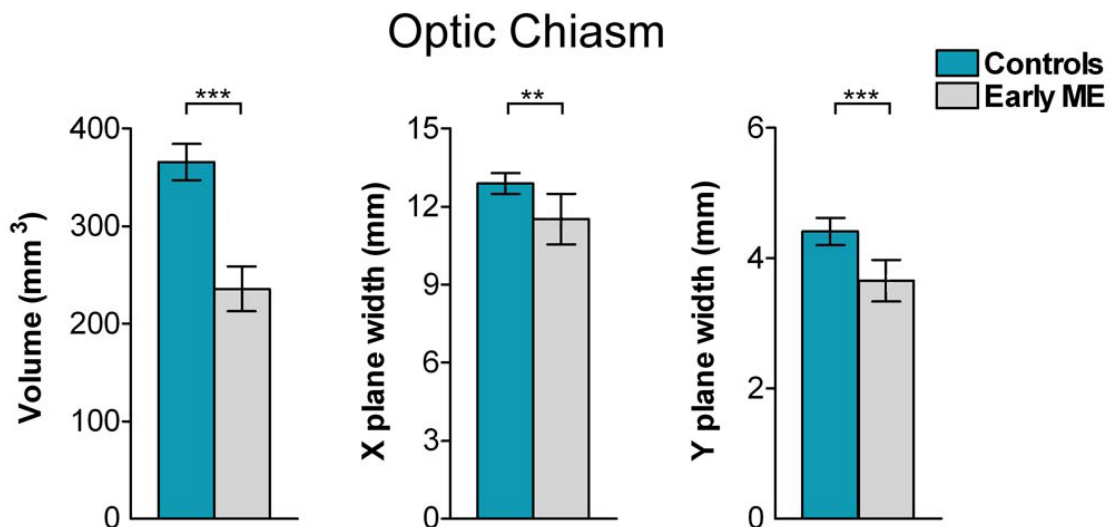


Figure 3.4. Bar graphs depicting mean optic chiasm volume (mm³), and mean optic chiasm width (mm) in the X and Y planes, for the control (blue bars) and early ME (grey

bars) groups. The early ME group exhibited significant decreases in all chiasm measures compared with the control group. Error bars represent $\pm 95\%$ confidence intervals (CIs). $**p < 0.01$; $***p < 0.001$.

Optic Nerve and Optic Tract Diameter

No significant difference in diameter between left and right optic nerves, and left and right optic tracts, was found in the control group ($ps \geq 0.570$) and these diameters were within the range previously reported for healthy controls (Parravano et al., 1993; Schmitz et al., 2003; Wagner et al., 1997). Consistent with other research (Jonas, Schmidt, Müller-Bergh, Schlötzer-Schrehardt, & Naumann, 1992), no significant sex differences in optic nerve and optic tract diameter were found for the control group ($ps \geq 0.354$). (See Table 3.2 for information regarding the left and right optic nerves and tracts of the control group.)

Table 3.2. Mean (SD) left and right optic nerve and optic tract diameter, and LGN volume in the control group.

| | Optic nerve diameter (mm) | Optic tract diameter (mm) | LGN Volume (mm ³) |
|-------|------------------------------|------------------------------|----------------------------------|
| Left | 4.7(0.5) | 4.2(0.4) | 155(32) |
| Right | 4.8(0.5) | 4.3(0.4) | 164(32) |

A $2 \times 2 \times 2$ ANOVA with age as a covariate, group (control, early ME) as the between-groups variable, and side (ipsilateral, contralateral) and diameter (optic nerve, optic tract) as the within-groups variables revealed a significant group \times side \times diameter interaction, $F(1,37) = 36.01$, $p < 0.001$. A trend towards a diameter \times group interaction approached significance, $F(1,37) = 3.39$, $p = 0.074$. Significant main effects of diameter, $F(1,37) = 11.69$, $p = 0.002$, and group, $F(1,37) = 44.08$, $p < 0.001$, were also found.

Post-hoc pairwise comparisons (Bonferroni-adjusted alphas = 0.013) revealed that the early ME group had significantly decreased contralateral optic nerve, and contralateral and ipsilateral optic tract diameters compared with the control group ($ps < 0.001$). There was no significant difference for ipsilateral optic nerve ($p = 0.271$) between groups. The early ME group exhibited asymmetries (Bonferroni-adjusted alphas = 0.025) where the contralateral optic nerve diameter was significantly decreased relative to the ipsilateral optic nerve, and the contralateral optic tract diameter was significantly increased relative to the ipsilateral optic tract ($ps < 0.001$). No significant asymmetries in optic nerve or tract diameter were found for the control group ($ps \geq 0.569$). Figure 3.5 shows optic chiasms from (A) typical control and (B) early ME participants, and bar graphs for mean (C) optic nerve and (D) optic tract diameter per group. (See also Table 3.4 at the end of the results section for optic nerve/tract diameters per group).

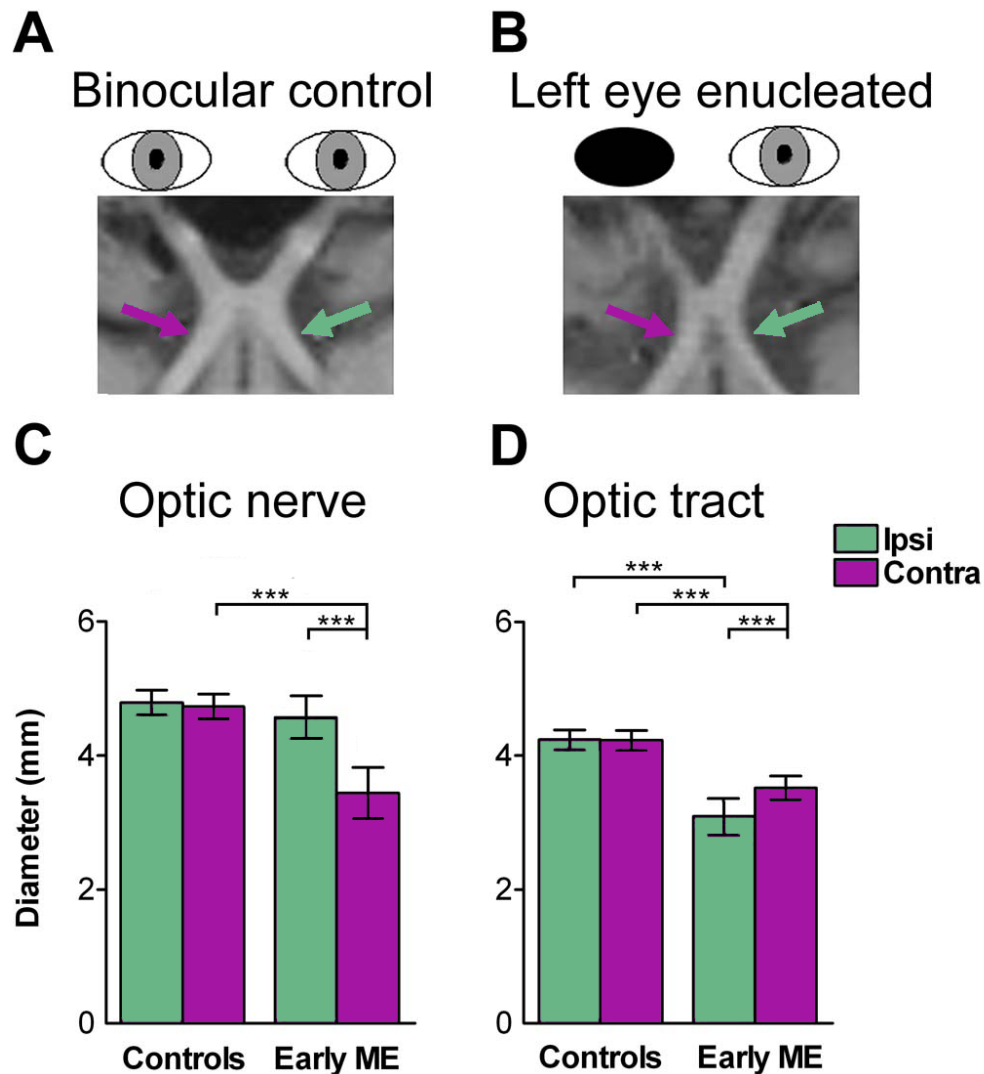


Figure 3.5. The optic nerves, chiasm, and tracts of a (A) typical control and (B) early ME participant are shown in reformatted T₁ weighted images. Bar graphs are also shown depicting the mean diameter (mm) for (C) optic nerves and (D) optic tracts ipsilateral (Ipsi: green bars) and contralateral (Contra: purple bars) to the dominant eye in the control group and remaining eye in the early ME group. The early ME group exhibited significantly decreased diameter for the contralateral optic nerve and both optic tracts compared with the control group. The early ME group also exhibited an asymmetry that

was not present in the control group: the contralateral optic tract (purple arrow) was significantly increased compared with the ipsilateral optic tract (green arrow) relative to the remaining eye. Error bars represent $\pm 95\%$ CIs. *** $p < 0.001$.

LGN Volume

No significant difference in volume between left LGN and right LGN was found for the control group ($p = 0.200$), and these volumes were within the range previously reported for healthy controls (Andrews et al., 1997; Dai et al., 2011; Putnam, 1926). Consistent with other research (Li et al., 2012), no significant sex differences in LGN volume were found for the control group ($ps \geq 0.322$).

A 2×2 ANOVA with age as a covariate, group (control, early ME) as the between-groups variable and side (ipsilateral, contralateral) as the within-groups variable revealed a significant group \times side interaction, $F(1,20) = 5.56$, $p = 0.029$, and a significant main effect of group, $F(1,20) = 14.21$, $p = 0.001$. No significant main effect of side was found, $F(1,20) = 0.35$, $p = 0.558$.

Post-hoc pairwise comparisons (Bonferroni-adjusted alphas = 0.025) revealed that compared with the control group, the early ME group had significantly decreased ipsilateral LGN volume ($p < 0.001$) and a tendency for significantly decreased contralateral LGN volume ($p = 0.045$) that approached significance. Further, post-hoc pairwise comparisons (Bonferroni-adjusted alphas = 0.025) revealed that the early ME group exhibited a significant asymmetry with a decrease in ipsilateral compared with contralateral LGN volume ($p = 0.017$). The control group did not exhibit this asymmetry

($p = 0.658$). Figure 3.6 shows PD weighted images of (A) typical control and (B) early ME participants, as well as a (C) bar graph for mean LGN volume per group. (See Table 3.3 for percent differences in the early ME group compared with controls for optic nerve, chiasm, and tract measurements and LGN volume).

Upon exploration of the data, only one early ME participant (ME05) showed the opposite asymmetry pattern where the ipsilateral LGN was larger relative to the contralateral LGN. When this participant was removed from the analyses, we see no significant group difference for the contralateral LGN ($p = 0.10$), and an even larger within group difference for the early ME group where the contralateral LGN (Mean = 133 mm³, SD = 26 mm³) was significantly smaller than the ipsilateral LGN (Mean = 98 mm³, SD = 24 mm³) ($p = 0.003$). We could not find any reason to account for this participant's differences from other early ME participants (i.e., no cognitive deficits or neural disease, no visual abnormalities in remaining eye) and individual variability in LGN size and shape may be a contributing factor (Andrews et al., 1997; Hickey & Guillery, 1979).

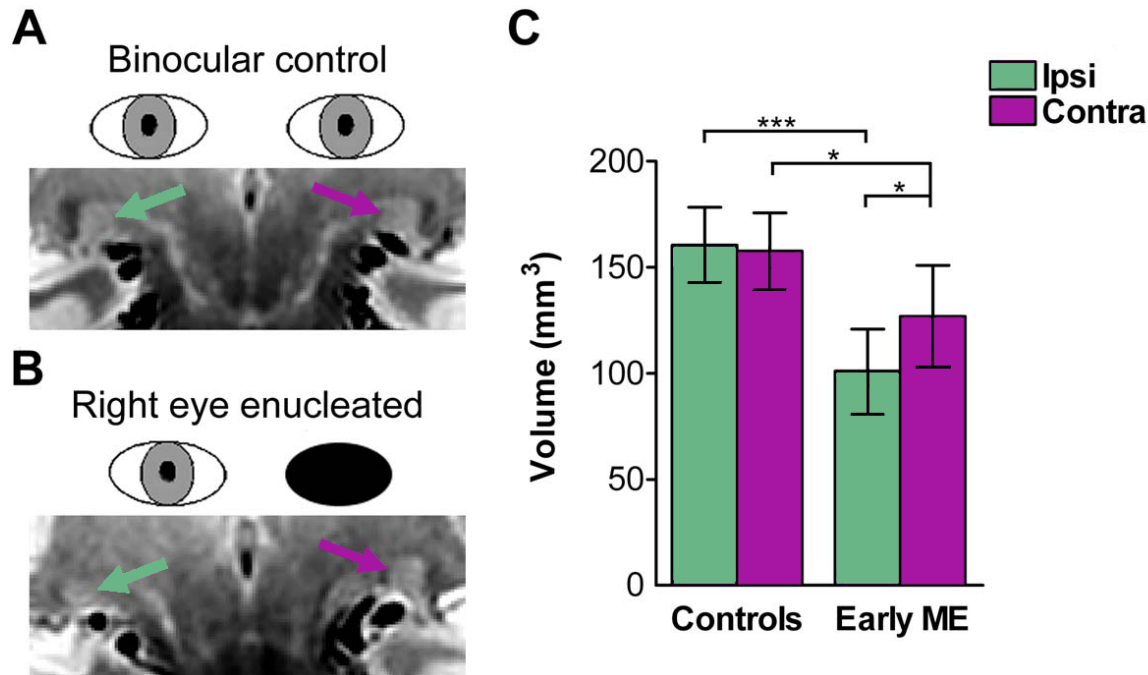


Figure 3.6. PD weighted images depicting the LGN ipsilateral (green arrow) and contralateral (purple arrow) to the dominant eye for a (A) typical control and remaining eye in a (B) typical early ME participant. A bar graph is shown (C) depicting mean LGN volumes (mm³) ipsilateral (Ipsi: green bars) and contralateral (Contra: purple bars) to the dominant eye in the control group and remaining eye in the early ME group. Compared with the control group, the early ME group exhibited volume decreases in both LGN. The early ME group also exhibited an asymmetry that was not present in the control group: contralateral LGN volume was significantly increased relative to ipsilateral LGN relative to the remaining eye. Error bars represent $\pm 95\%$ CIs. * $p < 0.05$; *** $p < 0.001$.

Timing of Deprivation

Partial correlations controlling for age (uncorrected alpha) revealed a significant positive correlation between AAE in the early ME group and the enucleated eye's optic nerve morphology such that earlier eye removal was associated with smaller optic nerve width, $r(9) = 0.63$, $p = 0.039$. However, the participant enucleated at 48 months of age was an outlier, and this correlation became non-significant after this participant was removed from the analysis, $r(8) = 0.26$, $p = 0.474$. Therefore no significant relationship with AAE was found for any of the chiasm measurements ($ps \geq 0.177$) or for LGN volume ($ps \geq 0.600$).

Late ME Participant

We gathered morphological data from one late ME participant (Table 3.4 and Figure 3.7). We used a modified t-test (Crawford & Garthwaite, 2002) designed to compare one individual case (i.e., the late ME participant) to a group of individuals (i.e., control and early ME groups). Table 3.4 shows chiasm measurements and LGN volume for the late ME participant. See Table 3.3 for percent differences in chiasm and LGN volume in the late ME participant relative to the control group and to the early ME group. Percent difference for each chiasm measurement and LGN volume were calculated using the following formula: % difference = (Comparison – late ME)/Comparison \times 100.

Late ME versus control group. Compared with the control group, the late ME participant exhibited decreased ipsilateral optic tract diameter, $t(27) = -2.04$, p (one-tailed) < 0.050 . No other differences between the late ME participant and control group were found for any of the remaining chiasm measurements. The late ME participant exhibited significantly decreased volume for both ipsilateral, $t(7) = -2.55$, p (one-tailed) < 0.025 , and contralateral, $t(7) = -2.44$, p (one-tailed) < 0.025 , LGN compared with the control group. When the late ME participant was compared to age- and sex-matched controls, the same pattern of results was found, with the addition of further decreases in chiasm width in the Y plane, $t(1) = -3.55$, p (one-tailed) < 0.05 , and in chiasm volume, $t(1) = -7.27$, p (one-tailed) < 0.05 . However, only two age-matched controls were available for chiasm measurements, and one for LGN volume suggesting this comparison should be interpreted with caution.

Late ME versus early ME group. Compared with the early ME group, the late ME participant exhibited increased contralateral optic tract diameter, $t(11) = 2.90$, p (one-tailed) < 0.01 , and increased chiasm volume, $t(11) = 2.07$, p (one-tailed) < 0.05 . No other difference between the late ME participant and early ME group was found. The same pattern of results was found for chiasm measurements when the late ME was compared to an age- and sex-matched early ME participant, although no matched early ME participant was available for LGN volume comparison. While the late ME participant did exhibit the pattern of increased contralateral relative to ipsilateral optic tract diameter, this participant did not exhibit the LGN asymmetry found in the early ME group.

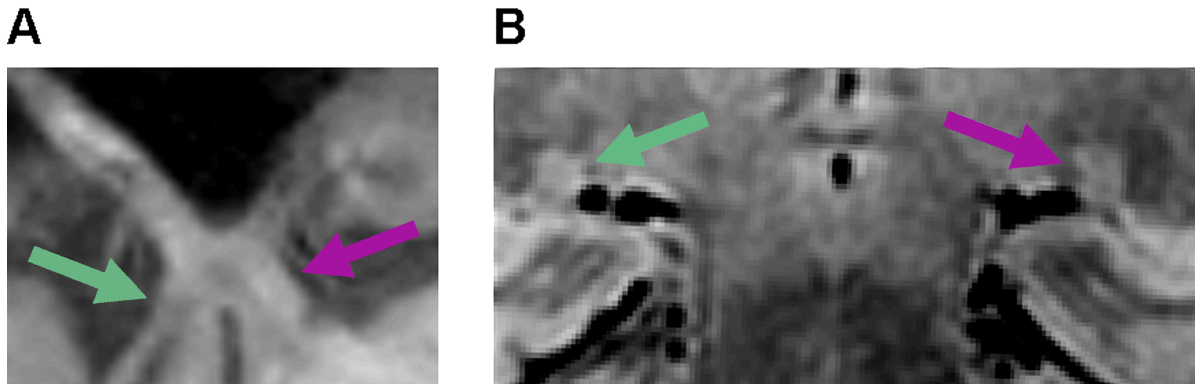


Figure 3.7. A T₁ weighted image showing the (A) optic nerves, chiasm, and tracts, and (B) an averaged PD image showing both LGN from the late ME (right eye enucleated) participant. The chiasm and LGN were decreased in size compared with controls. While the late ME participant showed an increase in contralateral (purple arrow) relative to ipsilateral (green arrow) optic tract diameter, there was no asymmetry between ipsilateral and contralateral LGN volumes.

Table 3.3. Percent (%) decrease of chiasm structures and LGN volume for the early ME group and the late ME participant relative to controls. Percent decrease relative to the average of two age- and sex-matched controls and one age- and sex-matched early ME participant for the chiasm are also shown for the late ME participant for the chiasm structure, and relative to one age- and sex-matched control for LGN volume. [% decrease = (Controls – ME)/Controls × 100].

| Comparison | Optic nerve diameter (mm) | | Optic chiasm width (mm) | | Optic chiasm volume (mm ³) | Optic tract diameter (mm) | | LGN Volume (mm ³) | |
|---------------------------|------------------------------|--------|----------------------------|------------|-------------------------------------------|------------------------------|--------|----------------------------------|--------|
| | Ipsi | Contra | X Plane | Y Plane | | Ipsi | Contra | Ipsi | Contra |
| | | | | | | | | | |
| Early ME: Controls | 4% | 28% | 11% | 16% | 35% | 26% | 17% | 37% | 19% |
| Late ME: Controls | -10% | 13% | 9% | 16% | 16% | 19% | -2% | 49% | 50% |
| Late ME: Matched Controls | 3% | 26% | 20% | 28% | 21% | 26% | -5% | 45% | 55% |
| Late ME: Early ME | -15% | 21% | -2% | 0% | -30% | -10% | -23% | 20% | 39% |
| Late ME: Matched Early ME | -13% | -11% | 8% | -2% | -51% | 3% | -9% | N/A | N/A |

Table 3.4. Descriptive statistics for the control and early ME groups showing the mean ($\pm 95\%$ CIs) optic nerve diameter, optic chiasm width in the X and Y planes, optic chiasm volume, optic tract diameter, LGN volume, and whole brain volume. Values for each measurement are also shown for one late ME participant.

| | Optic nerve diameter (mm) | | Optic chiasm width (mm) | | Optic chiasm volume (mm ³) | Optic tract diameter (mm) | | LGN Volume (mm ³) | Whole brain volume (cm ³) | |
|----------|------------------------------|-----------|----------------------------|-----------|-------------------------------------------|------------------------------|------------------|----------------------------------|------------------------------------------|----------|
| Group | Ipsi ^a | Contra | X Plane | Y Plane | | Ipsi | Contra | Ipsi | Contra | |
| Control | 4.8(0.2) | 4.7(0.2) | 12.9(0.4) | 4.4(0.2) | 365(18) | 4.2(0.2) | 4.2(0.2) | 160(18) | 157(18) | 1098(41) |
| Early ME | 4.6(0.3) | 3.4(0.4)* | 11.5(1.0)* | 3.7(0.3)* | 236(23)* | 3.1(0.3)* | 3.5(0.2)* | 101(20)* | 127(24)* | 1130(61) |
| Late ME | 5.3 | 4.1 | 11.7 | 3.7 | 307 [†] | 3.4* | 4.3 [†] | 81* | 78* | 1069 |

^aIpsilateral to the dominant eye for controls or the remaining eye for ME participants.

* Significantly different from control group.

[†]Significantly different from early ME group.

Discussion

Compared with binocularly intact controls, we found morphological changes in the adult anterior visual system subsequent to early monocular enucleation due to retinoblastoma. Consistent with previous research (Beatty et al., 1982; Goldby, 1957; Hickey & Guillery, 1979; Horton, 1997), the early ME group exhibited significant degeneration of this system, which is expected given that half of visual inputs to the brain are removed during development. Surprisingly, however, we found an asymmetry in morphology where optic tracts and LGN decreases were less severe contralateral to the remaining eye. This novel finding has not previously been reported by enucleated monkey and human studies (Beatty et al., 1982; Goldby, 1957; Hendrickson & Tigges, 1985; Horton, 1997; Hubel et al., 1977; Matthews, 1964; Rakic, 1981; Sloper et al., 1987a), which may reflect the failure of these other studies to assess long-term survival following eye enucleation that occurs early in life. This notion is supported by the large LGN volume decreases but a lack of asymmetry in contralateral/ipsilateral LGN volume in our late-enucleated participant, coupled with marked geniculate cell degeneration in previous late enucleation studies (e.g., Beatty et al., 1982; Goldby 1957). Our findings suggest that the complex postnatal organization of the visual system is altered following monocular enucleation that occurs during postnatal critical periods when the brain is still developing. Our data also suggest that although the anterior visual system is morphologically adult-like by 9 months of age (de Courten & Garey, 1982; Garey & de Courten, 1983), its critical developmental period extends beyond this age.

Morphological Asymmetry

The optic tract and LGN morphological asymmetry observed in our study with early monocular enucleation is consistent with stronger functional activation in primary visual cortex (V1) contralateral to the remaining eye of anaesthetized early-enucleated children (Barb et al., 2011), and in contralateral LGN and V1 of monocular viewing controls during ipsilateral eye stimulation (Miki et al., 2001; Toosy et al., 2001). The asymmetry is also consistent with morphological studies of enucleated rodents and rabbits that exhibit a contralateral bias in retinal projections and LGN size (Godement et al., 1987; Guillery, 1989; Khan, 2005). It is speculated that the disparity in previous results between enucleated primates and rodents is due to the difference in spatial layout of the chiasm during development. In binocularly intact rodents, retinal fibres mingle within the chiasm prior to projecting to either hemisphere. Axon guidance is considered to rely on this mingling and abnormal projections occur when retinal fibres from one eye are lacking (Neveu et al., 2006). In primates, enucleation is thought to have no impact on the remaining eye's projections since retinal projections are spatially segregated and no mingling occurs (Jeffery et al., 2008; Taylor & Guillery, 1995). Our data, however, do not support this theory since we do see asymmetries comparable to those found in rodents. Our findings therefore indicate the importance of surviving past the developmental stage in order to observe effects that early enucleation may have on the visual system. Possible explanations of this altered development must be explored.

Possible Mechanisms of Altered Visual Development

Normal visual development depends on the presence of activity-driven binocular interactions during postnatal maturation that are lacking with monocular enucleation (Sloper, 1993). For example, segregation of eye-specific laminae in the LGN and area V1 relies on balanced binocular competition for space. Subsequent cell maintenance relies on binocular cooperation, but enucleation eliminates this cooperation and results in geniculate cell shrinkage (Sloper, 1993; Sloper et al., 1987a). The LGN asymmetry found in our study may reflect changes in response to the loss of these binocular interactions. Here, we posit several possible mechanisms of altered visual development. First, aberrant connections may be formed between the remaining eye and geniculate cells associated with the enucleated eye, a phenomenon that has been observed in enucleated monkeys (Rakic, 1981). The contralateral bias in the optic tracts of our early ME participants, as well as that previously seen for enucleated rodents (Godement et al., 1987; Guillery, 1989), suggests that the crossed nasal fibres may be behind this cell recruitment. In line with this are behavioural data showing a preference for nasalward over temporalward motion for eye movement responses, specifically optokinetic nystagmus (Day, 1995; Reed et al., 1991), and for coherent motion discrimination (Steeves, González, Gallie, & Steinbach, 2002) in early monocularly enucleated patients. Further supporting this notion are behavioural findings of earlier development of peripheral acuity in the temporal visual field (i.e., nasal retina) compared with nasal visual field (i.e., temporal retina) (Courage & Adams, 1996; Lewis & Maurer, 1992), and morphological data showing higher cone density in the nasal relative to temporal retina in adults (Curcio, Sloan, Kalina, & Hendrickson, 1990). Evidence against this notion

stems from the prenatal establishment of retinal projections and laminar distribution of geniculate cells (Blakemore & Vital-Durand, 1986; de Courten & Garey, 1982; Rakic, 1976), and postnatally equivalent growth rates of geniculate cells in layers receiving crossed and uncrossed inputs in monkeys (Gottlieb, Pasik, & Pasik, 1985). The late ME participant in our study exhibited an optic tract asymmetry comparable to that found for the early ME group, but no LGN asymmetry since volume in both LGN was decreased by about half compared with controls. Hence, the recruitment of geniculate cells via crossing nasal fibres may not be the only factor contributing to the LGN asymmetry found in our early ME group and additional factors must be considered. For example, it is also possible that optic tract asymmetries reflect, in part, altered development of the retinotectal pathway, as seen in early-enucleated rodents (Woo, Jen, & So, 1985). Further, neurons within parvocellular laminae of monkeys are more adversely affected by early monocular enucleation compared with neurons in magnocellular laminae (Sloper et al., 1987a). This discrepancy may account for some of the observed volume asymmetry in the LGN, particularly given that parvocellular layers comprise a larger proportion of the LGN.

Another plausible mechanism for the observed asymmetry is that feedback connections from V1 are promoting the retention of deafferented geniculate cells during development, and this retention is stronger in the hemisphere contralateral to the remaining eye. Support for feedback from V1 stems from data showing the presence of binocular rivalry within the LGN of healthy controls (Wunderlich, Schneider, & Kastner, 2005), and by retrograde degeneration of the right, but not left, LGN following right occipital lobe removal (Beatty et al., 1982). Geniculate axons pass through the optic

radiation to synapse with neurons in layer IV of area V1 and form ocular dominance columns — alternating columns of cells that are eye-specific. Binocularly intact monkeys have a greater contribution of crossed nasal retinal inputs to ocular dominance columns (Tychsen & Burkhalter, 1997) and monocular viewing controls and early-enucleated children exhibit a contralateral bias in functional activity in V1 (Barb et al., 2011; Toosy et al., 2001). Together, these findings suggest that V1 receives stronger physiological inputs from the contralateral eye. Similar to geniculate laminae, ocular dominance columns require binocular interactions such as competition to develop in a normal fashion; however, they are only partially segregated at birth (Horton & Hocking, 1998a; Rakic, 1976; Sloper, 1993). Since monocular enucleation completely obliterates ocular dominance columns in monkeys and humans (Horton & Hocking, 1998a; Rakic, 1981), the remaining eye may be recruiting deafferented space within V1 while it is still maturing. A greater portion of visual cortex devoted to the remaining eye, particularly in the contralateral hemisphere, would translate into a stronger feedback signal to the LGN and cell preservation could occur predominantly in the LGN contralateral to the remaining eye. Consequently, some retinal fibres, especially the crossed nasal fibres, would also be preserved.

Alternatively, it could be argued that the observed LGN asymmetry solely reflects disproportionate neuronal degeneration due to the slightly unequal distribution of crossed versus uncrossed (~ 58:42) fibres found in the human and non-human primate visual systems (Chacko, 1948; Horton, 1997). However, the decreases in optic tract width and LGN volume in the early ME group relative to the control group does not reflect this slight proportional asymmetry — decreases were much less than 50%, which

would not be expected if neuronal degeneration was the sole determinant of changes in this population. While contralateral reductions were mild relative to the control group (optic tract = 17%; LGN = 19%), ipsilateral reductions were much more severe in the early ME group (optic tract = 26%; LGN = 37%) (Table 3.3). For example, when comparing to controls, volume decrease in the ipsilateral LGN of the early ME participants was almost double compared with that found in the contralateral LGN. Asymmetries should also be reflected with late monocular enucleation, yet an asymmetry has not been observed in previous late enucleation studies, nor in our late ME participant who exhibited large volume decreases in both LGN (~ 50%) compared with controls and in the contralateral LGN (~40%) compared with the early ME group. One study found a ratio of 53:47 for crossed versus uncrossed projections in a late enucleated man (Kupfer, Chumbley, & Downer, 1967), which is less asymmetrical than that found for binocularly intact human and non-human primates (~ 58:42) (Chacko, 1948; Horton, 1997). Lastly, anophthalmic patients born with only one eye exhibit symmetrical visual evoked potentials (VEPs) in visual cortex, reflecting an equal decussation of retinal fibres at the chiasm (Neveu et al., 2006). Therefore, an unequal number of nasal versus temporal retinal projections to the visual system cannot completely account for the asymmetries observed in our study. It is more likely that the asymmetry reflects reorganization during development via aberrant synaptic connections and/or feedback from contralateral V1 to retain deafferented geniculate cells.

Anterior Visual System Degeneration

Although altered visual development was apparent in our early ME group, relative decreases were nonetheless present in both chiasm and LGN measures compared with binocularly intact controls. Wallerian degeneration of axons can occur when the optic nerve is severed and explains the decreases in chiasm structures found with our early ME group and late ME participant. However, the mean diameter of the enucleated eye's optic nerve was not even decreased by half, which suggests the presence of Wilbrand's knee — an artefact of enucleation where crossed fibres of the remaining eye loop into the contralateral optic nerve before heading to the chiasm and tract. This phenomenon may be caused by the shrinkage of the optic chiasm (Horton, 1997).

While we cannot say with certainty that decreases observed in MRI volumes and diameters represent an actual decrease in neuron counts, neuron size, or smaller versus fewer fibres, we know that the total chiasm diameters are smaller and total LGN volumes are smaller. As mentioned earlier, maintenance of cells within the LGN relies on activity-driven cooperation between the two eyes (Sloper, 1993; Sloper et al., 1987a). Since the LGN is well developed at birth (de Courten & Garey, 1982; Garey & de Courten, 1983), decreases in the LGN of our early ME participants likely reflect a decrease in neuron size (Sloper et al., 1987a), and/or transneuronal degeneration as a result of the loss of synaptic input and binocular cooperation (Goldby, 1957). Unbalanced binocular cooperation has been shown to disrupt LGN development in other forms of monocular deprivation such as amblyopia where the quality of visual input from both eyes is unequal (Barnes et al., 2010). Degeneration was also found with the late ME participant in our study, and at least for the LGN, these decreases were larger than the early ME

group. Degeneration of the anterior visual system occurs with visual deprivation at any age; however, this degeneration is less severe with earlier monocular enucleation suggesting altered development that may be compensating for early eye loss.

Conclusions

In conclusion, we examined morphological development of the anterior visual system in a group of adults who had one eye enucleated early in life due to retinoblastoma. In contrast to previous research, we observed an asymmetry in morphology where decreases were less severe in the optic tracts and LGN contralateral to the remaining eye. This novel finding indicates a possible recruitment of deafferented geniculate cells via the crossing nasal fibres and/or stronger feedback signals from contralateral V1 that aids in the retention of deafferented cells. Altered visual system development may help explain the lack of spatial form vision deficits in this population. In line with previous notions of plasticity and consistent with previous research on late enucleation, a lack of asymmetry but substantial decrease in volume of both geniculate nuclei in the late-enucleated participant indicates a stronger malleability of the brain following visual deprivation that occurs earlier rather than later in life. These data highlight the importance of balanced binocular input during postnatal maturation for anterior visual system morphology. Future studies should expand on these data to determine whether visual areas and white matter integrity within the visual cortex are also affected by early monocular enucleation in humans.

CHAPTER IV

ALTERED CORTICAL DEVELOPMENT FOLLOWING EARLY MONOCULAR ENUCLEATION

The visual system is only partially developed at birth and takes years to fully mature (for reviews see Atkinson, 2000 and Daw, 2006). Studies on animals and humans with postnatal monocular deprivation from lid suture, congenital cataracts, and strabismus show adverse effects during visual system development on visual behaviour (e.g., Barnes et al., 2010; Ellemberg, Lewis, Maurer, & Brent, 2000; Wiesel & Hubel, 1963a,b, 1965). For example, postnatal monocular deprivation in humans results in deficits in both spatial form vision (e.g., acuity, contrast sensitivity) and motion perception (e.g., direction discrimination) that persist later in life in the deprived and non-deprived eyes (Ellemberg et al., 2000; Ellemberg, Lewis, Maurer, Brar, & Brent, 2002; Lewis, Maurer, Tytla, Bowering, & Brent, 1992; McKee, Levi, & Movshon, 2003; Reed, Steeves, Steinbach, Kraft, & Gallie, 1996; Simmers, Ledgeway, Hess, & McGraw, 2003; Woo & Irving, 1991). Further, monocular deprivation from strabismus and anisometropia leads to morphological changes of the visual system, including reductions in grey matter concentration in lateral geniculate nuclei (LGN) (Barnes et al., 2010) and in grey matter volume in visual cortex (Mendola et al., 2005; Xiao et al., 2007). These findings suggest that it is imperative for the postnatal visual system to receive balanced binocular input for typical development. Although these forms of deprivation provide an excellent model for studying monocular deprivation, the brain nonetheless receives anomalous visual input from the deprived eye. As a result, the effects of complete monocular deprivation cannot be easily inferred.

Studying individuals who have had one eye enucleated (surgically removed) early in life due to retinoblastoma (cancer of the retina) can aid in determining the effects of *total* monocular deprivation on visual system development. Retinoblastoma has a high

survival rate (97%), and eye enucleation is the most frequent and effective treatment due to the aggressive nature of the tumour. Although retinoblastoma is rare, it accounts for 6% of all childhood cancers and generally occurs before 5 years of age (Broaddus, Topham, & Singh, 2009a,b). Monocular enucleation at such a young age is likely to alter visual system development since half of the inputs are deafferented at a time when the brain is not fully mature.

In the present study, we focus on morphological development of visual cortex following long-term survival from enucleation due to retinoblastoma in human adults. Visual information in the binocularly intact primate visual pathway is first sent to the LGN, a bilateral thalamic nucleus that processes information from each eye in separate layers. LGN afferents then travel to the ipsilateral occipital lobe to terminate in primary visual cortex (V1) in layer IVc, which consists of alternating bands of eye-specific ocular dominance columns (Horton, Dagi, McCrane, & de Monasterio, 1990; Hubel & Wiesel, 1969; LeVay, Hubel, & Wiesel, 1975). Information from cells in layer IV project to cells in other layers of V1 where information from both eyes is finally integrated and sent to areas beyond V1, including visual area V2 (Hubel & Livingstone, 1987). Although V1 is adult size in volume by 4 months of age (Garey & de Courten, 1983; Huttenlocher & De Courten, 1987), it is still quite immature and continues to develop morphologically into adolescence. For example, synapses continue to form postnatally, a process called synaptogenesis, and synaptic density reaches its maximum between 6 and 9 months of age (Garey & de Courten, 1983). Following this, a period of synaptic loss occurs where half of the synapses are pruned to adult levels by 11 years of age (Garey & De Courten, 1983; Huttenlocher, 1990; Huttenlocher, de Courten, Garey, & Van der Loos, 1982).

Further, myelination of axons in cerebral cortex occurs rapidly during the first few years of life and continues more slowly into adolescence (Barnea-Goraly et al, 2005; Gao et al, 2009; Giedd et al., 1999). Finally, ocular dominance columns are partially segregated at birth and cells are equally innervated by both eyes (LeVay, Wiesel, & Hubel, 1980; Rakic, 1976, 1977; Sloper, 1993). Segregation completes by 6 months of age and relies on Hebbian competition between the two eyes for cortical space (Hickey & Peduzzi, 1987; Horton & Hocking, 1998a; reviewed in Howard, 2002 & Katz & Crowley, 2002).

Given the immaturity of the postnatal visual system, removing half of the inputs during the postnatal critical period is likely to disrupt development. Behaviourally, early monocular enucleation impairs motion perception in adults (e.g., speed discrimination, motion-defined letter recognition) (Kelly, Zohar, Gallie, & Steeves, 2013b; Steeves, González, Gallie, & Steinbach, 2002), indicating that balanced binocular input is crucial for development of this visual ability. However, spatial form vision (e.g., contrast sensitivity and discrimination, global shape discrimination) remains intact or is enhanced in this group (Kelly, et al., 2013b; Nicholas, Heywood, & Cowey, 1996; Steeves, Wilkinson, González, Wilson, & Steinbach, 2004), suggesting that reorganization occurs in regions associated with spatial form vision to compensate for the loss of an eye early in life. (See Kelly, Moro, & Steeves, 2013a and Steeves, González, & Steinbach, 2008 for a review).

Behavioural visual development is well-documented following early enucleation; however, less is understood regarding the long-term consequences on morphological visual development in adult humans. Animal models of enucleation are well established and show that non-primate mammals such as mice, ferrets, and rabbits

exhibit increased crossed, but decreased uncrossed, projections from the remaining eye (Godement, Salaun, & Metin, 1987; Grigonis, Pearson, & Murphy, 1986; Guillery, 1989), and rabbits exhibit a 50% reduction in volume of the deafferented LGN (Grigonois et al., 1986). Within visual cortex, early-enucleated mice display an expansion and accelerated refinement of retinotopic area V1 (Faguet, Maranhao, Smith, & Trachtenberg, 2009; Smith & Trachtenberg, 2007), as well as decreased neuronal density and metabolic activity in visual cortex contralateral to the enucleated eye (Chow et al., 2011; Heumann & Rabinowicz, 1982). The non-primate mammalian visual pathway is inherently different from primates given the cross-over of the majority of retinal projections in non-primates but hemisdecussation in primates. As a result, the findings from non-primate mammals cannot fully generalize to the human enucleated system; therefore, we must compare to non-human primates. In monkeys, postnatal monocular enucleation is associated with cell degeneration, and a reduction in or lack of geniculate layers and ocular dominance columns associated with the enucleated eye (Horton & Hocking, 1998a; Rakic, 1981; Sloper, Headon, & Powell, 1987a,b). However, one study found the typical pattern of stripes within area V2 using cytochrome oxidase staining, suggesting that morphologically, V2 remains unaffected by early enucleation (Horton & Hocking, 1998a).

The majority of monocular enucleation studies in humans consist of post-mortem brains of children whose visual system had not yet reached maturity, or adults who lost an eye during adulthood when the critical period for development has long been surpassed. Individuals enucleated during adulthood exhibit degeneration of the optic chiasm and LGN in deafferented laminae (Beatty, Sadun, Smith, Vonsattel, & Richardson, 1982; Goldby, 1957; Hardmann, Halpin, Hourihan, Mars, & Lane, 1997;

Horton, 1997; Kelly, McKetton, Schneider, Gallie, & Steeves, 2014). Within visual cortex, results for late enucleation are inconsistent. Decreased ocular dominance columns have been associated with the enucleated eye (Adams, Sincich, & Horton, 2007), a finding consistent with late-enucleated monkeys (Horton & Hocking, 1998b). In contrast, others report no changes in ocular dominance columns (Beatty et al., 1982). Physiologically, children who have been enucleated early in life have stronger functional activity in V1 contralateral to the remaining eye (Barb et al., 2011). Morphologically, early enucleation at 6 years of age has been shown to result in degenerated LGN layers (Hickey & Guillery, 1979). More recently, we have assessed long-term morphological development of the anterior visual system comprising the optic chiasm and LGN in adults who experienced early monocular enucleation (Kelly, et al., 2014). We found decreases in both structures compared with binocularly intact controls; however this decrease was less severe in the optic tract and LGN contralateral to the remaining eye. These data suggest a relative sparing of geniculate cells contralateral to the remaining eye, which may be attributed to recruitment of deafferented cells and/or feedback from ipsilateral V1 with early eye enucleation. One study examining visual cortex in children following early enucleation revealed a lack of ocular dominance columns (Horton & Hocking, 1998a), suggesting that the lack of binocular competition for cortical space alters the development of primary visual cortex. However, this study was conducted on children who died before their visual system was able to fully mature.

In the present study, we used structural magnetic resonance imaging (MRI) to conduct surface-based methods of analysis that are shown to be more sensitive to cortical changes in morphology than volume-based methods such as voxel-based

morphometry (VBM) (Ghosh, et al., 2010; Tucholka, Fritsch, Poline, & Thirion, 2012; Fischl et al., 2008). Cortical volume can be broken down into two measures, cortical thickness and surface area, that reflect distinct characteristics of brain morphology (Sanabria-Diaz et al., 2010; Winkler et al., 2010). These measures have been used to assess developmental disorders affecting vision, such as albinism (Bridge et al., 2012), congenital anophthalmia (Bridge, Cowey, Ragge, & Watkins, 2009) and congenital blindness (Jiang et al., 2009; Park et al., 2009; Qin, Liu, Jiang, & Yu, 2013). In general, these studies report increased cortical thickness but decreased surface area in early visual cortex in these patient groups.

Our aim was to expand upon our recent findings at the level of the optic chiasm and LGN (Kelly et al., 2014) to determine whether similar morphological changes are present in the posterior portion of the early-enucleated visual pathway following long-term survival in adult humans. We measured mean cortical thickness and total surface area of the cortical grey matter in a group of individuals who experienced early monocular enucleation due to retinoblastoma and compared their results to binocularly intact controls. We conducted: 1) whole brain analyses to examine regional differences across the entire cortical surface, 2) region-of-interest (ROI) analyses to examine differences in regions known to process spatial form vision (V1, V2) (Anzai, Peng, & Van Essen, 2007; Hubel & Livingstone, 1990; Tootell, Hamilton, & Switkes, 1988), and 3) correlations with age at enucleation to examine the effect of timing of deprivation on each morphology measure. Since this is the first study to examine morphology of the cortex following long-term survival from enucleation, it is difficult to predict what changes we will observe. On one hand, monocular enucleation may result in decreased surface

area but increased cortical thickness in early visual areas such as V1, consistent with previous visual deprivation studies (e.g., Jiang et al., 2009; Park et al., 2009). This finding would indicate altered morphological development of visual cortex as a result of early enucleation. Consistent with altered development, early monocular enucleation may also be associated with hemisphere asymmetries in early visual cortex, similar to the contralateral biases found for LGN volume (Kelly et al., 2014) and cortical activity in V1 (Barb et al., 2011). On the other hand, monocular enucleation may have no effect on morphological development in early visual cortex, consistent with studies reporting intact spatial form vision in this group (Kelly et al., 2013b; Nicholas et al., 1996; Steeves et al., 2004). This would suggest that the stream of normal visual input from the remaining eye, coupled with a lack of binocular competition, may aid in preserving visual cortex during development. Findings from this study will help elucidate the effects of early monocular enucleation on long-term, morphological visual development, and will provide insight into the requirements for typical visual system development.

Methods

Participants

Early Monocular Enucleation (ME) group. We tested a rare group of twelve adults (6 males) who were former patients at The Hospital for Sick Children in Toronto. Early ME participants had one eye enucleated (3 left eye removed) early in life due to retinoblastoma (cancer of the retina). Mean age (\pm SD) was 27.42 ± 11.90 years (range = 17 – 54 years) and mean age at enucleation (AAE) (\pm SD) was 18.67 ± 11.27 months

(range = 4 – 48 months). Based on the size and position of the tumour under retinal examination, it is estimated that the average tumour would have lead to disrupted vision approximately 6 months prior to enucleation. All participants had normal or corrected-to-normal acuity as assessed by an EDTRS eye chart (Precision VisionTM, La Salle, IL). Early ME participants are regularly seen by their ophthalmologist, and no known neurological or ocular abnormalities in the remaining eye were reported. (Table 4.1 lists individual patient histories).

Late ME_L participant. We also tested one male (age 65 years) who experienced trauma to the right eye at 50 years of age that eventually resulted in a detached retina and subsequent eye enucleation approximately 6 years prior to testing (AAE = 708 months). (See Table 4.1 for late ME_L participant history).

Table 4.1. Patient histories for ME participants including age, sex, Snellen acuity, enucleated eye, and age at enucleation (AAE).

| Patient | Age (years) | Sex | Acuity | Enucleated Eye | AAE (months) |
|-----------|----------------|--------|------------|-------------------|-----------------|
| ME01 | 54 | Male | 20/16 -1 | Right | 24 |
| ME02 | 43 | Female | 20/12.5 +2 | Right | 18 |
| ME03 | 21 | Male | 20/20 | Right | 23 |
| ME04 | 18 | Female | 20/20 | Right | 48 |
| ME05 | 18 | Male | 20/20 +4 | Right | 13 |
| ME06 | 17 | Male | 20/20 +2 | Right | 9 |
| ME07 | 29 | Female | 20/20 | Left | 11 |
| ME08 | 28 | Male | 20/16 | Right | 4 |
| ME09 | 30 | Male | 20/20 +3 | Left | 13 |
| ME10 | 18 | Female | 20/16 +3 | Right | 17 |
| ME11 | 17 | Female | 20/12.5 +1 | Right | 26 |
| ME12 | 36 | Female | 20/16 +4 | Left | 18 |
| ME13 | 65 | Male | 20/20 | Right | 708 |
| (Late ME) | | | | | |

Control group. Twenty-five binocularly intact controls (14 males) were tested who were approximately age- and sex-matched to the early ME group. Mean age (\pm SD) was 28.60 ± 10.16 years (range = 18 – 57 years). Participants had normal or corrected-to-normal acuity (Precision Vision TM, La Salle, IL) and normal Titmus stereoacuity (Stereo Optical Co., Inc. Chicago, IL). We also collected data from one 60-year old male to serve as an age-matched control for our late ME_L participant. Due to the younger

mean age of our early ME group, the 60-year old male's data was not included in the control group analysis for comparisons to the early ME group.

Data Acquisition and Processing

This research followed the Declaration of Helsinki doctrine and was approved by the Research Ethics Boards of both The Hospital for Sick Children and York University. Informed consent was obtained from all participants prior to testing and after explanation of the nature and possible consequences of the study.

A high-resolution, T_1 weighted three-dimensional MPRAGE was obtained from all participants using a Siemens MAGNETOM Trio 3T MRI scanner with a 32-channel head coil at the Sherman Health Sciences Research Centre at York University (Toronto, Canada). A scan of the entire head was acquired sagittally with the following parameters: rapid gradient echo, 1 mm^3 isotropic voxels, $TR = 1900\text{ ms}$, $TE = 2.52\text{ ms}$, 256×256 matrix, and flip angle = 9° .

To determine cortical thickness and surface area estimates for each participant, cortical surface reconstruction of each T_1 weighted image was performed with the FreeSurfer (version 5.3) image analysis suite described by Fischl and Dale (2000) (<http://surfer.nmr.mgh.harvard.edu/>). This process includes removal of non-brain tissue using a hybrid watershed/surface deformation procedure (Segonne et al., 2004), automated Talairach transformation, segmentation of the subcortical white matter and deep grey matter volumetric structures (Fischl et al., 2002; Fischl et al., 2004a), intensity

normalization (Sled, Zijdenbos, & Evans, 1998), tessellation¹⁰ of the grey matter/white matter boundary, automated topology correction (Fischl, Liu, & Dale, 2001; Segonne, Pacheco, & Fischl, 2007), and surface deformation following intensity gradients to optimally place the grey/white and grey/cerebrospinal fluid borders at the location where the greatest shift in intensity defines the transition to the other tissue class (Dale, Fischl, & Sereno, 1999; Dale & Sereno, 1993; Fischl & Dale, 2000). Once the cortical models are complete, a number of deformable procedures can be performed for further data processing and analysis including surface inflation (Fischl, Sereno, & Dale, 1999a), registration to a spherical atlas which utilizes individual cortical folding patterns to match cortical geometry across subjects (Fischl, Sereno, Tootell, & Dale, 1999b), parcellation of the cerebral cortex into units based on gyral and sulcal structure (Desikan et al., 2006; Destrieux, Fischl, Dale, & Halgren, 2010; Fischl et al., 2004b), and creation of a variety of surface-based data including maps of curvature and sulcal depth. This method uses both intensity and continuity information from the entire three-dimensional MR volume to perform segmentation and deformation procedures that produce representations of cortical thickness. (Figure 4.1 depicts automatic segmentation of grey matter/white matter and grey matter/pial matter borders). The maps are created using spatial intensity gradients across tissue classes and are therefore not simply reliant on absolute signal intensity. The maps produced are not restricted to the voxel resolution of the original data and thus are capable of detecting submillimeter differences between groups. Procedures for the measurement of cortical thickness have been validated against

¹⁰Tessellation is performed by covering the entire cortical surface using triangles as vertices so that no gaps or overlaps are present.

histological analysis (Rosas et al., 2002) and manual measurements (Kuperberg et al., 2003; Salat et al., 2004).

Mean cortical thickness estimates were calculated as the average distance between the grey matter/white matter boundary and the grey matter/pial matter boundary at each vertex on the tessellated surface. Total surface area was calculated at the pial matter surface (Fischl & Dale, 2000). Both cortical thickness and surface area estimates were derived from the native space of each participant. Cortical surfaces were visually evaluated for errors in talarach registration, brain extraction, and segmentation, and any necessary corrections were made.

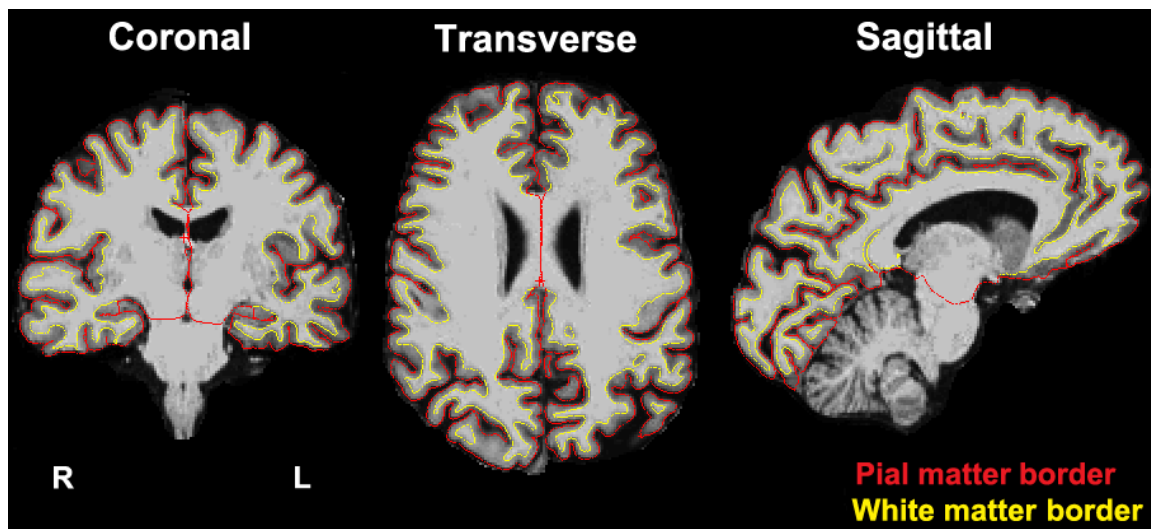


Figure 4.1. Coronal, transverse, and sagittal views of an extracted brain depicting automatic segmentation of the pial matter (red) and white matter (yellow) borders.

Data Analyses

Global differences. Global morphometry differences in surface area and cortical thickness of the entire cortical grey matter surface were assessed using a 2×2 analysis of variance (ANOVA) with group (control, early ME) as the between-groups variable, and hemisphere (left, right) as the within-groups variable.

Regional differences. Because we recently reported asymmetries in the anterior visual system following early monocular enucleation that show a relative sparing of the LGN contralateral to the remaining eye (Kelly et al., 2014) and others have reported structural asymmetries in the binocularly intact visual system (right > left) (e.g., Schultz et al., 2013; Zhou, Lebel, Evan, & Beaulieu, 2013), we divided the early ME group into two sub-groups; left eye intact (early ME_L; n = 9) and right eye intact (early ME_R; n = 3). The rest of our analyses were conducted using these subgroups.

Regional morphometry differences in surface area and cortical thickness of the entire cortical grey matter surface were assessed using a vertex-by-vertex general linear model conducted in FreeSurfer's GUI-based Qdec (Query, Design, Estimate, Contrast) application. Statistical analyses were performed at 163,842 vertices per hemisphere. Three separate comparisons were conducted: 1) control versus early ME_L, 2) control versus early ME_R, and 3) early ME_L versus early ME_R.

First, cortical surfaces from each participant were transformed to an average template surface space that is provided by FreeSurfer and created in MNI305 space. Second, surface area and cortical thickness maps were smoothed using a surface-based Gaussian kernel [full-width half maximum (FWHM) = 10] to reduce noise. Third,

contiguous clusters of significant vertex-wise group differences were identified by controlling for multiple comparisons across the whole brain using a false discovery rate (FDR) (Benjamini & Hochberg, 1995) set at $p < 0.05$ and a minimum cluster size of 20 mm². Significant regions were identified according to one of FreeSurfer's implemented parcellation schemes (aparc.a2009s – Destrieux atlas) that segments the cortical surface into 154 labels based on gyral and sulcal structure (Destrieux et al., 2010).

Region-of-interest (ROI) differences. We restricted our ROI analysis of visual cortex to anatomical V1 and V2 labels that have previously been validated (Fischl et al. 2008; Hinds et al., 2008, 2009) and are implemented in FreeSurfer's automatic processing stream. V1 and V2 labels are based on cortical folding patterns that correspond to Brodmann areas 17 and 18, respectively. These labels were mapped to each individual brain using a previously tested thresholded p level of 0.80 (Hinds et al., 2009). Averages for surface area and cortical thickness were calculated for each label and participant. (See Figure 4.2 for examples of thresholded V1 and V2 labels).

A $3 \times 2 \times 2$ ANOVA with group (control, early ME_L, early ME_R) as the between-groups variable, and hemisphere (left, right) and ROI (V1, V2) as the within-groups variables was conducted for surface area and cortical thickness measures. Post-hoc analyses were conducted on significant ANOVAs.¹¹

¹¹ In cases where homogeneity of variance was violated, independent t-tests with Satterwaite approximation for degrees of freedom was performed for between-groups analyses.

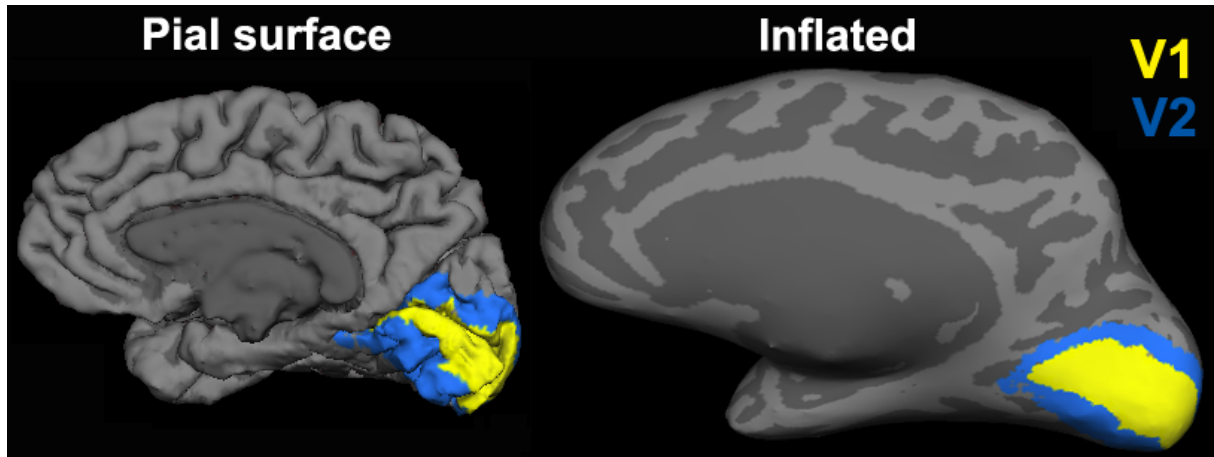


Figure 4.2. Three-dimensional examples of thresholded V1 (yellow) and V2 (blue) ROIs on the pial and inflated surface of a typical binocularly intact control.

Timing of deprivation. Correlations controlling for sex and age were conducted for the entire cortical surface area on a vertex-by-vertex basis using QDec to determine whether there was a relationship between AAE and surface area or cortical thickness ($p < 0.05$, FDR-corrected). Partial correlations were also conducted on V1 and V2 ROIs controlling for sex and age to determine whether there was a relationship between AAE and surface area or cortical thickness. All correlations were conducted for the early ME_L group only; no correlations were conducted for the early ME_R group due to the small number of participants ($n = 3$).

Late ME_L participant. Modified t-tests (Crawford & Garthwaite, 2002) designed to compare one individual case (i.e., late ME_L participant) to a group of individuals were used. Data from the late ME_L participant was compared to three age- and sex-matched

controls with a mean age of 55.70 years (range = 50 – 60 years), and to the early ME_L since his left eye remained intact. Due to the young mean age of the early ME_L group, we also compared the late ME_L participant to one matched early ME_L participant (male, 54); however, statistical tests could not be performed.

Results

Global Differences

Global surface area and cortical thickness of both groups were within the range previously reported for healthy controls (Im et al., 2006; Meyer, Liem, Hirsiger, Jäncke, & Hänggi, 2013; Van Essen, Glasser, Dierker, Harwell, & Coalson, 2012). (See Table 4.2 for global surface area and cortical thickness for each group). No significant age, $t(35) = 0.31$, $p = 0.755$, or sex, $\chi^2(1, N = 37) = 0.12$, $p = 0.502$, differences between the control and early ME group were found. Therefore, sex and age were not considered when conducting between-groups analyses for global morphometry.

Surface area. There was no significant group \times hemisphere interaction, $F(1,35) = 1.45$, $p = 0.237$, or main effect of group, $F(1, 35) = 2.25$, $p = 0.142$. However, there was a significant main effect of hemisphere, $F(1, 35) = 622.65$, $p < 0.001$. Post-hoc pairwise comparisons (Bonferroni-adjusted alpha = 0.025) revealed that the control and early ME groups had significantly larger surface area in the right compared with the left hemisphere ($ps < 0.001$).

Cortical thickness. There was no significant group \times hemisphere interaction, $F(1,35) = 0.43$, $p = 0.518$, or main effect of group, $F(1, 35) = 0.89$, $p = 0.352$. However, there was a significant main effect of hemisphere, $F(1, 35) = 5.64$, $p = 0.023$. Post-hoc pairwise comparisons (Bonferroni-adjusted $\alpha = 0.025$) revealed that the early ME group trended towards having larger cortical thickness in the left relative to right hemisphere, but this trend was not significant ($p = 0.074$) and the control group did not exhibit this trend ($p = 0.140$). See Table 4.2 for means [\pm standard error of the mean (SEM)] for each global morphometry measure for each group. Due to the lack of between-group differences for global morphometry measures, global surface area and global cortical thickness were not considered a factor for subsequent analyses.

Table 4.2. Descriptive statistics for the control and early ME groups showing the mean (\pm SEM) global estimates for surface area and cortical thickness of the cortical grey matter in the right and left hemisphere.

| Group | Surface area (cm ²) | | Cortical thickness (mm) | |
|----------|---------------------------------|----------|-------------------------|------------|
| | Right | Left | Right | Left |
| Control | 1102(21) | 1037(20) | 2.55(0.02) | 2.56(0.02) |
| Early ME | 1155(32) | 1096(32) | 2.57(0.03) | 2.59(0.03) |

Regional Differences

There were no significant age ($ps \geq 0.501$) or sex ($ps \geq 0.457$) differences between any combinations of the three groups (control, early ME_L, early ME_R). Therefore, age and sex were not factored into the regional differences analyses.

Surface area. Three main clusters in the left hemisphere were flagged as significantly larger in the early ME_L compared with the control group ($p < 0.05$, FDR corrected) These clusters were located in the inferior supramarginal, superior parietal, and superior temporal regions based on the Destrieux atlas parcellation (Destrieux et al., 2010). (See Figure 4.3 and Table 4.3). No other significant regional group differences were found for surface area in either hemisphere.

Cortical thickness. One cluster in the middle occipital region in the left hemisphere was flagged as significantly larger in the early ME_L compared with the early ME_R group ($p < 0.05$, FDR corrected). No other significant regional group differences were found for cortical thickness in either hemisphere.

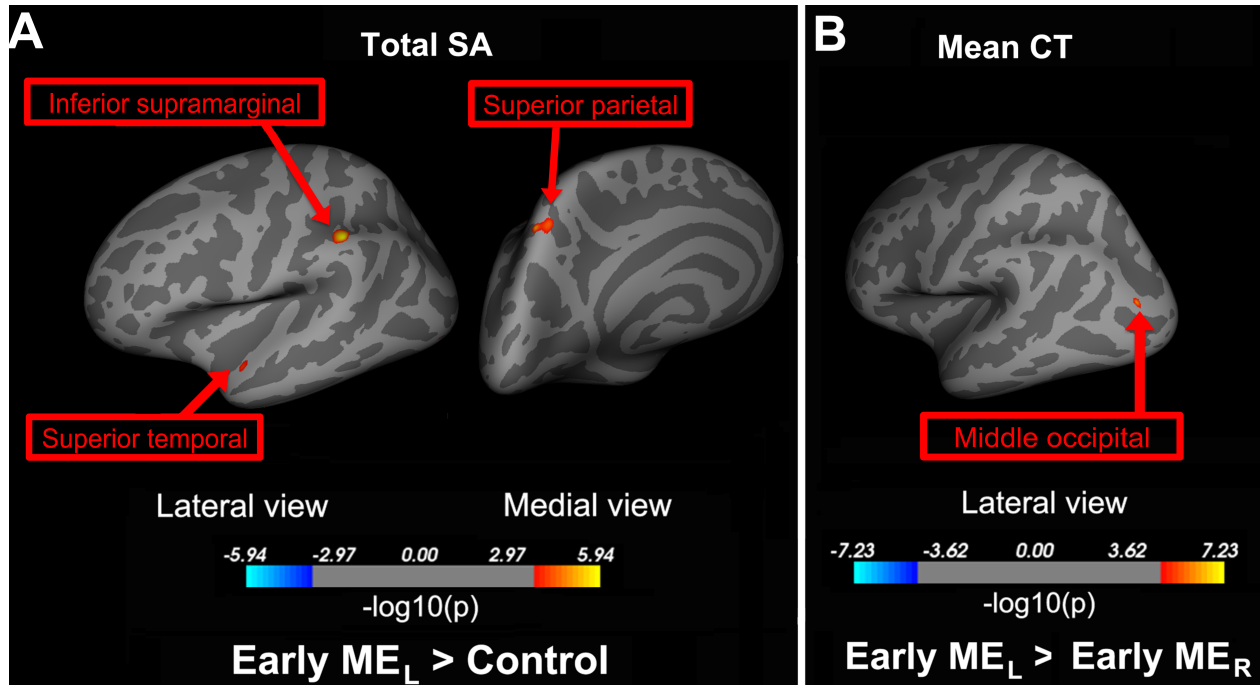


Figure 4.3. Average inflated brain showing regional group differences in the left hemisphere for (A) surface area between the control and early ME_L groups, and for (B) cortical thickness between the early ME_L and early ME_R groups. (A) The early ME_L group exhibited significantly larger surface area compared with the control group in three clusters located in the inferior supramarginal, superior temporal, and superior parietal regions ($p < 0.05$, FDR corrected). (B) The early ME_L group also exhibited significantly larger cortical thickness compared with the early ME_R group in one cluster located in the middle occipital region ($p < 0.05$, FDR corrected).

Table 4.3. Information for clusters flagged as significantly different between groups, including region, cluster size (mm^2), maximum $-\log(10)p$ value, and MNI coordinates.

| Measure | Comparison | Region | Cluster Size (mm^2) | Max $-\log(10)p$ | MNI Coordinates | | |
|--------------------|-----------------------------------------------|-----------------------------|--------------------------------|------------------|-----------------|-----|-----|
| | | | | | X | Y | Z |
| Surface area | Early ME _L > Control | Left Inferior Supramarginal | 164 | 6.0 | -50 | -40 | 44 |
| | | Left Superior Parietal | 117 | 5.1 | -11 | -69 | 52 |
| | | Left Superior Temporal | 33 | 4.1 | -52 | 4 | -11 |
| Cortical thickness | Early ME _L > Early ME _R | Left Middle Occipital | 26 | 6.1 | -35 | -88 | -12 |

Region-of-Interest (ROI) Differences

Surface area and cortical thickness estimates for V1 and V2 in the control group were within the range previously reported for healthy controls (Andrews, Halpern, Scott, & Purves, 1997; Hinds et al., 2009; Schultz et al., 2013; Stensaas, Eddington, & Dobelle, 1974).

Surface area. No significant group \times hemisphere \times ROI, $F(2,34) = 1.41$, $p = 0.257$, group \times hemisphere, $F(2,34) = 0.43$, $p = 0.657$, or group \times ROI, $F(2,34) = 0.97$, $p = 0.388$, interactions were found. No significant main effect of hemisphere was found, $F(1,34) = 1.48$, $p = 0.233$. However, there was a significant hemisphere \times ROI interaction, $F(1,34) = 13.54$, $p = 0.001$, and a significant main effect of group, $F(1,35) = 3.72$, $p = 0.035$.

Collapsed across hemisphere, post-hoc pairwise comparisons (Bonferroni-adjusted alphas = 0.017) revealed that the early ME_L group exhibited significantly increased surface area in V1 compared with the early ME_R group ($p = 0.015$). The early ME_L group also exhibited trends toward increased surface area in V1 compared with the control group ($p = 0.044$), and increased surface area in V2 compared with the control ($p = 0.040$) and early ME_R ($p = 0.047$) groups, but these trends were not significant. No other group differences were found ($ps \geq 0.149$).

Simple effects analysis for V1 (Bonferroni-adjusted alphas = 0.008) revealed that the early ME_L group had significantly increased surface area in the right hemisphere compared with the control ($p = 0.006$) and early ME_R ($p = 0.003$) groups. The early ME_L group also exhibited a trend towards increased surface area in the left hemisphere

compared with the early ME_R group ($p = 0.074$), but this trend was not significant. No other differences were found for V1 ($ps \geq 0.122$).

Simple effects analysis for V2 (Bonferroni-adjusted alphas = 0.008) revealed that the early ME_L group exhibited a trend towards increased surface area in the right hemisphere compared with the control ($p = 0.090$) and early ME_R ($p = 0.031$) groups, and in the left hemisphere compared with the control group ($p = 0.054$), but these trends were not significant. Further, the control group had significantly increased surface area in the right relative to left hemisphere ($p < 0.001$). The early ME_L group also exhibited increased surface area in the right relative to left hemisphere ($p = 0.028$), but this trend was not significant. No differences were found for V2 ($ps \geq 0.163$). (See Figure 4.4A and Table 4.4 for group averages of surface area per ROI).

Cortical thickness. No significant group \times hemisphere \times ROI, $F(2,34) = 1.08$, $p = 0.351$, group \times hemisphere, $F(2,34) = 0.15$, $p = 0.863$, or hemisphere \times ROI, $F(1,34) < 0.01$, $p > 0.99$, interactions were found. However, there was a significant group \times ROI interaction, $F(2,34) = 3.76$, $p = 0.034$. No significant main effect of group was found, $F(1,35) = 2.00$, $p = 0.151$. A trend towards a main effect of hemisphere was found, but this trend was not significant, $F(1,35) = 3.05$, $p = 0.090$.

Collapsed across hemisphere (Bonferroni-adjusted alphas = 0.017), post-hoc pairwise comparisons revealed that the early ME_L group had significantly increased cortical thickness in V2 compared with the early ME_R group ($p = 0.013$). Further, the control group exhibited a trend towards increased cortical thickness in V2 compared with

the early ME_R group ($p = 0.062$), but this trend was not significant. No other group differences were found ($ps \geq 0.155$).

Simple effects analysis for V2 (Bonferroni-adjusted alphas = 0.008) revealed that the early ME_L group had significantly increased cortical thickness in the left hemisphere compared with the early ME_R group ($p = 0.001$). The early ME_L group also exhibited trends towards significantly increased cortical thickness in the right hemisphere compared with the early ME_R group ($p = 0.032$), and in the left hemisphere compared with the control group ($p = 0.056$), but these trends were not significant. The control group had significantly increased cortical thickness in the right ($p = 0.006$) and left ($p = < 0.001$) hemispheres compared with the early ME_R group. Further, the control group exhibited a trend towards increased cortical thickness in the right relative to left hemisphere ($p = 0.073$), but this trend was not significant. No other differences were found for V2 ($ps \geq 0.155$). (See Figure 4.4B and Table 4.4 for group averages of cortical thickness per ROI).

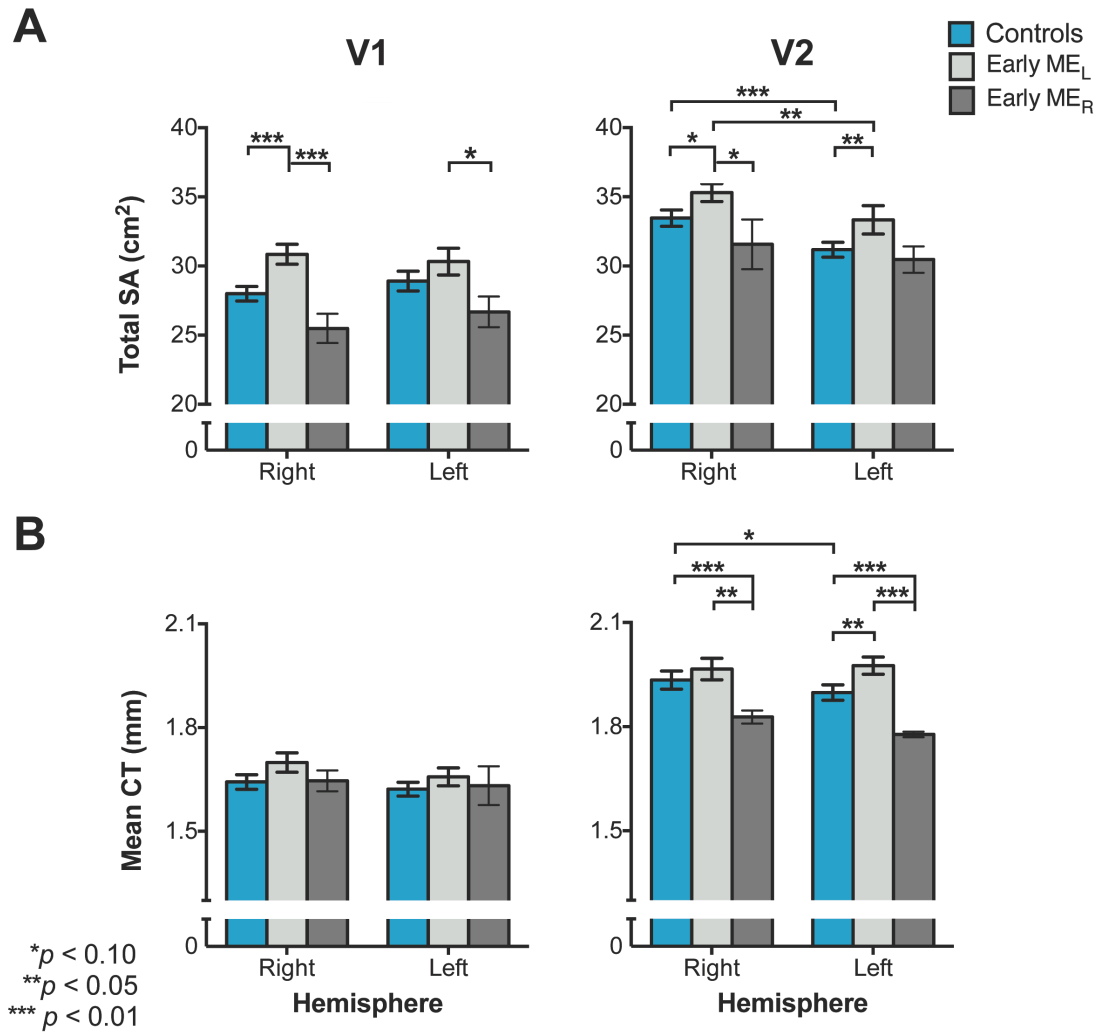


Figure 4.4. Bar graphs depicting group averages for (A) surface area (cm²) and (B) cortical thickness (mm) for right and left V1 and V2 in the control (blue), early ME_L (light grey), and early ME_R (dark grey) groups. In general, the early ME_L group exhibited increases in surface area and cortical thickness compared with controls and the early ME_R group, while the early ME_R group exhibited decreases in cortical thickness compared to the control group. Error bars represent \pm SEM. * $p < 0.10$; ** $p < 0.05$; *** $p < 0.01$.

Timing of Deprivation

Regional differences. No significant correlations were found between AAE and surface area or cortical thickness for the regional differences analyses ($p > 0.05$, FDR-corrected).

ROI differences. The early ME_L group exhibited a trend for a positive correlation between AAE and cortical thickness in right V2, $r = 0.75$, $p = 0.053$, but this trend was not significant. Further, the participant enucleated at 48 months of age was an outlier, and this trend became non-existent after this participant was removed from the analysis, $r = 0.47$, $p = 0.346$. Therefore, no significant relationships with AAE were found for surface area or cortical thickness in the ROI differences analyses ($ps \geq 0.287$).

Late ME_L Participant

Surface area. The late ME_L participant exhibited significantly decreased surface area in right V2 compared with the early ME_L group, $t(8) = -2.26$, $p < 0.050$, one-tailed. No other differences were found for surface area in the late ME_L participant compared with the early ME_L and matched control groups. Descriptively, the late ME_L participant also showed large decreases in surface area for V1 and V2 in both hemispheres compared with the matched early ME_L participant (see Figure 4.5 A and Table 4.4).

Cortical thickness. The late ME_L participant exhibited significantly decreased cortical thickness in right V1, $t(2) = -4.98$, $p < 0.025$, one-tailed, and left V1, $t(2) = -3.58$, $p < 0.050$, one-tailed, compared with the matched control group. He also exhibited a

trend towards decreased cortical thickness in right V2, $t(2) = -2.55$, $p < 0.100$, one-tailed, and left V2, $t(2) = -2.34$, $p < 0.100$, one-tailed, compared with the matched control group, but these trends were not significant.

The late ME_L participant exhibited decreased cortical thickness in right V1, $t(8) = -2.80$, $p < 0.025$, one-tailed, right V2, $t(8) = -2.72$, $p < 0.025$, one-tailed, and left V2, $t(8) = -3.31$, $p < 0.010$, one-tailed compared with the early ME_L group. Descriptively, the late ME_L participant also showed large decreases in cortical thickness for V1 and V2 in both hemispheres compared with the matched early ME_L participant (see Figure 4.5B and Table 4.4).

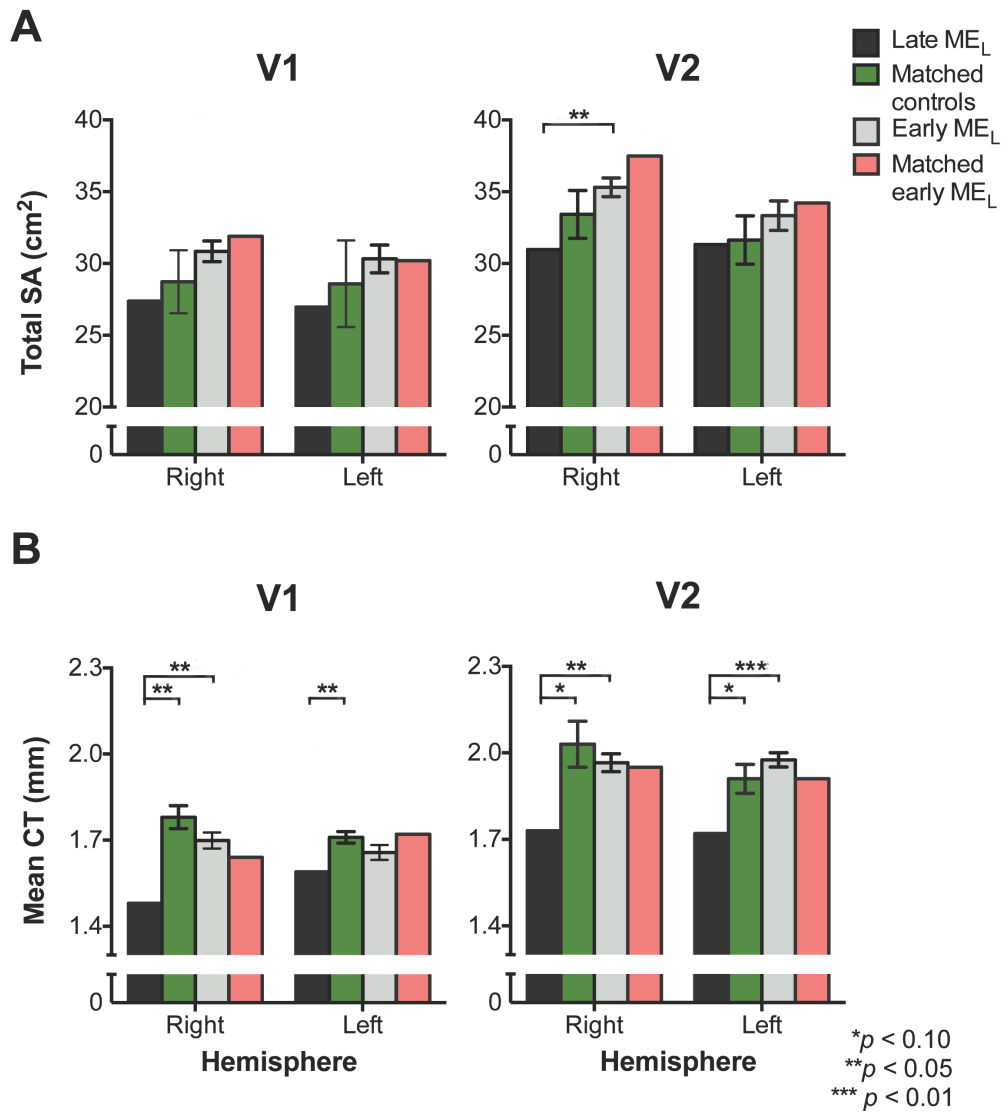


Figure 4.5. Bar graphs depicting (A) surface area (cm²) and (B) cortical thickness (mm) for V1 and V2 for the late ME_L participant (black), an age- and sex-matched control group (green), the early ME_L group (light grey), and one age- and sex-matched early ME_L participant (pink). The late ME_L participant exhibited decreases in surface area in V2 compared with the early ME_L group, and overall decreases in cortical thickness compared to all groups. Error bars represent \pm SEM. * $p < 0.10$; ** $p < 0.05$; *** $p < 0.01$.

Table 4.4. Descriptive statistics for the control, early ME_L and early ME_R groups showing group averages (\pm SEM) for surface area (cm₂) and cortical thickness (mm) estimates for V1 and V2 in the right and left hemispheres. Surface area and cortical thickness estimates are also shown for the late ME_L participant, a group of controls and one early ME_L participant age- and sex-matched to the late ME_L participant.

| Group | Total SA (cm ²) | | | | Mean CT (mm) | | | |
|-------------------------------|-----------------------------|-------------|-------------|-------------|--------------|------------|------------|------------|
| | V1 | | V2 | | V1 | | V2 | |
| | Right | Left | Right | Left | Right | Left | Right | Left |
| Control | 28.00(0.52) | 28.90(0.71) | 33.46(0.59) | 31.17(0.53) | 1.64(0.02) | 1.62(0.02) | 1.93(0.03) | 1.90(0.02) |
| Early ME _L | 30.84(0.72) | 30.31(0.97) | 35.30(0.65) | 33.33(1.03) | 1.70(0.03) | 1.66(0.03) | 1.97(0.03) | 1.98(0.03) |
| Early ME _R | 25.48(1.06) | 26.68(1.11) | 31.57(1.80) | 30.46(0.96) | 1.65(0.03) | 1.63(0.06) | 1.83(0.02) | 1.78(0.01) |
| Late ME _L | 27.38 | 26.96 | 30.97 | 31.32 | 1.48 | 1.59 | 1.73 | 1.72 |
| Matched Controls | 28.73(2.19) | 28.59(3.02) | 33.42(1.67) | 31.64(1.68) | 1.78(0.04) | 1.71(0.02) | 2.03(0.08) | 1.91(0.05) |
| Matched Early ME _L | 31.90 | 30.19 | 37.49 | 34.22 | 1.64 | 1.72 | 1.95 | 1.91 |

Discussion

We report the first instance of morphological changes in human cortex following long-term survival from early monocular enucleation due to retinoblastoma. Surprisingly, these changes differed depending on eye removed and morphological measure assessed. Generally speaking, the early ME_L (i.e., left eye intact) group exhibited increases whereas the early ME_R (i.e., right eye intact) group exhibited decreases in grey matter morphometry. We also report increased surface area in non-visual areas for the early ME_L group compared with controls. These changes suggest altered neural development following long-term survival subsequent to early monocular enucleation.

Visual Cortices

Compared with the control group, the early ME_L group displayed increased surface area in V1 and V2, and increased thickness in V2. While the increase in thickness is consistent with previous atypical development studies assessing visual cortex in albinism (Bridge et al., 2012), congenital anophthalmia (Bridge et al., 2009) and congenital blindness (Jiang et al., 2009; Park et al., 2009; Qin et al., 2013), the increase in surface area is inconsistent with decreased surface area in bilaterally enucleated monkeys (Rakic, 1988), and congenitally blind humans (Park et al., 2009). This discrepancy is expected given that the remaining eye in enucleated individuals allows one stream of normal visual input to the brain, unlike bilateral blindness. Studies of other forms of monocular deprivation (i.e., strabismus, amblyopia) have not examined cortical thickness or surface area, yet decreases in grey matter volume have been established in visual cortex in cases of amblyopia (Mendola et al., 2005; Xiao et al., 2007). It has been

shown that cortical volume is more closely correlated with surface area than cortical thickness in typical controls (Winkler et al., 2010). Although we did not assess volume, the lack of change in thickness coupled with the increase in surface area is indicative of either no volume changes or increased volume in visual regions of our early ME_L group. Our finding of increased surface area in regions known to process spatial form vision (i.e., V1 and V2) (Anzai et al., 2007; Hubel & Livingstone, 1990; Tootell et al., 1988) is also consistent with behavioural studies showing intact or enhanced spatial form vision in adults enucleated early in life (e.g., Kelly et al., 2013b; Nicholas et al., 1996; Steeves et al., 2004; reviewed in Kelly et al., 2013a & Steeves et al., 2008), and mouse models showing that early enucleation expands and accelerates the refinement of retinotopic area V1 (Faguet et al., 2009; Smith & Trachtenberg, 2007).

Our findings suggest that long-term survival from early monocular enucleation results in altered development of the cortex, which is consistent with changes found in the anterior visual pathway (Kelly et al., 2014). Here we posit several possible mechanisms of altered development following early enucleation. First, columnar segregation of V1 is dependent upon binocular interactions that are present during maturation, such as competition (Horton & Hocking, 1998a; Sloper, 1993). Early enucleation completely removes visual input from the deafferented eye and thus, removes the presence of binocular competition during a time of rapid development. Due to the lack of binocular competition, the remaining eye may recruit deafferented cells within V1 while still developing. This notion is not only supported by a lack of segregation of ocular dominance columns in early-enucleated monkeys and humans (Horton & Hocking, 1998a; Rakic, 1981), but also by rabbit and monkey models of

enucleation showing that aberrant connections are formed between the remaining intact eye and deafferented geniculate cells (Grigonis et al., 1986; Rakic 1981). More cortical space in V1 devoted to the remaining eye would then affect development of areas “higher-up” in the visual system, which would explain the increases in surface area and thickness also observed for V2. It could also be the case that feedback from higher-order visual areas such as V2 that have a larger proportion of binocular cells may aid in the retention of cortical cells within V1. Indeed, inactivation of V2 in monkeys suppresses V1 neuron responses (Hupé, James, Girard, & Bullier, 2001; Nassi, Lomber, & Born, 2013). Monkey data also show that early enucleation does not affect staining within V2 (Horton & Hocking, 1998a), lending support to the notion that visual information from both eyes in the intact visual system is integrated when it reaches V2.

Another plausible explanation for increased thickness and surface area in our enucleation group that has been put forth as an explanation for the same result in the congenitally blind is a disruption in synaptic pruning during development (e.g., Park et al., 2009). Synaptogenesis typically is complete by 9 months of age (Garey & de Courten, 1983) and is followed by a period of synaptic pruning that continues until 11 years of age (Huttenlocher, 1990; Huttenlocher et al., 1982, Garey & De Courten, 1983). In addition, early enucleation in mice, ferrets, and rabbits results in increased contralateral retinogeniculate connections (Godement et al., 1987; Grigonis et al., 1986; Guillery, 1989). A disruption in pruning may serve to reduce the instance of degeneration of visual neurons, and consequently spare visual function in a population whose brain is receiving only half of its typical visual input during development. However, increased thickness in congenital blindness is associated with decreased

surface area (Park et al., 2009), which is inconsistent with our results. Therefore, it appears that different mechanisms are involved in the different forms of visual deprivation and we cannot say for certain that a lack of pruning is responsible for the surface area and cortical thickness increases in our group. Instead, increases within visual cortex of our early ME_L group may reflect increased metabolic activity. Metabolic increases have been documented at rest in congenitally blind individuals compared with sighted controls (Kupers, Christiansen, Grey, & Ptito, 2009; Kupers, Pietrini, Ricciardi, & Ptito, 2011). This change may occur as a result of recruitment of visual cortex by cognitive functions (Kupers et al., 2011). Our population of enucleated individuals is not blind and the pattern of stronger functional activation contralateral to the remaining eye within visual cortex is akin to binocular controls viewing monocularly (Barb et al., 2011; Toosy et al., 2001). Thus, metabolic increases are not likely to account for the increases observed in our group. Other possible explanations include: 1) stronger connections to/from other sensory regions, which is supported by increases in non-visual areas found in our early ME_L group (discussed in detail below), and 2) changes in local gyrification, a morphological measure that is positively correlated with surface area (Hogstrom, Westlye, Walhovd, & Fjell, 2012). Future research should examine these possibilities.

While surface area increases were observed bilaterally within V2 for the early ME_L group, the increase in V1 was restricted to the right hemisphere, contralateral to the remaining eye. This asymmetry is consistent with our previous study showing a contralateral bias for LGN volume (Kelly et al., 2014), and with behavioural studies showing a nasalward bias for motion processing (Day, 1995; Reed et al., 1991; Steeves et al., 2002) in the early enucleation population. Further, monocularly enucleated

children (Barb et al., 2011) and binocularly intact controls viewing monocularly (Toosy et al., 2001) exhibit a contralateral bias in functional activity in V1. Since nasal retinal fibres cross-over, these fibres may be behind the recruitment of cells within deafferented geniculate laminae or ocular dominance columns. This claim is supported by research showing an increase in optic tract width contralateral to the remaining eye in humans enucleated early in life (Kelly et al., 2014), and a greater contribution of nasal retinal fibers to ocular dominance columns in binocularly intact monkeys (Tychsen & Burkhalter, 1997). Further, acuity in the nasal retina develops earlier than that in the temporal retina (Courage & Adams, 1996; Lewis & Maurer, 1992). However, retinal projections are established prenatally (Rakic, 1976), and geniculate cells innervated by either eye grow at equal rates in binocularly intact monkeys (Gottlieb et al., 1985). Further, visual evoked potentials (VEPs) in anophthalmic patients born with only one eye are symmetrical (Neveu et al., 2006), indicating that retinal fibres may be equal in their influence on visual cortex development. However, cortical changes in anophthalmia are likely operating *in utero*, which is different from postnatal enucleation. Other possible explanations for the contralateral bias within V1 must be considered. One hypothesis is that the right hemisphere develops earlier than the left, which is supported by the fact that increases were only observed for our early ME_L group and not our early ME_R group.

Left Eye Versus Right Eye Remaining

In contrast to the early ME_L group, the early ME_R group exhibited decreased thickness in V2 in both hemispheres compared with controls. Decreases in the early ME_R group may reflect a disruption in synaptogenesis, myelination, and/or degeneration of cortical neurons during development. Yet, synaptogenesis occurs independent of visual experience (Bourgeois & Rakic, 1996; Winfield, 1981). Therefore, it is more likely that cell degeneration and a disruption in myelination are occurring due to a loss of visual input. Indeed, myelin and cell degeneration have been found in the visual pathway of enucleated rabbits (Khan, 2005), monkeys (Hendrickson & Tigges, 1985; Hubel et al., 1977; Matthews, 1964; Sloper et al., 1987a), and humans (Beatty et al., 1982; Goldby, 1957; Hickey & Guillery, 1979; Horton, 1997). However, enucleation of the left eye appears to solely affect V2 since, compared with controls, no thickness or surface area differences were observed in V1. An intact V1 may explain the lack of spatial form vision deficits in this group (reviewed in Kelly et al., 2013a & Steeves et al., 2008). It is also important to note that surface area was not affected in the early ME_R group compared to controls, further supporting the notion that cortical thickness and surface area measures reflect distinct characteristics of brain morphology (Sanabria-Diaz et al., 2010; Winkler et al., 2010).

In line with decreases compared with controls, the early ME_R group also exhibited overall decreases in surface area and cortical thickness compared with the early ME_L group, with the exception of V1 thickness that remained intact. The early ME_R group also displayed a decrease in cortical thickness in the middle occipital gyrus compared with the early ME_L group. The middle occipital gyrus is a region known to process vision in

binocularly intact individuals (Braddick, O'Brien, Wattam-Bell, Atkinson, & Turner, 2000), and has been implicated in auditory and tactile processing in early blind participants (Renier et al, 2010).

We did not expect to find a differential effect of which eye was enucleated, especially given that this result has not been previously reported for LGN volume (Kelly et al., 2014), or for any behavioural measures assessed in this population. It has been suggested the right hemisphere develops earlier than the left, particularly for visuospatial abilities (Chiron et al., 1997; Geschwind & Galaburda, 1985), and this may explain our findings. According to this notion, functions required for survival are less likely to be disrupted if they develop more quickly (Geschwind & Galaburda, 1985). For example, face identification in infants is lateralized to the right hemisphere (de Schonen & Deruelle, 1991). Colour discrimination is also lateralized to the right hemisphere in infants, but is more lateralized to the left hemisphere in adults (Franklin et al., 2008). Further, infants up to three years of age display right hemisphere dominance in cerebral blood flow at rest in posterior regions (Chiron et al., 1997). Since visual cortex receives a stronger signal from the contralateral eye (e.g., Barb et al., 2011; Toosy et al., 2001), left-eye enucleation early in life would consequently deafferent visual input to the earlier developing right hemisphere. This would result in more severe deficits than removing visual information to the left hemisphere via right-eye enucleation. To address this concern, future studies should compare left- and right eye-enucleation that has occurred later in life, preferably after 4 years of age, but before the visual system has reached adult levels (approximately 11 years of age) (Garey & De Courten, 1983). However, the size of our early ME_R group was quite small ($n = 3$), and due to the rarity of these

patients, it is often difficult to obtain a large sample size. Thus, the results for this group must be interpreted with caution.

Non-Visual Cortices

Compared with controls, the early ME_L group exhibited increased surface area in regions that are not devoted solely to visual processing. These regions reside in superior parietal, superior temporal, and inferior supramarginal areas. The superior parietal lobule has been associated with visually-guided reaching (Inouchi, et al., 2013; Gallivan, Cavina-Pratesi, & Culham; reviewed in Culham & Valyear, 2006) and processing the spatial location of one's body (Felician, et al., 2004). A previous study shows that early-enucleated individuals generate larger head movements (i.e., motion parallax) during visually-guided reaching in order to perceive depth (Marotta, Perrot, Nicolle, Servos, & Goodale, 1995). More importantly, this strategy resulted in intact reaching compared to controls. Coupled with this finding, our data suggest that reorganization within the superior parietal lobule enables the enucleated population to execute reaching comparable to binocularly intact controls.

The inferior supramarginal gyrus, particularly in the left hemisphere, is considered the phonological store for short-term memory of auditory information, including language (Paulesu, Frith, & Frackowiak, 1993). This region has also been implicated in visual word recognition (Stoeckel, Gough, Watkins, & Devlin 2009), speech sound disorders (Tkach et al., 2011) and auditory hallucinations in schizophrenia (Gaser, Nenadic, Volz, Büchel, & Sauer, 2004). The superior temporal sulcus, particularly in the left hemisphere, has been implicated in audiovisual multisensory integration (Beauchamp,

Lee, Argall, & Martin, 2004; Stevenson & James, 2009). Increased surface area for the early ME_L group in the supramarginal and superior temporal regions are consistent with previous behavioural research showing that early monocular enucleation results in moderately enhanced sound localization (Hoover, Harris, & Steeves, 2012) and equal reliance on visual and auditory information during audiovisual processing (Moro & Steeves, 2012, 2013) following early monocular enucleation. Morphological changes within these regions have also been observed in the congenitally blind (Park et al., 2009). Congenitally blind individuals also have superior hearing abilities for certain tasks such as pitch discrimination (e.g., Gougoux et al., 2004) and sound localization (e.g., Lessard, Pare, Lepore, & Lassonde, 1998).

Increased surface area in our study was found only for regions within the left hemisphere, ipsilateral to the remaining eye. With right-eye enucleation, the intact left eye projects stronger signals to the contralateral (right) relative to the ipsilateral (left) hemisphere. Recruitment of non-visual regions in the left hemisphere that receives weaker visual input may serve as adaptive compensation during atypical visual development. Future neuroimaging studies should examine non-visual cortices following early monocular enucleation to determine whether morphological differences are correlated with functional activity.

Timing of Deprivation and Late Enucleation

No timing of deprivation effects were found for either early ME group, which is consistent with previous behavioural studies of spatial form vision (González, Steeves, Kraft, Gallie, & Steinbach, 2002; Kelly et al., 2013b; Reed et al., 1996, Reed, Steeves, &

Steinbach, 1997; Steeves et al., 2004), and our previous structural LGN volume study (Kelly et al., 2014). Unfortunately, we were unable to recruit participants enucleated past the age of 4 years, which may be outside the developmental critical periods or may not span a large enough range of time for developmental relationships to emerge. This is not surprising given synaptic pruning and myelination if the cortex is not complete until well into adolescence (Barnea-Goraly et al, 2005; Gao et al, 2009; Garey & De Courten, 1983; Giedd et al., 1999; Huttenlocher, 1990; Huttenlocher et al., 1982).

Our study focused on long-term development following early monocular enucleation; however, we did have the opportunity to test one participant whose eye was removed during adulthood. In contrast to early enucleation, the late ME_L participant exhibited severe decreases in cortical thickness throughout visual areas V1 and V2 compared with age-matched controls and the early ME group. These data coincide with severe decreases in LGN volume in this participant (reported in Kelly et al., 2014), as well as previous monkey and human studies of late enucleation showing atrophy of optic chiasm, optic tracts, and LGN, and a shrinkage of ocular dominance columns years following enucleation (Beatty et al., 1982; Goldby, 1957; Hardmann, et al., 1997; Horton, 1997). From our data, it is evident that late enucleation results in degeneration of neurons at multiple levels of the visual pathway. While most of the increases observed in our early ME_L group were found for surface area, the decreases found in our late ME_L participant were predominantly in cortical thickness. This further supports the notion that surface area and cortical thickness reflect different characteristics of morphology.

Conclusions

In summary, we report morphological changes in visual cortex following long-term survival from early monocular enucleation. Increases in surface area were not restricted to visual cortex as increases were also observed in other sensory regions. However, these increases were restricted to individuals whose right eye was enucleated early in life. Further, the increase for V1 was restricted to the right hemisphere, indicating a contralateral bias that has previously been observed for geniculate volume and behavioural motion abilities. Increased surface area and cortical thickness in visual cortex may reflect recruitment of deafferented cells by the remaining eye, feedback from higher visual areas, and/or a disruption in synaptic pruning. In contrast, decreases were found for those whose left eye was enucleated, suggesting neuronal and myelin degeneration as a result of the loss of visual input from the enucleated eye. These data suggest a differential effect of enucleated eye, possibly due to hemispheric differences during development.

Our findings highlight the importance of receiving balanced binocular input during postnatal development of grey matter within visual cortex. Further, data from our late-enucleated participant indicate that plasticity of visual cortex is much weaker when the critical periods for development have been surpassed. Future studies should expand on these data to determine whether functional activity and white matter integrity within the visual cortex are also affected by early monocular enucleation in humans.

CHAPTER V

GENERAL DISCUSSION

Summary and Conclusions

Humans rely on vision more than any other sense not only to identify objects and individuals, but also to navigate and manipulate their environment. Vision develops quite early in life but depends on normal levels of visual input through each eye to mature. For decades, scientists have been researching early visual deprivation to determine the circumstances required for typical visual development, and to tease apart the consequences of atypical circumstances on maturation of the visual system. From these studies, it is evident that visual deprivation can hinder behavioural, morphological, and physiological visual development. Nonetheless, it is also evident that some compensatory reorganization occurs if deprivation begins during a time when the brain is still maturing.

My dissertation has focused on behavioural and morphological development of the visual system following long-term survival following early monocular enucleation. In Chapter II, I report impaired speed perception but intact and somewhat enhanced luminance contrast perception in this group, which is consistent with previous reports of a dissociation in visual ability. These data point to compensatory reorganization that occurs as a result of the enucleation. However, the mechanisms behind this reorganization remain unclear, a notion which led to the following two experiments. In Chapter III, I investigated subcortical regions in the enucleated visual pathway to determine whether behavioural changes are associated with morphological changes during development. The main finding from this experiment was that optic tract and LGN decreases were less severe contralateral to the remaining eye. In Chapter IV, I expanded my investigation of the effects of enucleation on morphology of the cortex.

From these data, I found increased grey matter morphology in regions associated with spatial form vision (i.e., V1, V2) compared with binocularly intact controls. Similar to the anterior visual pathway, these increases were predominantly observed in the contralateral hemisphere. Surprisingly, these increases depended on which eye was removed, suggesting hemispheric differences in critical period development, at least in early visual cortex. Regions associated with processing auditory, motor, and multisensory information were also found to be increased following early monocular enucleation. Data from one late-enucleated participant was collected in order to compare to the early monocular enucleation group for both subcortical and cortical morphological experiments. In general, this participant exhibited severe decreases on all measures, suggesting that enucleation that occurs past the critical developmental period does not allow for compensatory reorganization within the visual system.

Based on findings from Chapters III and IV, I can speculate as to the possible reorganization mechanisms that lead to intact, and sometimes enhanced, spatial form vision reported following early monocular enucleation. These mechanisms include, but are not limited to: 1) recruitment of deafferented cells by the remaining (contralateral) eye, 2) feedback signals from visual cortical regions, and 3) a disruption in synaptic pruning. In summary, data from the experiments in this dissertation suggest that not all behavioural aspects of vision (i.e., spatial form vision, motion perception) are affected in an equal manner. These data also support the notion of compensatory reorganization that encompasses not only the visual system, but other sensory systems, following long-term survival from early monocular enucleation in humans; however, late enucleation

does not afford the same advantage. I discuss each experimental chapter in more detail below.

Chapter II. I sought to further examine behavioural motion perception following early monocular enucleation. The motivation behind this experiment came from inconsistencies in the literature regarding motion perception in this group. For example, individuals with early monocular enucleation exhibit impaired motion-defined form recognition (Steeves, González, Gallie, & Steinbach, 2002) and the perception of motion in depth (Steeves, Gray, Steinbach, & Regan, 2000), but intact relative velocity detection (Bowns, Kirshner, & Steinbach, 1994) and direction discrimination (Steeves et al., 2002). I examined an ability not before tested in this group, namely speed perception, and compared performance to controls viewing binocularly and monocularly. Participants completed a series of speed discrimination tasks that consisted of vertical gratings moving either to the left or right at various speeds. Participants also completed a series of luminance contrast detection and discrimination control tasks that consisted of static vertical gratings at varying levels of luminance contrast. The early monocular enucleation group exhibited impaired speed perception at almost all speeds, but intact luminance contrast perception compared to controls. Further, the early monocular enucleation group displayed enhanced luminance contrast perception compared with controls viewing monocularly. These findings are consistent with previous research showing a dissociation in visual ability (reviewed in Kelly, Moro, & Steeves, 2013a and Steeves González, & Steinbach, 2008), and with enhancements in some aspects of spatial form vision, such as contrast sensitivity (Nicholas, Heywood, & Cowey, 1996)

and low-contrast global shape discrimination (Steeves, Wilkinson, González, Wilson, & Steinbach, 2004). These data further suggest that spatial form vision and motion perception systems are affected differently during development by this form of deprivation. Based on these findings, it is evident that compensatory reorganization occurs in response to losing an eye early in life that spares, and in some cases actually enhances, spatial form vision. However, this reorganization is not sufficient for the development of motion perception, an ability that appears vulnerable to early visual deprivation and that likely requires two streams of normal visual input for typical maturation.

Chapter III. My goal was to investigate the morphological development of the optic chiasm and LGN. The motivations behind this experiment were twofold. First, while there has been some research in early-enucleated non-primate mammals, and late-enucleated non-human and human primates, none have examined long-term development following early monocular enucleation in humans. Thus, one goal of this study was to fill this gap in the literature. The second goal was to investigate the effects of enucleation on the morphology of subcortical visual structures to understand the behavioural patterns observed in these individuals. To test these goals, I obtained high-resolution T_1 weighted and proton density weighted images from early monocular enucleation and binocularly intact control participants using a 3T MRI scanner. From these images, raters who were blind to group membership manually took several measures of the optic chiasm (optic nerve, chiasm, and tract width, optic chiasm volume) and LGN volume.

I found that early monocular enucleation results in a general decrease in optic chiasm and LGN measures, which was expected given the fact that half of visual inputs are removed. Interestingly, however, these decreases were remarkably less severe in the optic tract and LGN contralateral to the remaining eye. Data from one late enucleation participant was also collected in order to compare to controls and the early monocular enucleation group. This participant showed marked volume decreases in both LGN that were about half of that of controls. Further, unlike the early monocular enucleation group, the late enucleation participant did not exhibit an asymmetry. Geniculate volume decreases likely reflect a degree of neuronal degeneration in the LGN as suggested by previous monkey (Hendrickson & Tigges, 1985; Hubel, Wiesel, & LeVay, 1977; Matthews, 1964; Sloper, Headon, & Powell, 1987a,b) and human (Hickey & Guillery, 1979) data. However, the fact that the decrease was much less in the contralateral LGN for the early monocular enucleation group indicates recruitment of deafferented cells by the crossing nasal fibres of the remaining eye. This notion is consistent with previous reports of the formation of aberrant connections between the remaining eye and deafferented geniculate cells in early-enucleated rabbits (Grigonis, Pearson, & Murphy, 1986) and monkeys (Rakic, 1981; Wefers, Dehay, Berland, Kennedy, & Chalupa, 2000). Or, it could be the case that stronger feedback signals from ipsilateral cortical V1 (contralateral to the remaining eye) are aiding in the retention of geniculate cells, as is evidenced by a contralateral bias in functional activity in V1 in enucleated children (Barb et al., 2011) and monocular viewing controls (Toosy et al., 2001). Data from this experiment suggest that degeneration of the visual system can

occur with visual deprivation at any age; however, if the enucleation occurs early enough in development, some reorganization occurs to prevent geniculate cell death.

Chapter IV. I sought to further investigate the morphological development of the visual system following early monocular enucleation and to determine whether the LGN asymmetry observed in this group was also present in visual cortical regions. From high-resolution T_1 weighted images obtained in the previous experiment, measures of total surface area and mean cortical thickness were estimated using the automated FreeSurfer image analysis suite. Between-groups analyses were conducted on the whole brain as well as anatomically defined ROIs associated with processing spatial form vision (V1, V2). I found that early enucleation was associated with increases in surface area in visual cortex, including right V1, and bilateral V2, and in non-visual regions, including supramarginal, superior parietal, and superior temporal regions. An increase in cortical thickness was also found for left V2. Increases in early visual cortices may reflect: 1) recruitment of deafferented cells by the remaining eye, particularly in the contralateral hemisphere, 2) feedback from higher visual areas, and/or 3) a disruption in synaptic pruning during development. Increases in non-visual regions suggest that other sensory modalities are recruited to compensate for the loss of an eye, which is consistent with previous behavioural data showing altered auditory and multisensory processing (Hoover, Harris, & Steeves 2012; Moro & Steeves, 2012, 2013), and intact visually-guided reaching (Marotta, Perrot, Nicolle, Servos, & Goodale, 1995) in this group.

Surprisingly, there was an effect of which eye was removed; the increases mentioned above were restricted to those whose right eye was enucleated. Individuals whose left eye was enucleated showed a different pattern of results where they exhibited decreased cortical thickness in bilateral V2 compared with controls, and in bilateral V1 and right V2 compared with individuals with their right eye enucleated. A decrease compared to controls may reflect neuronal and myelin degeneration following deprivation from early eye enucleation. It is important to note that this decrease was restricted to V2 while V1 was comparable to controls, and this finding may explain the intact spatial form vision in this group. A differential effect of eye of removal may reflect different developmental critical periods for each hemisphere. Morphological changes along the visual pathway highlight the importance of receiving balanced binocular input during visual development and suggest that altered development occurs following early eye loss.

Similar to the previous LGN experiment, data from one late enucleation participant was compared to controls and the early monocular enucleation group. This participant displayed severe decreases in cortical thickness and surface area compared with age-matched controls and early enucleation participants in the examined ROIs. Decreases in surface area and cortical thickness in the late enucleation participant are consistent with the previous LGN experiment and point to a weaker malleability of visual cortex when deprivation occurs after the critical periods for development.

Limitations

The techniques used in my dissertation were carefully planned, chosen from previously established methods, and controlled for many potential confounds. However, some limitations are inherent in not only working with patient populations, but also when using psychophysics and neuroimaging methods. The potential limitations of this thesis will be discussed in detail and should be considered during interpretation of the results.

Patient group. I recruited from a unique database of adults who had one eye enucleated in early in life due to unilateral retinoblastoma. Although this group can provide a great deal of insight into the requirements for typical visual development, a number of limitations are worth mentioning. First, it is impossible to control for the timing of visual deprivation as the tumour can develop at any point postnatally, and may or may not encroach upon the fovea prior to enucleation. This means that some individuals would likely have had a brief period of normal vision prior to tumour development. However, participants in my dissertation were enucleated before 4 years of age, which is well before the critical periods for visual development have been surpassed. Further, we suggest that the cancerous eye would have had little or no vision approximately 6 months prior to enucleation based on inspection of the size and position of the tumour on the retina from patient records. Finally, there were no correlations between age at enucleation and any of the behavioural or morphological measures assessed. Therefore, this limitation should pose no issues when interpreting the results in this dissertation.

Second, changes observed in the enucleation group may be a result of the disease itself rather than the treatment. However, unilateral retinoblastoma is localized to the affected eye, is treated before the cancer extends beyond the eye, and is rarely associated with cancer in the other eye or in any other form. Further, enucleation participants are regularly seen by their ophthalmologist, and no further ocular or neurological abnormalities have been reported. Thus, it can be said that the retinoblastoma did have an effect on the visual system, but only in that it affected retinal ganglion cells at the tumour site and therefore, altered the sensory input from that eye. In animal models, there is no cancer, hence a “normal” visual system prior to enucleation, and our data show the same pattern of morphological results (e.g., an asymmetry). If the changes observed in our study were linked solely to the disease process with retinoblastoma, it is unlikely that our data would be consistent with non-primate animal models. In any case, it may be advantageous to assess individuals who lost their eye for reasons other than retinoblastoma such as trauma or infection, to determine whether the pattern of results remains.

Third, as with any rare disease, it is often difficult to obtain a large sample size (i.e., $n > 10$). While this was not a problem for the first experiment in this dissertation ($n = 12$), sample sizes were smaller for LGN volume ($n = 8$) in Chapter III, and when the eye of enucleation was considered, the subgroups were also smaller [left-eye ($n = 9$) and right-eye ($n = 3$) intact] in Chapter IV. To compensate for this, we ensured that the enucleation groups were compared to larger control samples that were age- and sex-matched.

Fourth, in line with the third limitation, morphological measures were assessed in only one participant enucleated during adulthood to determine whether late enucleation differs from early enucleation. While it is difficult to interpret data from only one participant, his results were compared to controls and the early enucleation group using a significance test specifically designed to compare one individual case to a group. Additionally, he showed the same pattern of results as those previously reported for late-enucleated individuals, indicating that our findings for late enucleation are real.

Speed discrimination methodology. One limitation of the behavioural methodology employed in my dissertation was the fact that I neglected to use a dichoptic presentation set-up when presenting stimuli to the monocular viewing group. Dichoptic viewing consists of presenting stimuli to the viewing eye, and a uniformly-lit blank field to the non-viewing eye rather than patching that eye. This form of viewing eliminates binocular rivalry due to patching and has been shown to be superior to patching while testing visual functions monocularly in binocular controls (Steeves et al., 2004). Nonetheless, enucleated participants have been shown to perform better than monocular controls viewing dichoptically on some tasks (Steeves et al., 2004). Further, monocular viewing participants in our study were tested not with a black patch over their non-dominant eye, but with transparent tape that allowed some light but not form information to filter through, thereby reducing rivalry and consensual pupillary effects. Therefore, it is likely that the enhanced luminance contrast perception of the enucleation group compared with monocular viewing controls observed in Chapter II is not due to rivalry from patching.

Structural MRI methodology. Two main limitations exist with structural neuroimaging methods. First, it is impossible to know the actual causes of the morphological changes observed in the enucleation group. The resolution of the techniques ($1 - 2\text{mm}^3$) in this dissertation render it difficult to image geniculate laminae and ocular dominance columns. Therefore, I cannot say with certainty that LGN volume decreases in the enucleation group represent an actual decrease in neuron counts or neuron size, or whether the decrease occurs in all laminae or only the deafferented laminae. However, based on previous research showing a decrease in neuron count of deafferented cells (Sloper et al., 1987a,b), and a shrinkage of both deafferented and non-deafferented cells (Hendrickson & Tigges, 1985; Hubel et al., 1977), the geniculate decreases found in this dissertation likely reflect a combination of these potential scenarios. Further, I cannot confirm that deafferented cells within the LGN and V1 are recruited by the remaining eye, particularly in the contralateral hemisphere. However, previous research strongly indicates recruitment of deafferented geniculate cells by the remaining eye in enucleated rabbits (Grigonis et al., 1986), and monkeys (Rakic, 1981; Wefers et al., 2000), as does a lack of ocular dominance columns in monkeys and humans.

Second, structural neuroimaging methods cannot reveal changes in functional activation. LGN volume was determined by manual tracings of three independent raters, and the surface-based measurements from FreeSurfer were determined by anatomical landmarks such as gyri and sulci. Thus, I cannot say for certain how the cells within the LGN and visual cortices respond to visual input from structural measurements alone.

However, brain functioning depends partly on brain structure, and we are able to make certain inferences based on morphological measures. For example, given that anatomical V1 and V2 labels accurately predict functional boundaries (Fischl et al. 2008; Hinds et al., 2008, 2009), I can speculate that intact and enhanced spatial form vision reported for the enucleation group reflect the increases in morphology found in these ROIs. However, it could be that other factors are contributing to this increase, such as changes in cortical folding. For example, cortical folding increases have been found in V1 and V2 of people with schizophrenia (Schultz et al., 2013) and changes such as these may explain increases found in our enucleation group. Yet, V1 and V2 ROIs have not been validated in patient populations and these results must be interpreted with caution.

Future Directions

An array of studies, including the experiment in Chapter II, have established that behaviourally, early monocular enucleation results in a dissociation in visual ability such that spatial form vision is intact but motion perception is mildly impaired (see Kelly et al, 2013a and Steeves et al., 2008 for reviews). Future research should further probe this dissociation, behaviourally, using other tasks of spatial form vision and motion perception not yet implemented in this group. Many tasks of low- to mid-level spatial visual ability have been assessed in this group; yet only one previous study has assessed one form of higher-order spatial form vision, namely face perception. This study found mild face perception deficits following early monocular enucleation (Kelly, Gallie, & Steeves, 2012), but intact house perception. This face perception deficit should

be examined further, as should other higher-order spatial visual tasks, including those that assess object and place perception and have separate visual pathways (Mullin & Steeves, 2011; Steeves et al., 2004).

With the inconsistencies found for motion perception in this group, it would be advantageous to examine other forms of motion perception, such as biological motion. Although some aspects of motion processing are impaired in amblyopia, biological motion has been shown to be intact (Luu & Levi, 2013), which may also be the case for the enucleation group given that distinct neural substrates are associated with biological motion (e.g., Puce & Perrett, 2003). Further, future research could examine the effects of training to determine whether it is possible to improve aspects of motion perception that are impaired following early monocular enucleation. Training has been shown to improve direction discrimination in binocularly intact adults (Ball & Sekuler, 1982), and motion detection and discrimination in amblyopic adults (Hou et al., 2011), suggesting a degree of plasticity of the motion perception system even in adulthood. Thus, training may improve some aspects of motion impaired in the early monocular enucleation group. Indeed, preliminary results from one study examining perceptual learning in two early enucleation participants found improved motion-defined letter recognition following practice (González, Steeves, & Steinbach, 1998).

Functional neuroimaging studies should also probe this dissociation to determine its underlying neural mechanisms by using tasks to assess regions implicated in low-level spatial form vision (e.g., V1, V2) and motion (e.g., MT/MST) perception. With the exception of one study that examined functional activity in early visual cortex of sedated enucleated children (Barb et al., 2011), no fMRI studies have been conducted

in the early monocular enucleation population to assess low-level spatial form vision. Preliminary data from one fMRI study found a decrease in functional activity of enucleation participants in regions associated with face perception, but not in regions associated with scene perception (Kelly, Tcherassen, Gallie, & Steeves, 2014), which is consistent with behavioural data showing mild deficits for face perception (Kelly et al., 2012). However, these brain regions encode higher-level spatial form vision categories and it is unknown how early visual cortex would respond to low-level spatial visual stimuli. Data from fMRI studies will provide insight into functional mechanisms of altered visual development and can be correlated with behavioural measures of spatial form vision and motion perception in this population.

Aside from behavioural and functional techniques, more research should be conducted on the long-term consequences of early monocular enucleation on morphological development of the visual pathway. While this has been extensively studied in animal populations such as mice and rabbits, only a handful of studies have assessed these consequences in non-human and human primates. In fact, apart from the two neuroimaging studies presented in this thesis (Chapters III and IV), there has only been one other neuroimaging study to assess structure (i.e., white matter connectivity) in alive early-enucleated children (Barb et al., 2011). This study failed to find significant changes in measures of white matter integrity in enucleated participants; thus, it is crucial to further investigate this population using state-of-the-art neuroimaging techniques, such as cortical folding, and white matter integrity and connectivity within the visual pathway of alive, adults enucleated early in life. Since rodent models of enucleation show increased crossed projections from the remaining eye, and this

dissertation shows a contralateral bias in both LGN volume and visual cortex surface area, it is likely that changes in white matter connectivity may also show the same bias.

I was only able to procure one participant enucleated during adulthood, and although findings from this participant are consistent with previous studies on late enucleation, it would nonetheless be beneficial to directly compare results from a late enucleation group to those of an early enucleation group. Further, early monocular enucleation in humans is often indirectly compared to other forms of early monocular deprivation, such as cataract and strabismus, or in animals directly compared to those who have had one eyelid sutured shut. However, enucleation results in only one stream of normal visual input from the remaining eye while other forms of monocular deprivation result in an imbalance of visual input from the two eyes. Only a handful of studies exist that compare behaviourally, the differences between early monocular enucleation and one other form of monocular deprivation (strabismus) (Reed, Steinbach, Ono, Kraft, & Gallie, 1995; Reed, Steeves, & Steinbach, 1997; Reed, Steeves, Steinbach, Kraft, & Gallie, 1996). Therefore, it would be informative to directly compare early versus late monocular enucleation, and to compare enucleation to other forms of early monocular deprivation to determine whether the effects found in this dissertation are unique to the group tested. The latter comparison would aid in assessing the effects of quality versus quantity of visual input on visual system development.

Lastly, additional research should investigate the morphological development of other non-visual sensory and multisensory systems in the early monocular enucleation group. Studying these systems would add to the morphological changes in non-visual and auditory regions found in this dissertation (Chapter IV), and would corroborate

previously reported behavioural research showing that early monocular enucleation alters auditory (Hoover et al., 2012) and audiovisual (Moro & Steeves, 2012, 2013) development. Data from such experiments would elucidate the role that other sensory modalities play during compensatory reorganization following the loss of one eye during visual development. Preliminary data on the structure of the medial geniculate body (MGB), the auditory relay station of the thalamus, show that early enucleation results in increased volume in the left relative to the right MGB (Moro, Kelly, McKetton, & Steeves, 2014). This asymmetry may reflect an increased interaction between the left MGB and primary auditory cortex for aspects of auditory processing that are left hemisphere-dominant, such as language perception (e.g., Geschwind, 1970).

Concluding Remarks

The experiments in my dissertation highlight the importance of receiving normal levels of binocular visual input during early visual development. The absence of binocular interactions (i.e., competition/cooperation) that result from early monocular enucleation clearly disrupt typical visual development. Coupled with previous research, the behavioural motion impairments and morphological changes at various levels of the visual pathway found in the experiments of this dissertation support this claim. However, findings from the experiments in this dissertation also point to a degree of compensatory reorganization that occurs as a result of losing an eye before the critical periods for development end. While this reorganization may not be sufficient for some aspects of visual development (e.g., motion perception), it appears to aid in sparing others (e.g., spatial form vision). Understanding the mechanisms that allow the brain to change in

response to atypical circumstances is a very important line of research. Although not a new topic of research, the consequences of monocular deprivation from early eye loss are still unclear and must continue to be examined. Data from these experiments not only provide theoretical advances for basic science, but also have the potential for informing clinical research and rehabilitation for more severe sensory deprivation, atypical development, and brain trauma populations. The advances in state-of-the-art neuroimaging techniques allow us to delve deeper into the brains of alive individuals and aid in unlocking the mysteries of this complex organ.

REFERENCES

- Adams, R.J. & Courage, M.L. (2002). Using a single test to measure human contrast sensitivity from early childhood to maturity. *Vision Research*, 42, 1205-1210.
- Adams, R.J. & Courage, M.L. (1993). Contrast sensitivity in 24- and 36-month-olds as assessed with the contrast sensitivity card procedure. *Optometry & Vision Science*, 70, 97–101.
- Adams, D.L., Sincich, L.C., & Horton, J.C. (2007). Complete pattern of ocular dominance columns in human primary visual cortex. *Journal of Neuroscience*, 27, 10391-10403.
- Ahmed, I.J., Lewis, T.L., Ellemberg, D., & Maurer, D. (2005). Discrimination of speed in 5-year-olds and adults: are children up to speed? *Vision Research*, 45, 2129-2135.
- Allen, J.S., Damasio, H., & Grabowski, T.J. (2002). Normal neuroanatomical variation in the human brain: an MRI-volumetric study. *American Journal of Physical Anthropology*, 118, 341–348.

Andrews, T.J., Halpern, S.D., Scott, D., & Purves, D. (1997). Correlated size variation in human visual cortex, lateral geniculate nucleus, and optic tract. *Journal of Neuroscience*, 17, 2859–2868.

Anzai, A., Peng, X., & Van Essen, D.C. (2007). Neurons in monkey visual area V2 encode combinations of orientations. *Nature Neuroscience*, 10, 1313-1321.

Aslin, R.N. & Shea, S.L. (1990). Velocity thresholds in human infants: implications for the perception of motion. *Developmental Psychology*, 26, 589-598.

Atkinson, J. (2000). *The Developing Visual Brain*. New York: Oxford University Press.

Atkinson, J., Braddick, O., & Braddick, F. (1974). Acuity and contrast sensitivity of infant vision. *Nature*, 247, 403-404.

Atkinson, J., Braddick, O., & Moar, K. (1977). Development of contrast sensitivity over the first 3 months of life in the human infant. *Vision Research*, 17, 1037-1044.

Atkinson, J., King, J., Braddick, O., Nokes, L., Anker, S., & Braddick, F. (1997). A specific deficit of dorsal stream function in Williams' syndrome. *Neuroreport*, 8, 1919-1922.

- Backus, B.T., Fleet, D.J., Parker, A.J., & Heeger, D.J. (2001). Human cortical activity correlates with stereoscopic depth perception. *Journal of Neurophysiology*, 86, 2054-2068.
- Baker, D.H. & Meese, T.S. (2007). Binocular contrast interactions: dichoptic masking is not a single process. *Vision Research*, 47, 3096-3107.
- Ball, K. & Sekuler, R. (1982). A specific and enduring improvement in visual motion discrimination. *Science*, 218, 697-698.
- Banks, M.S. & Bennett, P.J. (1988). Optical and photoreceptor immaturities limit the spatial and chromatic vision of human neonates. *Journal of the Optical Society of America A*, 5, 2059-2079.
- Banks, M.S. & Salapatek, P. (1978). Acuity and contrast sensitivity in 1-, 2-, and 3-month-old human infants. *Investigative Ophthalmology & Visual Science*, 17, 361-365.
- Banton, T., Bertenthal, B., & Seaks, J. (1999). Infants sensitivity to statistical distributions of motion direction and speed. *Vision Research*, 39, 3417–3340.
- Banton, T., Dobkins, K., & Bertenthal, B.I. (2001). Infant direction discrimination thresholds. *Vision Research*, 41, 1049-1056.

Banton, T. & Levi, D.M. (1991). Binocular summation in vernier acuity. *Journal of the Optical Society of America. A, Optics, Image Science, and Vision*, 8, 673-680.

Barb, S.M., Rodriguez-Galindo, C., Wilson, M.W., Phillips, N.S., Zou, P., Scoggins, M., Li, Y., Qaddoumi, I., Helton, K.J., Bikhazi, G., Haik, B.G., & Ogg, R. J. (2011). Functional neuroimaging to characterize visual system development in children with retinoblastoma. *Investigative Ophthalmology & Visual Science*, 52, 2619-2626.

Barnea-Goraly, N., Menon, V., Eckert, M., Tamm, L., Bammer, R., Karchemskiy, A. Dant, C., & Reiss, A. (2005). White matter development during childhood and adolescence: a cross-sectional diffusion tensor imaging study. *Cerebral Cortex*, 15, 1848–1854.

Barnes, G.R., Li, X., Thompson, B., Singh, K.D., Dumoulin, S.O., & Hess, R.F. (2010). Decreased gray matter concentration in the lateral geniculate nuclei in human amblyopes. *Investigative Ophthalmology and Visual Science*, 51, 1432-1438.

Barrett, B.T., Bradley, A., & McGraw, P.V. (2004). Understanding the neural basis of amblyopia. *Neuroscientist*, 10, 106-117.

- Baudouin, J.Y., Gallay, M., Durand, K., & Robichon, F. (2010). The development of perceptual sensitivity to second-order facial relations in children. *Journal of Experimental Child Psychology*, 107, 195-206.
- Beatty, R.M., Sadun, A.A., Smith, L., Vonsattel, J.P., & Richardson, E.P. (1982). Direct demonstration of transsynaptic degeneration in the human visual system: a comparison of retrograde and anterograde changes. *Journal of Neurology, Neurosurgery, and Psychiatry*, 45, 143-146.
- Beauchamp, M.S., Lee, K.E., Argall, B.D., Martin, A. (2004). Integration of auditory and visual information about objects in superior temporal sulcus. *Neuron*, 41, 809–823.
- Benjamini, Y. & Hochberg, Y. (1995). Controlling the false discovery rate: a practical and powerful approach to multiple testing. *Journal of the Royal Statistical Society Series B*, 57, 289–300.
- Bertone, A., Hanck, J., Cornish, K.M., & Faubert, J. (2008). Development of static and dynamic perception for luminance-defined and texture-defined information. *Neuroreport*, 19, 225-228.
- Birch, E.E. (1985). Infant acuity differences and binocular vision. *Vision Research*, 25, 571–576.

Birch, E.E., Fawcett, S., & Stager, D. (2000). Co-development of VEP motion response and binocular vision in normal infants and infantile esotropes. *Investigative Ophthalmology & Visual Science*, 41, 1719-1723.

Birch, E.E., Shimojo, S., & Held R. (1985). Preferential-looking assessment of fusion and stereopsis in infants aged 1 to 6 months. *Investigative Ophthalmology & Visual Science*, 26, 366–370.

Birch, E.E. & Swanson, W. H. (1992). Probability summation of acuity in the human infant. *Vision Research*, 32, 1999–2003.

Blakemore, C. & Vital-Durand, F. (1986). Organization and post-natal development of the monkey's lateral geniculate nucleus. *Journal of Physiology*, 380, 453-491.

Blakemore, C., Garey, L.J., & Vital-Durand, F. (1978). The physiological effects of monocular deprivation and their reversal in the monkey's visual cortex. *Journal of Physiology*, 283, 223-262.

Blasdel, G.G. & Fitzpatrick, D. (1984). Physiological organization of layer 4 in macaque striate cortex. *Journal of Neuroscience*, 4, 880-895.

- Boothe, R.G., Greenough, W.T., Lund, J.S., & Wrege, K. (1979). A quantitative investigation of spine and dendrite development of neurons in visual cortex (area 17) of *Macaca nemestrina* monkeys. *Journal of Comparative Neurology*, 186, 473-489.
- Bosworth, R.G. & Birch, E.E. (2005). Motion detection in normal infants and young patients with infantile esotropia. *Vision Research*, 45, 1557-1567.
- Bosworth, R.G. & Birch, E.E. (2007). Direction-of-motion detection and motion VEP asymmetries in normal children and children with infantile esotropia. *Investigative Ophthalmology and Visual Science*, 48, 5523-5531.
- Bourgeois, J.P. & Rakic, P. (1996) Synaptogenesis in the occipital cortex of macaque monkey devoid of retinal input from early embryonic stages. *European Journal of Neuroscience*, 8, 942-950.
- Bowns, L., Kirshner, L., & Steinbach, M. (1994). Hemifield relative motion bias in adults monocularly enucleated at an early age. *Vision Research*, 34, 3389-3395.
- Braddick, O. (1996). Motion processing: Where is the naso-temporal asymmetry? *Current Biology*, 6, 250-253.

Braddick, O., Atkinson, J., & Wattam-Bell, J. (2003). Normal and anomalous development of visual motion processing: motion coherence and 'dorsal-stream vulnerability'. *Neuropsychologia*, 41, 1769-1784.

Braddick, O.J., O'Brien, J.M., Wattam-Bell, J., Atkinson, J., & Turner R. (2000). Form and motion coherence activate independent, but not dorsal/ventral segregated, networks in the human brain. *Current Biology*, 10, 731-734.

Brady, F. (2004). *A Singular View: The Art of Seeing with One Eye*. Oradell, New Jersey: Medical Economics Company.

Bradley, A. & Freeman, R.D. (1982). Contrast sensitivity in children. *Vision Research*, 22, 953-959.

Brauer, K., Leuba, G., Garey, L.J., & Winkelman, E. (1985). Morphology of axons in the human lateral geniculate nucleus: a Golgi study in prenatal and postnatal material. *Brain Research*, 359, 21-33.

Bridge, H., Cowey, A., Ragge, N., & Watkins, K. (2009). Imaging studies in congenital anophthalmia reveal preservation of brain architecture in "visual" cortex. *Brain*, 132, 3467-3480.

Bridge, H., Thomas, O., Jbabdi, S., & Cowey, A. (2008). Changes in connectivity after visual cortical brain damage underlie altered visual function. *Brain*, 131, 1433–1444.

Bridge, H., von dem Hagen, E.A.H., Davies, G., Chambers, C., Gouws, A., Hoffmann, M., & Morland, A.B. (2012). Changes in brain morphology in albinism reflect reduced visual acuity. *Cortex*, 1–9.

Broaddus, E., Topham, A., & Singh, A.D. (2009a). Incidence of retinoblastoma in the USA: 1975-2004. *British Journal of Ophthalmology*, 93, 21-23.

Broaddus, E., Topham, A., & Singh, A.D. (2009b). Survival with retinoblastoma in the USA: 1975-2004. *British Journal of Ophthalmology*, 93, 24-27.

Brosnahan, D., Norcia, A.M., Schor, C.M., & Taylor, D.G. (1998). OKN. perceptual and VEP direction biases in strabismus. *Vision Research*, 38, 2833-2840.

Bushnell, I.W.R. (2001). Mother's face recognition in newborn infants: learning and memory. *Infant and Child Development*, 10, 67-74.

Burkhalter, A., Van Essen, D.C. (1986). Processing of color, form and disparity information in visual areas VP and V2 of ventral extrastriate cortex in the macaque monkey. *Journal of Neuroscience*, 6, 2327-2351.

Cagnello, R., Arditi, A., & Halpern, D.L. (1993). Binocular enhancement of visual acuity. *Journal of the Optical Society of America, A, Optics, Image Science, and Vision*, 10, 1841-1848.

Chacko, L.W. (1948). The laminar pattern of the lateral geniculate body in the primates. *Journal of Neurology, Neurosurgery, and Psychiatry*, 11, 211–224.

Chalupa, L.M. & Lia, B. (1991). The nasotemporal division of retinal ganglion cells with crossed and uncrossed projections in the fetal rhesus monkey. *Journal of Neuroscience*, 11, 191-202.

Chawla, D., Phillips, J., Buechel, C., Edwards, R., & Friston, K.J. (1998). Speed-dependent motion-sensitive responses in V5: an fMRI study. *NeuroImage*, 7, 86-96.

Chen, Y., Bedell, H.E., & Frishman, L.J. (1996). Temporal-contrast discrimination and its neural correlates. *Perception*, 25, 505-522.

Chen, Y., Grossman, E.A., Bidwell, L., Yurgelun-Todd, D., Gruder, S.A., Levy, D.L., Nakayama, K.L., & Holzman, P.S. (2008). Differential activation patterns of occipital and prefrontal cortices during motion processing: evidence from normal and schizophrenic brains. *Cognitive, Affective and Behavioral Neuroscience*, 8, 293-303.

Chen, Y., Nakayama, K., Levy, D.L., Mathysse, S., & Holzman PS. (1999).

Psychophysical isolation of a motion-processing deficit in schizophrenics and their relatives and its association with impaired smooth pursuit. *Proceedings of the National Academy of Sciences of the United States of America*, 96, 4724-4729.

Chiron, C., Jambaque, I., Nabbout, R., Lounes, R., Syrota, A., & Dulac, O. (1997). The right brain hemisphere is dominant in human infants. *Brain*, 120, 1057–1065.

Chow, A. M., Zhou, I. Y., Fan, S. J., Chan, K. W. Y., Chan, K. C., & Wu, E. X. (2011).

Metabolic changes in visual cortex of neonatal monocular enucleated rat: a proton magnetic resonance spectroscopy study. *International Journal of Developmental Neuroscience*, 29, 25–30.

Cohen, B. (2001). Explaining Psychological Statistics, 2nd ed. John Wiley & Sons, Inc., New York.

Courage, M.L. & Adams, R.J. (1996). Infant peripheral vision: the development of monocular visual acuity in the first 3 months of postnatal life. *Vision Research* 36, 1207–1215.

- Crawford, J.R. & Garthwaite, P.H. (2002). Investigation of the single case in neuropsychology: confidence limits on the abnormality of test scores and test score differences. *Neuropsychologia*, 40, 1196–1208.
- Culham, J.C., & Valyear, K.F. (2006). Human parietal cortex in action. *Current Opinion in Neurobiology*, 16, 205-212.
- Curcio, C.A., Sloan, K.R., Kalina, R.E., & Hendrickson, A.E. (1990). Human photoreceptor topography. *Journal of Comparative Neurology*, 292, 497–523.
- Dai, H., Mu, K.T., Qi, J.P., Wang, C.Y., Shu, W.Z., Xia, L.M., Chen, Z.Q., Zhang, H., Ai, F., & Morelli, J.N. (2011). Assessment of lateral geniculate nucleus atrophy with 3 TMR imaging and correlation with clinical stage of glaucoma. *AJNR American Journal of Neuroradiology*, 32, 1347–1353.
- Dale, A.M., Fischl, B., & Sereno, M.I. (1999). Cortical surface-based analysis. I. Segmentation and surface reconstruction. *NeuroImage*, 9, 179-194.
- Dale, A.M. & Sereno, M.I. (1993). Improved localization of cortical activity by combining EEG and MEG with MRI cortical surface reconstruction: a linear approach. *Journal of Cognitive Neuroscience*, 5, 162-176.

Daw NW. (2006). Visual Development. 2nd ed. New York: Springer.

Day S. (1995). Vision development in the monocular individual: implications for the mechanisms of normal binocular vision development and the treatment of infantile esotropia. *Transactions of the American Ophthalmological Society*, 93, 523-581.

de Courten, C. & Garey, L. (1982). Morphology of the neurons in the human lateral geniculate nucleus and their normal development. *Experimental Brain Research*, 47, 159-171.

de Schonen, S. & Deruelle, C. (1991). Visual field asymmetries for pattern processing are present in infancy. A comment on T. Hatta's study on children's performances. *Neuropsychologia*, 29, 335-337.

Desikan, R.S., Segonne, F., Fischl, B., Quinn, B.T., Dickerson, B.C., Blacker, D., Buckner, R.L., Dale, A.M., Maguire, R.P., Hyman, B.T., Albert, M.S., & Killiany, R.J. (2006). An automated labeling system for subdividing the human cerebral cortex on MRI scans into gyral based regions of interest. *NeuroImage*, 31, 968-980.

Destrieux, C., Fischl, B., Dale, A., & Halgren, E. (2010). Automatic parcellation of human cortical gyri and sulci using standard anatomical nomenclature. *NeuroImage*, 53, 1-15.

- Derrington, A.M. & Lennie, P. (1984). Spatial and temporal contrast sensitivities of neurones in lateral geniculate nucleus of macaque. *Journal of Physiology*, 357, 219-240.
- Devlin, J.T., Sillery, E.L., Hall, D.A., Hobden, P., Behrens, T.E., Nunes, R.G., Clare, S., Matthews, P.M., Moore, D.R., & Johansen-Berg, H. (2006). Reliable identification of the auditory thalamus using multi-modal structural analyses. *NeuroImage*, 30, 112–1120.
- Distler, C. & Hoffmann, K.P. (2011). Visual pathway for the optokinetic reflex in infant macaque monkeys. *Journal of Neuroscience*, 31, 17659-17668.
- Drover, J.R., Morale, S.E., Wang, Y.Z., Stager, D.R. & Birch, E.E. (2010). Vernier acuity cards: examination of development and screening validity. *Optometry and Vision Science*, 87, E806-12.
- Du, H., Xie, B., Yu, Q., & Wang J. (2009). Occipital lobe's cortical thinning in ametropic amblyopia. *Magnetic Resonance Imaging*, 27, 637-640.
- Durand, A.C., & Gould, G.M. (1910). A method of determining ocular dominance. *JAMA*, 55, 369-370.

Ellemberg, D., Lewis, T.L., Defina, N., Maurer, D., Brent, H.P., Guillemot, J.P., & Lepore, F. (2005). Greater losses in sensitivity to second-order local motion than to first-order local motion after early visual deprivation in humans. *Vision Research*, 45, 2877-2884.

Ellemberg, D., Lewis, T.L., Dirks, M., Maurer, D., Ledgeway, T., Guillemot, J.P., & Lepore F. (2004). Putting order into the development of sensitivity to global motion. *Vision Research*, 44, 2403-2411.

Ellemberg, D., Lewis, T.L., Liu, C.H. & Maurer, D. (1999). Development of spatial and temporal vision during childhood. *Vision Research*, 39, 2325-2533.

Ellemberg, D., Lewis, T.L., Maurer, D., Brar, S., & Brent, H.P. (2002). Better perception of global motion after monocular than after binocular deprivation. *Vision Research*, 42, 169-179.

Ellemberg, D., Lewis, T.L., Maurer, D., & Brent, H.P. (2000). Influence of monocular deprivation during infancy on the later development of spatial and temporal vision. *Vision Research*, 40, 2383-2395.

Ellemberg, D., Lewis, T.L., Meghji, K.S., Maurer, D., Guillemot, J.P., & Lepore F. (2003). Comparison of sensitivity to first- and second-order local motion in 5-year-olds and adults. *Spatial Vision*, 16, 419-428.

Faguet, J., Maranhao, B., Smith, S.L., & Trachtenberg, J.T. (2009). Ipsilateral eye cortical maps are uniquely sensitive to binocular plasticity. *Journal of Neurophysiology*, 10, 855-861.

Felician, O., Romaiguère, P., Anton, J.L., Nazarian, B., Roth, M., Poncet, M., & Roll, JP. (2004). The role of human left superior parietal lobule in body part localization. *Annals of Neurology*, 55, 749-751.

Fischl, B. & Dale, A.M. (2000). Measuring the thickness of the human cerebral cortex from magnetic resonance images. *Proceedings of the National Academy of Sciences of the United States of America*, 97, 11050–11055.

Fischl, B., Liu, A., & Dale, A.M. (2001). Automated manifold surgery: constructing geometrically accurate and topologically correct models of the human cerebral cortex. *IEEE Transactions on Medical Imaging*, 20, 70-80.

Fischl, B., Rajendran, N., Busa, E., Augustinack, J., Hinds, O., Yeo, B.T., Mohlberg, H., Amunts, K., & Zilles, K. (2008). Cortical folding patterns and predicting cytoarchitecture. *Cereb Cortex*, 18, 1973-1980.

Fischl, B., Salat, D.H., Busa, E., Albert, M., Dieterich, M., Haselgrove, C., van de Kouwe, A., Killiany, R., Kennedy, D., Klaveness, S., Montillo, A., Makris, N., Rosen, B., & Dale, A.M. (2002). Whole brain segmentation: automated labeling of neuroanatomical structures in the human brain. *Neuron*, 33, 341-355.

Fischl, B., Salat, D.H., van der Kouwe, A.J., Makris, N., Segonne, F., Quinn, B.T., & Dale, A.M. (2004a). Sequence-independent segmentation of magnetic resonance images. *Neuroimage*, 23, S69-84.

Fischl, B., Sereno, M.I., & Dale, A.M. (1999a). Cortical surface-based analysis. II: Inflation, flattening, and a surface-based coordinate system. *NeuroImage*, 9, 195-207.

Fischl, B., Sereno, M.I., Tootell, R.B., & Dale, A.M. (1999b). High-resolution intersubject averaging and a coordinate system for the cortical surface. *Human Brain Mapping*, 8, 272-284.

Fischl, B., van der Kouwe, A., Destrieux, C., Halgren, E., Segonne, F., Salat, D.H., Busa, E., Seidman, L.J., Goldstein, J., Kennedy, D., Caviness, V., Makris, N., Rosen, B., & Dale, A.M. (2004b). Automatically parcellating the human cerebral cortex. *Cerebral Cortex*, 14, 11-22.

Fox, R., Aslin, R.N., Shea, S.L., & Dumais, S.T. (1980). Stereopsis in human infants. *Science*, 207, 323-324.

Franklin, A., Drivonikou, G.V., Bevis, L., Davies, I.R., Kay, P., Regier, T. (2008). Categorical perception of color is lateralized to the right hemisphere in infants, but to the left hemisphere in adults. *Proceedings of the National Academy of Sciences of the United States of America*, 105, 3221-3225.

Fukuda, Y., Sawai, H., Watanabe, M., Wakakuwa, K., & Morigiwa, K. (1989). Nasotemporal overlap of crossed and uncrossed retinal ganglion cell projections in the Japanese monkey (*Macaca fuscata*). *Journal of Neuroscience*, 9, 2353-2573.

Gallivan, J.P., Cavina-Pratesi, C., & Culham, J.C. (2009). Is that within reach?: fMRI reveals that the human superior parieto-occipital cortex (SPOC) encodes objects reachable by the hand. *Journal of Neuroscience*, 29, 4381-4391.

Gao, W., Lin, W., Chen, Y., Gerig, G., Smith, J.K., Jewells, V., & Gilmore, J.H. (2009). Temporal and spatial development of axonal maturation and myelination of white matter in the developing brain. *AJNR American Journal of Neuroradiology*, 30, 290–296.

- Garey, L.J. & de Courten, C. (1983). Structural development of the lateral geniculate nucleus and visual cortex in monkey and man. *Behavioral Brain Research*, 10, 3-13.
- Gaser, C. Nenadic, I., Volz, H.P., Büchel, C., & Sauer, H. (2004). Neuroanatomy of “Hearing Voices”: A frontotemporal brain structural abnormality associated with auditory hallucinations in schizophrenia. *Cerebral Cortex*, 14, 91–96.
- Ge, Y., Grossman, R.I., Babb, J.S., Rabin, M.L., Mannon, L.J., & Kolson, D.L. (2002). Age-related total gray matter and white matter changes in normal adult brain. Part I: volumetric MR imaging analysis. *AJNR American Journal of Neuroradiology*, 23, 1327–1333.
- Geschwind, N. & Galaburda, A.M. (1985). Cerebral lateralization. *Archives of Neurology*, 42, 428–459.
- Geschwind, N. (1970). The organization of language and the brain. *Science*, 170, 940–944.
- Giaschi, D., Narasimhana, S., Solski, A., Harrison, E., Wilcox, L.M. (2013). On the typical development of stereopsis: Fine and coarse processing. *Vision Research*, 89, 65-71.

Giedd, J.N., Blumenthal, J., Jeffries, N.O., Castellanos, F.X., Liu, H., Zijdenbos, Paus, T., Evans, A.C., Rapoport, J.L. (1999). Brain development during childhood and adolescence: a longitudinal MRI study. *Nature Neuroscience*, 2, 861–863.

Giolli, R.A. & Guthrie, M.D. (1969). The primary optic projections in the rabbit: An experimental degeneration study. *Journal of Comparative Neurology*, 136, 99-116.

Glass, L. (1969). Moiré effect from random dots. *Nature*, 223, 578-580.

Godement, P., Salaun, J., & Metin, C. (1987). Fate of uncrossed retinal projections following early or late prenatal monocular enucleation in the mouse. *Journal of Comparative Neurology*, 255, 97-109.

Goldby, F. (1957). A note on transneuronal atrophy in the human lateral geniculate body. *Journal of Neurology, Neurosurgery, and Psychiatry*, 20, 202-207.

Goltz, H.C., Steinbach, M.J. & Gallie, B.L. (1997). Head turn in 1-eyed and normally sighted individuals during monocular viewing. *Archives of Ophthalmology*, 115, 748–750.

González, E.G., Steeves, J.K. E. & Steinbach, M.J. (1998). Perceptual learning for motion-defined letters in unilaterally enucleated observers and monocularly viewing normal controls, *Investigative Ophthalmology and Visual Science Supplement*, 39, S400.

González, E.G., Steeves, J.K.E., Kraft, S.P., Gallie, B.L., & Steinbach, M.J. (2002). Foveal and eccentric acuity in one-eyed observers. *Behavioral Brain Research*, 128, 71–80.

González, E.G., Wong, A.M., Niechwiej-Szwedo, E., Tarita-Nistor, L., & Steinbach, M.J. (2012). Eye position stability in amblyopia and in normal binocular vision. *Investigative Ophthalmology and Visual Science*, 53, 5386-94.

Goodyear, B.G., Nicolle, D.A., Humphrey, K., & Menon, R.S. (2000). BOLD fMRI response of early visual areas to perceived contrast in human amblyopia. *Journal of Neurophysiology*, 84, 1907-1913.

Gottfried, J.A. & Zald, D.H. (2005). On the scent of human olfactory orbitofrontal cortex: meta-analysis and comparison to non-human primates. *Brain Research: Brain Research Reviews*, 50, 287-304.

- Ghosh, S.S., Kakunoori, S., Augustinack, J., Nieto-Castanon, A., Kovelman, I., Gaab, N., Christodoulou, J.A., Triantafyllou, C., Gabrieli, J.D., Fischl, B. (2010). Evaluating the validity of volume-based and surface-based brain image registration for developmental cognitive neuroscience studies in children 4 to 11 years of age. *NeuroImage*, 53, 85–93.
- Gottlieb, M.D., Pasik, P. & Pasik, T. (1985). Early postnatal development of the monkey visual system. I. Growth of the lateral geniculate nucleus and striate cortex. *Brain Research*, 17, 53–62.
- Gougoux, F., Lepore, F., Lassonde, M., Voss, P., Zatorre, R.J., & Belin P. (2004). Neuropsychology: pitch discrimination in the early blind. *Nature*, 430, 309.
- Gougoux, F., Zatorre, R.J., Lassonde, M., Voss, P., & Lepore, F. (2005). A functional neuroimaging study of sound localization: Visual cortex activity predicts performance in early-blind individuals. *PLoS Biology*, 3, e27.
- Grigonis, A.M., Pearson, H.E., & Murphy, E.H. (1986). The effects of neonatal monocular enucleation on the organization of ipsilateral and contralateral retinothalamic projections in the rabbit. *Brain Research*, 394, 9-19.
- Grill-Spector, K., Kourtzi, Z., & Kanwisher, N. (2001). The lateral occipital complex and its role in object recognition. *Vision Research*, 41, 1409-1422.

Guillery, R.W. (1989). Early monocular enucleations in fetal ferrets produce a decrease of uncrossed and an increase of crossed retinofugal components: a possible model for the albino abnormality. *Journal of Anatomy*, 164, 73-84.

Hadad, B.S., Maurer, D., & Lewis, T.L. (2011). Long trajectory for the development of sensitivity to global and biological motion. *Developmental Science*, 14, 1330-1339.

Han, X., Jovicich, J., Salat, D., van der Kouwe, A., Quinn, B., Czanner, S., Busa, E., Pacheco, J., Albert, M., Killiany, R., Maguire, P., Rosas, D., Makris, N., Dale, A., Dickerson, B., Fischl, B. (2006). Reliability of MRI-derived measurements of human cerebral cortical thickness: the effects of field strength, scanner upgrade and manufacturer. *Neuroimage*, 32, 180-194.

Hardman, J., Halpin, S.F.S., Hourihan, M. D., Mars, S., & Lane, C. (1997). MRI of the anterior optic pathways following enucleation. *Neuroradiology*, 39, 815-817.

Headon, M.P., Sloper, J.J., Hiorns, R.W., & Powell, T.P. (1981). Cell sizes in the lateral geniculate nucleus of normal infant and adult rhesus monkeys. *Brain Research*, 229, 183-186.

Hebb, D.O. (1949). *The Organization of Behaviour*. New York: John Wiley and Sons.

- Hendrickson, A.E. & Tigges, M. (1985). Enucleation demonstrates ocular dominance columns in Old World macaque but not in New World squirrel monkey visual cortex. *Brain Research*, 333, 340-344.
- Hess, R.F., & Howell, E.R. (1977). The threshold contrast sensitivity function in strabismic amblyopia: evidence for a two type classification. *Vision Research*, 17, 1049-1055.
- Hess, R.F., Wang, Y-Z., Demanins, R., Wilkinson, F., & Wilson, H.R. (1999). A deficit in strabismic amblyopia for global shape detection. *Vision Research*, 39, 901-914.
- Heumann, D. & Rabinowicz, T. (1982). Postnatal development of the visual cortex of the mouse after enucleation at birth. *Experimental Brain Research*, 46, 99-106.
- Hickey, T.L. (1977). Postnatal development of the human lateral geniculate nucleus: relationship to a critical period for the visual system. *Science*, 198, 836-838.
- Hickey, T.L. & Guillery, R.W. (1979). Variability of laminar patterns in the human lateral geniculate nucleus. *Journal of Comparative Neurology*, 183, 221-246.
- Hickey, T.L. & Peduzzi, J.D. (1987). Structure and development of the visual system. In P. Salapatek & L. Cohen (Eds.). *Handbook of Infant Perception* (pp 1-42). Orlando: Academic Press.

- Hickey, Ho, C.S., Giaschi, D.E., Boden, C., Dougherty, R., Cline, R., & Lyons, C. (2005). Deficient motion perception in the fellow eye of amblyopic children. *Vision Research*, 45, 1615-1627.
- Hinds, O., Polimeni, J. R., Rajendran, N., Balasubramanian, M., Amunts, K., Zilles, K., Schwartz, E.L., Fischl, B., & Triantafyllou, C. (2009). Locating the functional and anatomical boundaries of human primary visual cortex. *NeuroImage*, 46, 915–922.
- Hinds, O.P., Rajendran, N., Polimeni, J.R., Augustinack, J.C., Wiggins, G., Wald, L. L., Rosas, H.D., Potthast, A., Schwartz, E.L., & Fischl, B. (2008). Accurate prediction of V1 location from cortical folds in a surface coordinate system. *NeuroImage*, 39, 1585–1599.
- Ho, C.S. & Giaschi, D.E. (2009). Low- and high-level motion perception deficits in anisometropic and strabismic amblyopia: evidence from fMRI. *Vision Research*, 49, 2891-2901.
- Hogstrom, L.J., Westlye, L.T., Walhovd, K.B., & Fjell, A.M. (2012). The structure of the cerebral cortex across adult life: age-related patterns of surface area, thickness, and gyrification. *Cerebral Cortex*, 23, 2521-2530.

- Hoffmann, K.P. (1986). Visual inputs relevant for the optokinetic nystagmus in mammals. *Progress in Brain Research*, 64, 75-84.
- Hoffmann, K.P., Bremmer, F., Thiele, A., & Distler, C. (2002). Directional asymmetry of neurons in cortical areas MT and MST projecting to the NOT-DTN in macaques. *Journal of Neurophysiology*, 87, 2113–2123.
- Hohmann, A. & Haase, W. (1982). Development of visual line acuity in humans. *Ophthalmic Research*, 12, 107-112.
- Hoover, A.E.N., Harris, L.R. & Steeves, J.K.E. (2012). Sensory compensation in sound localization in people with one eye. *Experimental Brain Research*, 216, 565-574.
- Horton, J. (1997). Wilbrand's knee of the primate optic chiasm is an artefact of monocular enucleation. *Transactions of the American Ophthalmological Society*, 95, 579-609
- Horton, J.C. (2006). Ocular integration in the human visual cortex. *Canadian Journal of Ophthalmology*, 41, 584-593.
- Horton, J.C., Dagi, L.R., McCrane, E.P., & de Monasterio, F.M. (1990). Arrangement of ocular dominance columns in human visual cortex. *Archives of Ophthalmology*, 108, 1025-1031.

Horton, J.C., & Hocking, D.R. (1998a). Effect of early monocular enucleation upon ocular dominance columns and cytochrome oxidase activity in monkey and human visual cortex. *Visual Neuroscience*, 15, 289-303.

Horton, J.C., & Hocking, D.R. (1998b). Monocular core zones and binocular border strips in primate striate cortex revealed by the contrasting effects of enucleation, eyelid suture, and retinal laser lesions on cytochrome oxidase activity. *Journal of Neuroscience*, 18, 5433-5455.

Hou, F., Huang, C.B., Tao, L., Feng, L., Zhou, Y., & Lu, Z.L. (2011). Training in contrast detection improves motion perception of sinewave gratings in amblyopia. *Investigative Ophthalmology and Visual Science*, 52, 6501-6510.

Howard, I.P. (2002). Seeing in Depth. Vol. 1 Basic Mechanisms. Thornhill, Ontario, Canada: I Porteous.

Hubel, D.H. & Livingstone, M.S. (1987). Segregation of form, color, and stereopsis in primate area 18. *Journal of Neuroscience*, 7, 3378-3415.

Hubel, D.H. & Livingstone, M.S. (1990). Color and contrast sensitivity in the lateral geniculate body and primary visual cortex of the macaque monkey. *Journal of Neuroscience*, 10, 2223-2237.

Hubel, D.H. & Wiesel, T.N. (1969). Anatomical demonstration of columns in the monkey striate cortex. *Nature*, 221, 747-750.

Hubel, D.H. & Wiesel, T.N. (1977). Ferrier lecture. Functional architecture of macaque monkey visual cortex. *Proceedings of the Royal Society of London B Biological Science*, 198, 1-59.

Hubel, D.H., Wiesel, T.N., & LeVay, S. (1977). Plasticity of ocular dominance columns in monkey striate cortex. *Philosophical Transactions of the Royal Society of London. Series B, Biological sciences*, 278, 377-409.

Huk, A.C., & Heeger, D.J. (2000). Task-related modulation of visual cortex. *Journal of Neurophysiology*, 83, 3525-3536.

Hupé, J.M., James, A.C., Girard, P., & Bullier, J. (2001). Response modulations by static texture surround in area V1 of the macaque monkey do not depend on feedback connections from V2. *Journal of Neurophysiology*, 85, 146-163.

Huttenlocher, P.R. (1990). Morphometric study of human cerebral cortex. *Neuropsychologia*, 28, 517-527.

Huttenlocher, P.R. & de Courten, C. (1987). The development of synapses in striate cortex of man. *Human Neurobiology*, 6, 1-9.

Huttenlocher, P.R., de Courten, C., Garey, L.J., & Van der Loos, H. (1982).

Synaptogenesis in human visual cortex--evidence for synapse elimination during normal development. *Neuroscience Letters*, 33, 247-252.

Im, K., Lee, J.-M., Lee, J., Shin, Y.-W., Kim, I.Y., Kwon, J.S., & Kim, S.I. (2006). Gender difference analysis of cortical thickness in healthy young adults with surface-based methods. *NeuroImage*, 31, 31–38.

Inouchi, M., Matsumoto, R., Taki, J., Kikuchi, T., Mitsueda-Ono, T., Mikuni, N., Wheaton, L., Hallett, M., Fukuyama, H., Shibasaki, H., Takahashi, R., & Ikeda, A. (2013). Role of posterior parietal cortex in reaching movements in humans: clinical implication for 'optic ataxia'. *Clinical Neurophysiology*, 124, 2230-2241.

Jackson, E.F., Ginsberg, L.E., Schomer, D.F., & Leeds, N.E., (1997). A review of MRI pulse sequences and techniques used in neuroimaging. *Surgical Neurology*, 47, 185–199.

Jeffery, G., Cowey, A.C., & Kuypers, H.G.J.M. (1981). Birfurcating retinal ganglion cell axons in the rat, demonstrated by retrograde double labeling. *Experimental Brain Research*, 44, 34-40.

- Jeffery, G., Levitt, J.B., & Cooper, H.M. (2008). Segregated hemispheric pathways through the optic chiasm distinguish primates from rodents. *Neuroscience*, 157, 637-643.
- Jenkinson, M. & Smith, S.M. (2001). A global optimisation method for robust affine registration of brain images. *Medical Image Analysis*, 5, 143–156.
- Jenkinson, M., Bannister, P.R., Brady, J.M., & Smith, S.M. (2002). Improved optimisation for the robust and accurate linear registration and motion correction of brain images. *NeuroImage*, 17, 825–841
- Jiang, J., Zhu, W., Shi, F., Liu, Y., Li, J., Qin, W., Li, K., Yu, C., & Jiang, T. (2009). Thick visual cortex in the early blind. *Journal of Neuroscience*, 29, 2205–2211.
- Jonas, J.B., Schmidt, A.M., Müller-Bergh, J.A., Schlötzer-Schrehardt, U.M., & Naumann, G.O.H., 1992. Human optic nerve fiber count and optic disc size. *Investigative Ophthalmology and Visual Science*, 33, 2012–2018.
- Kandel, G.L., Grattan, P.E., & Bedell, H.E. (1980). Are the dominant eyes of amblyopes normal? *American Journal of Optometry and Physiological Optics*, 57, 1-6.

Kanwisher, N., McDermott, J., & Chun, M.M. (1997). The fusiform face area: A module in human extrastriate cortex specialized for face perception. *Journal of Neuroscience*, 17, 4302-4311.

Kaplan, E. & Shapley, R.M. (1982). X and Y cells in the lateral geniculate nucleus of macaque monkeys. *Journal of Physiology*, 330, 125-143.

Katz, L.C. & Crowley, J.C. (2002). Development of cortical circuits: lessons from ocular dominance columns. *Nature Reviews: Neuroscience*, 3, 34-42.

Kau, S., Strumpf, H., Merkel, C., Stoppel, CM., Heinze, H.J., Hopf, J.M., & Schoenfeld, M.A. (2013). Distinct neural correlates of attending speed vs. coherence of motion. *Neuroimage*, 64, 299-307.

Kelly, K.R., Gallie, B.L., & Steeves, J.K.E. (2012). Impaired face processing in early monocular deprivation from enucleation. *Optometry and Vision Science*, 89, 137-147.

Kelly, K.R., McKetton, L., Schneider, K.A. Gallie, B.L., & Steeves, J.K.E. (2013). Altered anterior visual system development following early monocular enucleation. *NeuroImage: Clinical*, 4, 72-81.

Kelly, K.R., Moro, S.S., & Steeves, J.K.E. (2013a). Living with one eye: plasticity in visual and auditory systems. In J.K.E. Steeves & L.R. Harris (Eds.), *Plasticity in Sensory Systems* (pp. 225-44). Cambridge: Cambridge University Press.

Kelly, K.R., Tcherassen, K., Gallie, B.L., & Steeves, J.K.E. (2014). Early monocular enucleation selectively disrupts the development of neural mechanisms for face perception. [Paper Presentation]. Vision Sciences Society annual meeting. May 16 – May 21, 2014, St. Pete's Beach, FL.

Kelly, K.R., Zohar, S.R., Gallie, B.L., & Steeves, J.K.E. (2013b). Impaired speed perception but intact luminance contrast perception in people with one eye. *Investigative Ophthalmology and Visual Science*, 54, 3058–3064.

Keys, R. (1981). Cubic convolution interpolation for digital image processing. *IEEE Transactions on Signal Processing, Acoustics, Speech, and Signal Processing*, 29, 1153–1160.

Khan, A.A., 2005. Effects of monocular enucleation on the lateral geniculate nucleus (LGN) of rabbit: a qualitative light and electron microscopic study. *Biomedical Research*, 16, 1–5.

- Khan, A.A., Wadhwa, S. & Bulani, B.V. (1994). Development of human lateral geniculate nucleus: An electron microscopic study. *International Journal of Developmental Neuroscience*, 12, 661-672.
- Koldewyn, K., Whitney, D., & Rivera, S.M. (2010). The psychophysics of visual motion and global form processing in autism. *Brain*, 133, 599-610.
- Kremenitzer, J.P., Vaughan, H.G. Kurtzberg, D., & Dowling, K. (1979). Smooth-pursuit eye movements in the newborn infant. *Child Development*, 50, 442-448.
- Kuperberg, G.R., Broome, M.R., McGuire, P.K., David, A.S., Eddy, M., Ozawa, F., Goff, D., West, W.C., Williams, S.C., van der Kouwe, A.J., Salat, D.H., Dale, A.M., & Fischl, B. (2003). Regionally localized thinning of the cerebral cortex in schizophrenia. *Archives of General Psychiatry*, 60, 878-888.
- Kupers, R., Christensen, R., Grey, M., & Ptito, M. (2009). Glucose metabolism of the occipital cortex in early blind subjects. *Society for Neuroscience Abstract*, 167.26.
- Kupers, R., Pietrini, P., Ricciardi, E., & Ptito, M. (2011). The nature of consciousness in the visually deprived brain. *Frontiers in Psychology*, 2, 19.

Kupfer, C., Chumbley, L., & Downer, J. C. (1967). Quantitative histology of optic nerve, optic tract and lateral geniculate nucleus of man. *Journal of Anatomy*, 101, 393-401.

Le Grand, R., Mondloch, C.J., Maurer, D., & Brent, H.P. (2003). Expert face processing requires visual input to the right hemisphere during infancy. *Nature Neuroscience*, 6, 1108-1112.

Le Grand, R., Mondloch, C.J., Maurer, D., & Brent, H.P. (2004). Impairment in holistic face processing following early visual deprivation. *Psychological Science*, 15, 762-768.

Legge, G.E. (1984). Binocular contrast summation. 1. Detection and discrimination. *Vision Research*, 24, 373-383.

Lessard, N., Paré, M., Lepore, F., & Lassonde, M. (1998). Early-blind human subjects localize sound sources better than sighted subjects. *Nature*, 395, 278-280.

Lewis, T.L. & Maurer, D. (1992). The development of temporal and nasal visual fields during infancy. *Vision Research*, 32, 903-911.

Lewis, T.L., Maurer, D., Chung, J.Y., Holmes-Shannon, R., & Van Schaik, C.S. (2000).

The development of symmetrical OKN in infants: quantification based on OKN acuity for nasalward versus temporalward motion. *Vision Research*, 40, 445-453.

Lewis, T.L., Maurer, D., Tytla, M.E., Bowering, E.R., & Brent, H.P. (1992) Vision in the

“good” eye of children treated for unilateral congenital cataract. *Ophthalmology*, 99, 1013-1017.

Lewis, T.L., Ellemberg, D., Maurer, D., Wilkinson, F., Wilson, H.R., Dirks, M., & Brent,

H.P. (2002). Sensitivity to global form in glass patterns after early visual deprivation in humans. *Vision Research*, 42, 939-948.

LeVay, S., Hubel, D.H., & Wiesel, T.N. (1975). The pattern of ocular dominance columns

in macaque visual cortex revealed by a reduced silver stain. *Journal of Comparative Neurology*, 159, 559-576.

LeVay, S., Wiesel, T. N., & Hubel, D. H. (1980). The development of ocular dominance

columns in normal and visually deprived monkeys. *The Journal of Comparative Neurology*, 191, 1-51.

- Li, M., He, H.G., Shi, W., Li, J., Lv, B., Wang, C.H., Miao, Q.W., Wang, Z.C., Wang, N.L., Walter, M., & Sabel, B.A. (2012). Quantification of the human lateral geniculate nucleus in vivo using MR imaging based on morphometry: volume loss with age. *AJNR American Journal of Neuroradiology*, 33, 915–921.
- Lohmann, D.R. & Gallie, B.L. (2013). Retinoblastoma. In: R.A. Pagon, M.P. Adam, M.P., T.D. Bird, et al. (Eds.), *GeneReviews™* [Internet]. Seattle, WA. Available from: <http://www.ncbi.nlm.nih.gov/books/NBK1452/>
- Luu, J.Y. & Levi, D.M. (2013). Sensitivity to synchronicity of biological motion in normal and amblyopic vision. *Vision Research*, 83, 9-18
- Marotta, J.J., Perrot, T.S., Nicolle, D., Servos, P., & Goodale, M.A. (1995). Adapting to monocular vision: grasping with one eye. *Experimental Brain Research*, 104, 107-114.
- Manning, C., Aagten-Murphy, D., & Pellicano E. (2012). The development of speed discrimination abilities. *Vision Research*, 70, 27-33.
- Mason, A.J., Braddick, O.J., & Wattam-Bell, J. (2003). Motion coherence thresholds in infants--different tasks identify at least two distinct motion systems. *Vision Research*, 43, 1149-1157.

Matthews, M.R. (1964). Further observations on transneuronal degeneration in the lateral geniculate nucleus of the macaque monkey. *Journal of Anatomy*, 98, 255-263.

Maunsell, J.H.R., & Van Essen, D.C. (1983). Functional-properties of neurons in middle temporal visual area of the macaque monkey. 2. Binocular interactions and sensitivity to binocular disparity. *Journal of Neurophysiology*, 49, 1148-1167.

Mayer, D.L. & Dobson, V. (1982). Visual acuity development in infants and young children, as assessed by operant preferential learning. *Vision Research*, 22, 1141-1151.

McKee, S.P., Levi, D.M., Movshon, J.A. (2003). The pattern of visual deficits in amblyopia. *Journal of Vision*, 3, 380-405.

McKeefry, D.J., Burton, M.P., Vakrou, C., Barrett, B.T., & Morland, A.B. (2008). Induced deficits in speed perception by transcranial magnetic stimulation of human cortical areas V5/MTp and V3A. *Journal of Neuroscience*, 28, 6848-6857.

Mendola, J.D., Conner, I.P., Roy, A., Chan, S.T., Schwartz, T.L., Odom, J.V., & Kwong, K.K. (2005). Voxel-based analysis of MRI detects abnormal visual cortex in children and adults with amblyopia. *Human Brain Mapping*, 25, 222-236.

- Menon, V., & Desmond, J.E. (2001). Left superior parietal cortex involvement in writing: integrating fMRI with lesion evidence. *Brain Research. Cognitive Brain Research*, 12, 337-340.
- Meyer, M., Liem, F., Hirsiger, S., Jäncke, L., & Hänggi, J. (2013). Cortical surface area and cortical thickness demonstrate differential structural asymmetry in auditory-related areas of the human cortex. *Cerebral Cortex*. doi: 10.1093/cercor/bht094
- Miki, A., Liu, G.T., Englander, S.A., van Erp, T.G., Bonhomme, G.R., Aleman, D.O., Liu, C.S., & Haselgrove, J.C. (2001). Functional magnetic resonance imaging of eye dominance at 4 tesla. *Ophthalmic Research*, 33, 276-282.
- Mishkin M, Ungerleider LG. (1982). Contribution of striate inputs to the visuospatial functions of parieto-preoccipital cortex in monkeys. *Behavioural Brain Research*, 6, 57-77.
- Moro, S.S., Kelly, K.R., McKetton, L., & Steeves, J.K.E. (2014). Asymmetrical MGB volume in people with one eye. [Paper Presentation]. Vision Sciences Society annual meeting. May 16 – May 21, 2014, St. Pete's Beach, FL.
- Moro, S.S. & Steeves, J.K.E (2012). No Colavita effect: equal auditory and visual processing in people with one eye. *Experimental Brain Research*, 216, 367-373.

- Moro, S.S. & Steeves, J.K.E (2013). No Colavita effect: Increasing temporal load maintains equal auditory and visual processing in people with one eye. *Neuroscience Letters*, 556, 186-190.
- Mullin, C.R., & Steeves, J.K.E. (2011). TMS to lateral occipital cortex disrupts object processing but facilitates scene processing *Journal of Cognitive Neuroscience*, 23, 4174-4184.
- Naegle, J.T. & Held, R. (1982). The postnatal development of monocular optokinetic nystagmus in infants. *Vision Research*, 22, 341-346.
- Nassi, J.J., Lomber, S.G., & Born, R.T. (2013). Corticocortical feedback contributes to surround suppression in V1 of the alert primate. *Journal of Neuroscience*, 33, 8504-8517.
- Neveu, M.M., Holder, G.E., Ragge, N.K., Sloper, J.J., Collin, J.R.O., & Jeffery, G. (2006). Early midline interactions are important in mouse optic chiasm formation but are not critical in man: a significant distinction between man and mouse. *European Journal of Neuroscience*, 23, 3034-3042.
- Nicholas, J.J., Heywood, C.A., & Cowey, A. (1996). Contrast sensitivity in one-eyed subjects. *Vision Research*, 36, 175-180.

- Norcia, A.M., Garcia, H., Humphrey, R., Holmes, A., Hamer, R.D., & Orel-Bixler, D. (1991). Anomalous motion VEPs in infants and in infantile esotropia. *Investigative Ophthalmology and Visual Science*, 32, 436-439.
- Norcia, A.M., Tyler, C.W., & Hamer, R.D. (1990). Development of contrast sensitivity in the human infant. *Vision Research*, 30, 1475-1486.
- Pan, M., Yang, X., & Tang, J. (2012). Research on interpolation methods in medical Image processing. *Journal of Medical Systems*, 36, 777-807.
- Pandya, D.N., Rosene, D.L., & Doolittle, A.M. (1994). Corticothalamic connections of auditory-related areas of the temporal lobe in the rhesus monkey. *Journal of Comparative Neurology*, 345, 447-471.
- Park, H.-J., Lee, J.D., Kim, E.Y., Park, B., Oh, M.-K., Lee, S., & Kim, J.-J. (2009). Morphological alterations in the congenital blind based on the analysis of cortical thickness and surface area. *NeuroImage*, 47, 98–106.
- Parravano, J.G., Toledo, A., & Kucharczyk, W. (1993). Dimensions of the optic nerves, chiasm, and tracts: MR quantitative comparison between patients with optic atrophy and normals. *Journal of Computer Assisted Tomography*, 17, 688–690.

Parrish, E.E., Giaschi, D.E., Boden, C., & Dougherty, R. (2005). The maturation of form and motion perception in school age children. *Vision Research*, 45, 827-837.

Paulesu, E., Frith, C.D., & Frackowiak, R.S. (1993). The neural correlates of the verbal component of working memory. *Nature*, 362, 342–345.

Perry, V.H. & Cowey, A. (1984). Retinal ganglion cells that project to the superior colliculus and pretectum in the macaque monkey. *Neuroscience*, 12, 1125–1137.

Perry, V.H., Oehler, R., & Cowey, A., 1984. Retinal ganglion cells that project to the dorsal lateral geniculate nucleus in the macaque monkey. *Neuroscience*, 12, 1101–1123.

Pirenne, M.H. (1954). Absolute visual thresholds. *Journal of Physiology*, 123, 40–41

Provis, J.M. & Watson, C.R. (1981). The distribution of ipsilaterally and contralaterally projecting ganglion cells in the retina of the pigmented rabbit. *Experimental Brain Research*, 44, 82-92.

Ptito, M., Fumal, A., Martens de Noordhout, Schoenen, J., Gjedde, A., Kupers. R. (2008). TMS of the occipital cortex induces tactile sensations in the fingers of blind Braille readers. *Experimental Brain Research*, 184, 193-200.

- Ptito, M., Moesgaard, S.M., Gjedde, A., & Kupers, R. (2005). Cross-modal plasticity revealed by electrotactile stimulation of the tongue in the congenitally blind. *Brain*, 128, 606-614.
- Puce, A. & Perrett, D. (2003). Electrophysiology and brain imaging of biological motion. *Philosophical Transactions of the Royal Society of London. Series B, Biological Science*, 358, 435-445.
- Putnam, T.J. (1926). Studies on the central visual system. IV. The details of the organization of the geniculostriate system in man. *Archives of Neurology*, 16, 683–707.
- Qin, W., Liu, Y., Jiang, T., & Yu, C. (2013). The development of visual areas depends differently on visual experience. *PLoS One*, 8, e53784.
- Qiu, Z., Xu, P., Zhou, Y., & Lu, Z.L. (2007). Spatial vision deficit underlies poor sine-wave motion direction discrimination in anisometropic amblyopia. *Journal of Vision*, 7, 1-16.
- Rakic, P. (1976). Prenatal genesis of connections subserving ocular dominance in the rhesus monkey. *Nature*, 261, 467-471.

- Rakic, P (1977). Prenatal development of the visual system in rhesus monkey. *Philosophical Transactions of the Royal Society of London. Series B, Biological sciences*, 278, 245-246.
- Rakic, P. (1981). Development of visual centers in the primate brain depends on binocular competition before birth. *Science*, 214, 928-931.
- Reed, M.J., Steeves, J.K.E., & Steinbach, M.J. (1997). A comparison of contrast letter thresholds in unilateral eye enucleated subjects and binocular and monocular subjects. *Vision Research*, 37, 2465-2469.
- Reed, M.J., Steeves, J.K.E, Steinbach, M.J., Kraft, S., & Gallie, B. (1996). Contrast letter thresholds in the non-affected eye of strabismic and unilateral eye enucleated subjects. *Vision Research*, 36, 3011-3018.
- Reed, M.J., Steinbach, M.J., Anstis, S.M., Gallie, B., Smith, D., & Kraft, S. (1991). The development of optokinetic nystagmus in strabismus and monocularly enucleated subjects. *Behavioural Brain Research*, 46, 31-42.
- Reed, M.J., Steinbach, M.J., Ono, H., Kraft, S., & Gallie, B. (1995). Alignment ability of strabismic and eye enucleated subjects on the horizontal and oblique meridians. *Vision Research*, 35, 2523-2528.

- Regal, D.M. (1981). Development of critical flicker frequency in human infants. *Vision Research*, 21, 549–555.
- Renier, L.A., Anurova, I., De Volder, A.G., Carlson, S., VanMeter, J., & Rauschecker, J.P. (2010). Preserved functional specialization for spatial processing in the middle occipital gyrus of the early blind. *Neuron*, 68, 138-148.
- Robinson, D.L. & Petersen S.E. (1992). The pulvinar and visual salience. *Trends in Neuroscience*, 15, 127-132.
- Rosas, H.D., Liu, A.K., Hersch, S., Glessner, M., Ferrante, R.J., Salat, D.H., van der Kouwe, A., Jenkins, B.G., Dale, A.M., & Fischl, B. (2002). Regional and progressive thinning of the cortical ribbon in Huntington's disease. *Neurology*, 58, 695-701.
- Rosset, A., Spadola, L., & Ratib, O. (2004). OsiriX: an open-source software for navigating in multidimensional DICOM images. *Journal of Digital Imaging*, 17, 205–216.
- Roy, J.P., Komatsu, H., & Wurtz, R.H. (1992). Disparity sensitivity of neurons in monkey extrastriate area MST. *Journal of Neuroscience*, 12, 2478-2492.

- Roy, M., Lachapelle, P., & Leporé, F. (1989). Maturation of the optokinetic nystagmus as a function of the speed of stimulation in fullterm and preterm infants. *Clinical Vision Sciences*, 4, 357–336.
- Salat, D.H., Buckner, R.L., Snyder, A.Z., Greve, D.N., Desikan, R.S., Busa, E., Morris, J.C., Dale, A.M., & Fischl, B. (2004). Thinning of the cerebral cortex in aging. *Cerebral Cortex*, 14, 721-730.
- Sanabria-Diaz, G., Melie-García, L., Iturria-Medina, Y., Alemán-Gómez, Y., Hernández-González, G., Valdés-Urrutia, Galán, L., & Valdés-Sosa, P. (2010). Surface area and cortical thickness descriptors reveal different attributes of the structural human brain networks. *NeuroImage*, 50, 1497–1510.
- Schiller, P.H., Logothetis, N.K., & Charles, E.R. (1990). Role of the color-opponent and broad-band channels in vision. *Visual Neuroscience*, 5, 321-346.
- Schmitz, B., Schaefer, T., Krick, C.M., Reith, W., Backens, M., & Käsmann-Kellner, B. (2003). Configuration of the optic chiasm in humans with albinism as revealed by magnetic resonance imaging. *Investigative Ophthalmology and Visual Science*, 44, 16–21.

- Schultz, C.C., Wagner, G., Koch, K., Gaser, C., Roebel, M., Schachtzabel, C., Nenadic, I., Reichenbach, J.R., Sauer, H., & Schlösser, R.G.M. (2013). The visual cortex in schizophrenia: alterations of gyrification rather than cortical thickness—a combined cortical shape analysis. *Brain Structure and Function*, 218, 51–58.
- Segonne, F., Dale, A.M., Busa, E., Glessner, M., Salat, D., Hahn, H.K., & Fischl, B. (2004). A hybrid approach to the skull stripping problem in MRI. *NeuroImage*, 22, 1060-1075.
- Segonne, F., Pacheco, J., & Fischl, B. (2007). Geometrically accurate topology-correction of cortical surfaces using nonseparating loops. *IEEE Transactions on Medical Imaging*, 26, 518-529.
- Shatz, C.J. & Stryker, M.P. (1988). Prenatal tetrodotoxin infusion blocks segregation of retinogeniculate afferents. *Science*, 242, 87-89.
- Simmers, A.J., Ledgeway, T., Hess, R.F., & McGraw, P.V. (2003). Deficits to global motion processing in human amblyopia. *Vision Research*, 43, 729-738.
- Skoczenski, A.M. & Norcia, A.M. (1999). Development of VEP vernier acuity and grating acuity in human Infants. *Investigative Ophthalmology and Visual Science*, 40, 2411-2417.

- Skoczenski, A.M. & Norcia, A.M. (2002). Late maturation of visual hyperacuity. *Psychological Science*, 13, 537-541.
- Sled, J.G., Zijdenbos, A.P., & Evans, A.C. (1998). A nonparametric method for automatic correction of intensity nonuniformity in MRI data. *IEEE Transactions on Medical Imaging*, 17, 87-97.
- Sloper, J.J. (1993). Edridge-Green Lecture. Competition and cooperation in visual development. *Eye*, 7, 319-331.
- Sloper, J.J., Headon, M.P., & Powell, T.P.S. (1987a). Effects of enucleation at different ages on the sizes of neurons in the lateral geniculate nucleus of infant and adult monkeys. *Developmental Brain Research*, 31, 259-265.
- Sloper, J.J., Headon, M.P., & Powell, T.P.S. (1987b). Changes in the size of cells in the monocular segment of the primate lateral geniculate nucleus during normal development and following visual deprivation. *Developmental Brain Research*, 31, 267-267.
- Smith, S.L. & Trachtenberg, J.T. (2007). Experience-dependent binocular competition in the visual cortex begins at eye opening. *Nature Neuroscience*, 10, 370-375.

Steeves, J.K.E., González, E.G., Gallie, B.L., & Steinbach, M.J. (2002). Early unilateral enucleation disrupts motion processing. *Vision Research*, 42, 143-150.

Steeves, J.K.E., González, E.G., & Steinbach, M.J. (2008). Vision with one eye: a review of visual function following unilateral enucleation. *Spatial Vision*, 21, 509-529.

Steeves, J.K.E., Gray, R., Steinbach, M.J., & Regan D. (2000). Accuracy of estimating time to collision using only monocular information in unilaterally enucleated observers and monocularly viewing normal controls. *Vision Research*, 40, 3783-3789.

Steeves, J.K.E., Wilkinson, F., González, E.G., Wilson, H.R., & Steinbach, M.J. (2004). Global shape discrimination at reduced contrast in enucleated observers. *Vision Research*, 44, 943-949.

Stensaas, S.S., Eddington, D.K., & Dobelle, W.H. (1974). The topography and variability of the primary visual cortex in man. *Journal of Neurosurgery*, 40, 747-755.

Stevenson, R.A. & James T.W. (2009). Audiovisual integration in human superior temporal sulcus: inverse effectiveness and the neural processing of speech and object recognition. *NeuroImage*, 44, 1210-1223.

- Stoeckel, C., Gough, P.M., Watkins, K.E., & Devlin, J.T. (2009). Supramarginal gyrus involvement in visual word recognition *Cortex*, 45, 1091–1106.
- Takai, Y., Sato, M., Tan, R., & Hirai, T. (2005). Development of stereoscopic acuity: Longitudinal study using a computer-based random-dot stereo test. *Japan Journal of Ophthalmology*, 49, 1-5.
- Teller, D.Y. (1997). First glances: The vision of infants. *Investigative Ophthalmology and Visual Science*, 38, 2183-2203.
- Thomson, L.C. (1947). Binocular summation within the nervous pathway of the pupillary light reflex. *Journal of Physiology*, 106, 59-65.
- Tkach , J.A., Chen, X., Freebairn, L.A., Schmithorst, V.J., Holland, S.K., & Lewis, B.A. (2011). Neural correlates of phonological processing in speech sound disorder: a functional magnetic resonance imaging study. *Brain and Language*, 119, 42-49.
- Toosy, A.T., Werring, D.J., Plant, G.T., Bullmore, E.T., Miller, D.H., & Thompson, A.J. (2001). Asymmetrical activation of human visual cortex demonstrated by functional MRI with monocular stimulation. *NeuroImage*, 14, 632-641.

- Tootell, R.B., Hamilton, S.L. & Switkes, E. (1988). Functional anatomy of macaque striate cortex. IV. Contrast and magno- parvo streams. *Journal of Neuroscience*, 8, 1594-1609.
- Tootell, R.B., Reppas, J.B., Kwong, K.K., Malach, R., Born, R.T., Brady, T.J., Rosen, B.R., & Belliveau, J.W. (1995). Functional analysis of human MT and related visual cortical areas using magnetic resonance imaging. *Journal of Neuroscience*, 15, 3215-3230.
- Tucholka, A., Fritsch, V., Poline, J. B., & Thirion, B. (2012). An empirical comparison of surface-based and volume-based group studies in neuroimaging. *Neuroimage*, 63, 1443–1453.
- Turati, C., Macchi Cassia, V., Simion, F., & Leo, I. (2006). Newborns' face recognition: Role of inner and outer facial features. *Child Development*, 77, 297–311.
- Tychsen, L. & Burkhalter, A. (1997). Nasotemporal asymmetries in V1: ocular dominance columns of infant, adult, and strabismic macaque monkeys. *Journal of Comparative Neurology*, 388, 32–46.
- Tychsen, L., & Lisberger, S.G. (1986). Maldevelopment of visual motion processing in humans who had strabismus with onset in infancy. *Journal of Neuroscience*, 6, 2495-2508.

Valmaggi, C., Rüttsche, A., Baumann, A., Pieh, C., Bellaiche Shavit, Y., Proudlock, F., & Gottlob, I. (2004). Age related change of optokinetic nystagmus in healthy subjects: a study from infancy to senescence. *British Journal of Ophthalmology*, 88, 1577-1581.

Van Boven, R.W., Hamilton, B.S., Kauffman, T., Keenan, J.P., & Pascual-Leon, A. (2000). Tactile spatial resolution in blind Braille readers. *Neurology*, 54, 223-226.

Van Essen, D. C., Glasser, M. F., Dierker, D. L., Harwell, J., & Coalson, T. (2012). Parcellations and hemispheric asymmetries of human cerebral cortex analyzed on surface-based atlases. *Cerebral Cortex*, 22, 2241–2262.

Vázquez, Y., Salinas, E., & Romo, R. (2013). Transformation of the neural code for tactile detection from thalamus to cortex. *Proceedings of the National Academy of Sciences of the United States of America*, 110, E2635-44.

Volkman, F. C., & Dobson, V. (1976). Infant responses of ocular fixation to moving visual stimuli. *Journal of Experimental Child Psychology*, 22, 86-99.

Wagner, A.L., Murtagh, F.R., Hazlett, K.S., & Arrington, J.A. (1997). Measurement of the normal optic chiasm on coronal MR images. *AJNR American Journal of Neuroradiology*, 18, 723–726.

- Wallace, M.T., Wilkinson, L.K., & Stein, B.E. (1996). Representation and integration of multiple sensory inputs in primate superior colliculus. *Journal of Neurophysiology*, 76, 1246-1266.
- Wandell, B.A., Dumoulin, S.O., & Brewer, A.A. (2007). Visual field maps in human cortex. *Neuron*, 56, 366–383.
- Wattam-Bell, J. (1994). Coherence thresholds for discrimination of motion direction in infants. *Vision Research*, 34, 877–883.
- Wattam-Bell, J. (1996). Visual motion processing in one-month-old infants: Preferential looking experiments. *Vision Research*, 36, 1671-1677.
- Wattam-Bell, J. (2003). Motion processing asymmetries and stereopsis in infants. *Vision Research*, 43, 1961-1968.
- Weber, E. H. (1834). De pulsu, resorptione, audita et tactu. *Annotationes anatomicae et physiologicae*, Leipzig: Koehler.
- Wefers, C.J., Dehay, C., Berland, M., Kennedy, H., & Chalupa, L.M. (2000). Binocular competition does not regulate retinogeniculate arbor size in fetal monkey. *Journal of Comparative Neurology*, 427, 362-369.

- Westheimer, G. (1975). Editorial: Visual acuity and hyperacuity. *Investigative Ophthalmology*, 14, 570-572.
- Wiesel, T.N., & Hubel, D.H. (1963a). Effects of visual deprivation on morphology and physiology of cells in the cats lateral geniculate body. *Journal of Neurophysiology*, 26, 978-993.
- Wiesel, T.N., & Hubel, D.H. (1963b). Single-cell responses in striate cortex of kittens deprived of vision in one eye. *Journal of Neurophysiology*, 26, 1003-1017.
- Wiesel, T.N., & Hubel, D.H. (1965). Comparison of the effects of unilateral and bilateral eye closure on cortical unit responses in kittens. *Journal of Neurophysiology*, 28, 1029-1040.
- Wilkinson, F., James, T.W., Wilson, H.R., Gati, J.S., Menon, R.S., & Goodale, M.A. (2000). An fMRI study of the selective activation of human extrastriate form vision areas by radial and concentric gratings. *Current Biology*, 10, 1455-1458.
- Winfield, D.A. (1981). The postnatal development of synapses in the visual cortex of the cat and the effects of eyelid closure. *Brain Research* 206, 166–171.

- Winkler, A.M., Kochunov, P., Blangero, J., Almasy, L., Zilles, K., Fox, P.T., Duggirala, R., & Glahn, D.C. (2010). Cortical thickness or grey matter volume? The importance of selecting the phenotype for imaging genetics studies. *NeuroImage*, 53, 1135–1146.
- Woo G.C. & Irving, E. (1991). The non-amblyopic eye of a unilateral amblyope: a unique entity. *Clinical and Experimental Optometry*, 74, 1-5.
- Woo, H.H., Jen, L.S., & So, K.F. (1985). The postnatal development of retinocollicular projections in normal hamsters and in hamsters following neonatal monocular enucleation: a horseradish peroxidase tracing study. *Brain Research*, 352, 1–13.
- Wunderlich, K., Schneider, K.A., & Kastner, S. (2005). Neural correlates of binocular rivalry in the human lateral geniculate nucleus. *Nature Neuroscience*, 8, 1595-1602.
- Xiao, J.X., Xie, S., Ye, J.T., Liu, H.H., Gan, X.L., Gong, G.L., & Jiang, X.X. (2007). Detection of abnormal visual cortex in children with amblyopia by voxel-based morphometry. *American Journal of Ophthalmology*, 143, 489-493.
- Zanker, J., Mohn, G., Weber, U., Zeitler-Driess, K., & Fahle, M. (1992). The development of vernier acuity in human infants. *Vision Research*, 32, 1557-1564.

Zhou, D., Lebel, C., Evans, A., & Beaulieu, C. (2013). Cortical thickness asymmetry from childhood to older adulthood. *NeuroImage*, 83, 66–74.

APPENDIX A: GLOSSARY OF TERMS

Amblyopia. An uncorrectable, permanent reduction of visual function in one eye that is not correctable optically. The clinical definition is a difference in acuity of two lines between the two eyes."

Anisometropia. Unequal refractive error between the two eyes.

Binocular summation. The advantage of viewing with two eyes compared with one when detecting a stimulus or discriminating between two stimuli.

Binocular competition. During visual development, the projections from the two eyes are in competition for synaptic space in visual regions of the brain. When one eye is enucleated, this competition is also removed.

Brain morphology. The study of the form and structure of the brain.

Congenital cataract. A cloudiness of the lens of the eye that is present at birth.

Critical (sensitive) period. The postnatal period during which rapid development of a function occurs, and during which that function is most vulnerable to abnormal experience. There are three types of critical periods relative to a function: 1) *critical period of development* where environmental experience can have a great impact on a

function during a time when that function is rapidly developing, 2) *critical period for disruption* where atypical postnatal experience can have adverse effects on development of a function, and 3) *critical period for recovery* where a function can be recovered after it has been disrupted. Critical periods for different functions can emerge at different times and have varying time courses.

Experience-dependent plasticity. The brain's ability to change on a functional or structural level in response to environmental circumstances, such as during typical development or in the case of visual deprivation.

Hemidecussation. The crossing over of approximately half of the retinal fibres at the optic chiasm.

Hyperacuity. The ability to resolve visual information to a level that is finer than the spacing of cones in the retina allows.

Lateral geniculate nucleus (LGN). A subcortical, thalamic nucleus that is bilateral, and is deemed the visual relay station of the brain. The LGN receives retinal projections in separate, eye-specific laminae, and sends projections to cortical visual regions.

Monocular enucleation. The surgical removal of one eye.

Nasalward motion. During monocular viewing, a stimulus is moving towards the nose.

Newton-Müller-Gudden law. The proportion of crossed/uncrossed retinal fibres is related to the size of the binocular visual field.

Ocular dominance columns. Alternating bands of neurons in primary visual cortex that respond preferentially to one eye or the other.

Optic chiasm. An X-shaped structure located at the anterior part of the visual pathway where fibres from the retina converge. Approximately half of these fibres (i.e., nasal retinal fibres) cross-over, whereas the other half (i.e., temporal retinal fibres) do not.

Optokinetic nystagmus. An involuntary reflex response to full-field horizontal motion of a visual stimulus. There are two phases: 1) a slow phase of pursuit where the eye follows the moving stimulus, 2) a fast phase where the eye has reached the end of the orbit and saccades back in order to continue following the stimulus.

Retinoblastoma. Cancer of the retina.

Spatial frequency. The number of light/dark cycles per degree of visual angle in a grating stimulus.

Spatial form vision. The ability to resolve the spatial features of objects and of our environment. Examples of low-level spatial visual abilities include acuity and contrast

sensitivity. Mid- to high-level spatial form vision tasks bring together many aspects of low-level spatial form vision, such as contrast and spatial frequency, and tasks include detecting and recognizing forms, such as letters, faces, and objects.

Stereopsis. The process of depth perception induced by using a binocular cue to depth — binocular disparity. Binocular disparity refers to the fact that each eye has a slightly different view of the world; when the brain perceives these two slightly different images, depth can be perceived.

Strabismus. Misalignment of the visual axes.

Synaptic pruning. Following a period of synaptogenesis, a period of pruning occurs characterized by a progressive loss of synapses and dendrites.

Synaptogenesis. The physiological process during development where synapse numbers and dendrite complexity increases.

Temporalward motion. During monocular viewing, a stimulus is moving away from the nose and toward the temple.

Tessellation. The process of breaking down components (i.e., voxels) into smaller components (i.e., triangles). The entire cortical surface is covered using these smaller triangles so that no gaps or overlaps are present. The places where the points of the

triangles meet are called vertices. This allows for sub-voxel precision during surface-based analysis.

Weber fraction. Weber fractions are often used in discrimination tasks and are based on Weber's Law that states that the just-noticeable-difference between two perceived stimuli is proportional to the magnitude of the stimuli. The formula is $K = \Delta X/X$, where K is a constant, X is the value of the initial stimulus, and ΔX is the just-noticeable difference between the initial stimulus and a second stimulus.

APPENDIX B: COPYRIGHT PERMISSIONS

Rightslink Printable License

14-03-02 1:54 PM

ELSEVIER LICENSE TERMS AND CONDITIONS

Mar 02, 2014

This is a License Agreement between Krista R Kelly ("You") and Elsevier ("Elsevier") provided by Copyright Clearance Center ("CCC"). The license consists of your order details, the terms and conditions provided by Elsevier, and the payment terms and conditions.

All payments must be made in full to CCC. For payment instructions, please see information listed at the bottom of this form.

| | |
|--------------------------------|------------------------------------------------------------------------------------------------|
| Supplier | Elsevier Limited The Boulevard, Langford Lane Kidlington, Oxford, OX5 1GB, UK |
| Registered Company Number | 1982084 |
| Customer name | Krista R Kelly |
| Customer address | 4700 Keele St Toronto, ON M3J1P3 |
| License number | 3340900450348 |
| License date | Mar 02, 2014 |
| Licensed content publisher | Elsevier |
| Licensed content publication | NeuroImage: Clinical |
| Licensed content title | Altered anterior visual system development following early monocular enucleation |
| Licensed content author | Krista R. Kelly, Larissa McKetton, Keith A. Schneider, Brenda L. Gallie, Jennifer K.E. Steeves |
| Licensed content date | 2014 |
| Licensed content volume number | 4 |
| Licensed content issue number | |
| Number of pages | 10 |
| Start Page | 72 |
| End Page | 81 |
| Type of Use | reuse in a thesis/dissertation |
| Portion | full article |
| Format | both print and electronic |
| Are you the author of this | Yes |

Elsevier article?

Will you be translating? No

Title of your thesis/dissertation VISUAL SYSTEM DEVELOPMENT IN PEOPLE WITH ONE EYE: BEHAVIOUR AND STRUCTURAL NEURAL CORRELATES

Expected completion date May 2014

Estimated size (number of pages) 200

Elsevier VAT number GB 494 6272 12

Permissions price 0.00 USD

VAT/Local Sales Tax 0.00 USD / 0.00 GBP

Total 0.00 USD

Terms and Conditions

INTRODUCTION

1. The publisher for this copyrighted material is Elsevier. By clicking "accept" in connection with completing this licensing transaction, you agree that the following terms and conditions apply to this transaction (along with the Billing and Payment terms and conditions established by Copyright Clearance Center, Inc. ("CCC"), at the time that you opened your Rightslink account and that are available at any time at <http://myaccount.copyright.com>).

GENERAL TERMS

2. Elsevier hereby grants you permission to reproduce the aforementioned material subject to the terms and conditions indicated.

3. Acknowledgement: If any part of the material to be used (for example, figures) has appeared in our publication with credit or acknowledgement to another source, permission must also be sought from that source. If such permission is not obtained then that material may not be included in your publication/copies. Suitable acknowledgement to the source must be made, either as a footnote or in a reference list at the end of your publication, as follows:

"Reprinted from Publication title, Vol /edition number, Author(s), Title of article / title of chapter, Pages No., Copyright (Year), with permission from Elsevier [OR APPLICABLE SOCIETY COPYRIGHT OWNER]." Also Lancet special credit - "Reprinted from The Lancet, Vol. number, Author(s), Title of article, Pages No., Copyright (Year), with permission from Elsevier."

4. Reproduction of this material is confined to the purpose and/or media for which permission is hereby given.

5. Altering/Modifying Material: Not Permitted. However figures and illustrations may be altered/adapted minimally to serve your work. Any other abbreviations, additions, deletions and/or any other alterations shall be made only with prior written authorization of Elsevier Ltd. (Please contact Elsevier at permissions@elsevier.com)

Debbie Chin <dchin@arvo.org>
To: Krista Kelly <kkelly@yorku.ca>

Wed, Apr 24, 2013 at 4:58 PM

Dear Dr. Kelly,

Permission is hereby granted to reprint the following article in your PhD dissertation for York University:

Kelly KR, Zohar SR, Gallie BL, Steeves JKE. Impaired speed perception but intact luminance contrast perception in people with one eye. *Invest Ophthalmol Vis Sci*. 2013;54:in press.

A reprint of this material must include a full article citation and acknowledge ARVO as the copyright holder.

Best regards,

Debbie Chin

Association for Research in Vision and Ophthalmology
1801 Rockville Pike, Suite 400

Rockville MD 20852 USA

Direct: +1.240.221.2926 | Main: +1.240.221.2900 | Fax: +1.240.221.0370

www.arvo.org

